O.V. Fomin, M.I. Gorbunov, O.V. Burlutski

THEORETICAL ASPECTS OF APPLIED TRANSPORT MECHANICS

Part 1

Monograph

Sievierodonetsk 2019

A u t h o r ' s   t e a m :
O. V. Fomin, M. I. Gorbunov, O.V. Burlutski,
O.A. Logvinenko, O. V. Kazanko, O. V.El Kassem

This monograph is recommended for printing by the Science Council
of Volodymyr Dahl East Ukrainian National University
(protocol No 07 dd 29.03.2019)

R e v i e w e r s :

R. V. Vovk,   doctor of Sciences (Physics and Mathematics), Dean of the Faculty of Physics, professor of the Department of Low Temperature Physics, VN Karazin Kharkiv National University ;

V.H Masliiev,   doctor of Technical Sciences, professor at Electronic system and complex of vehicle, National Technical University "Kharkiv Polytechnic Institute";

V.G. Puzyr,   doctor of Technical Sciences, Head of Department at Chair of Operation and Maintenance of Rolling Stock at Ukrainian State University of Railway Transport.

The monograph comprehensively defines theoretical designing principles for transport systems and mechanisms, as well as their individual components at the present stage. The results and peculiarities of the work conducted in terms of creation and investigation into carrying structures of transport facilities were previously published in some Ukrainian and international specialized editions, discussed and obtained approval at some international scientific and technical conferences.

We wrote this book for scientists and engineers whose fields of the professional expertise are related to design and research of railway rolling stock, it also could be useful for the university teachers, students, post-graduate students of the named sphere.

CONTENTS

3

ABSTRACT

The monograph deals with theoretical aspects and methodological basis of modern applied transport mechanics. A range of fundamental problems about operation of mechanisms of various transport facilities and their structural components were studied. The emphasis was on the mechanics of rail traction and non-traction rolling stock facilities.

The study presents theoretical aspects of development and research of the carrying systems of transport facilities and corresponding movable joints. Great attention is given to problems of optimization, research into kinematic characteristics, design refinements of capacity and strength for transportation facilities. The monograph presents the following novel theoretical and practical conceptual frameworks:

- improved methods of structural and kinematic research into mechanisms and machines;
- mathematic dependencies which describe a required law of motion of a follower, the use of which provides the highest limiting time/section values at given conditions and restrictions on design;
- revised dependencies in terms of capacity, rigidity and strength calculation of structural elements of engineering transport facilities;
- advanced approaches towards engineering solutions for improvements of the carrying structures of facilities of rail rolling stock; and
- standardized method for evaluation of the carrying capacity factor of structural elements of bodies of rail open wagons, which can be used, with minor correction, to solve similar tasks for other facilities of transport machine engineering.

The monograph comprehensively defines theoretical designing principles for transport systems and mechanisms, as well as their individual components at the present stage. The results and peculiarities of the work conducted in terms of creation and investigation into carrying structures of transport facilities were previously published in some Ukrainian and

international specialized editions, discussed and obtained approval at some international scientific and technical conferences.

The monograph is meant for experts in the field of transport engineering, the information presented can be of interest for design engineers, developers, researchers, and post graduate students. Besides, it can be used as a textbook for graduate students of rail transport engineering.

Keywords: transport engineering, applied transport mechanics, structural design, fundamentals of theory of mechanisms and machines, strength and reliability, detail design.

1. FUNDAMENTALS OF THEORY
OF MECHANISMS AND MACHINES

1.1. General information

A machine is defined as the technical device intended for certain mechanical transformation of energy, properties, sizes, forms, information and position of materials, in order to replace and facilitate human physical and mental labor by achieving higher efficiency [45, 92].

By functions machines are divided into the following groups.

1. *Energy machines:* used to transform energy (*electrical, hydraulic and internal combustion engines*).

If such machines transform any kind of energy into mechanical energy, they are called *engines*, and for inverse processes the machines are called *generators*.

2. *Working machines:* used to transform a material.

They are divided into *transport* machines used to displace bodies (*automobiles, conveyers, transporters, hoisting machines, etc.*) and *technological* machines used to change the form, condition and properties of a material (*metal-working machinery, rolling mill, breakers, grinders, etc.*).

3. *Information machines:* used to receive and process information.

They include *control machines,* used to process information in order to operate energy and working machines, to control and automatically adjust technological processes; and *mathematical machines,* used to transmit information in order to obtain mathematical images of the object's properties, i.e. to handle mathematical operations (*computers*).

4. *Cybernetic machines,* used to replace or simulate different mechanical, physiological or biological processes inherent to humans and nature. Besides, they are artificial intelligence machines.

The technical device, used to reproduce operating functions of human arms is called *a manipulator*. Automatic control manipulators can be used in harmful working environments, for automation of monotonous and tiresome tasks at quick-acting conveyers, transposition and package of details, etc. Such automatically operated manipulators are called industrial robots .

Transformation of energy, materials and information, performed by a machine, can sometimes be done without an operator. Such machines are

called automatic machines. A group of automatic machines connected and intended for a certain technological process is called an automated line.

A machine assembly is a technical system consisting of one or several connected in sequence or in parallel machines, and used to fulfill some needed functions. Generally, a machine assembly includes (Fig. 1.1): engine, transmission gear, working or energy and control machine. The primary function of a transmission gear is coordination of the mechanical characteristics of an engine and the mechanical characteristics of a working or energy machine.
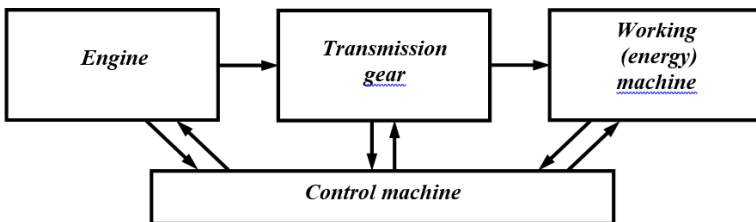
Fig. 1.1. Functional diagram of a machine assembly

Mechanism is the system of physical bodies used to transform a prescribed motion of one or several bodies into a needed motion of other bodies. *The basic feature of a mechanism is transformation of motion.*
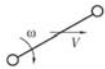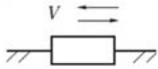
1.2. Structure of mechanism elements and their classification

The solid bodies of a mechanism are called links. The links can be movable and immovable. The immovable link is the link without relative mobility, i.e. it cannot move. Such links are called poles. In turn, movable links are divided into input (links which directly obtain motion transformed by a mechanism into a needed motion of the other links), output (links which perform the target motion of a mechanism) and connecting (links which directly transform motion in a mechanism) [31-32].

The link is named according to the type of motion it performs. Notably, (Table 1.1): crank is the link which performs a rotating motion around an immovable rotation axis (a complete revolution around the axis); connecting rod is the link which performs a plane-parallel (plane) motion; crosshead is the link which performs progressive motion; rocker is the link which performs reciprocating rotary motion around the rotation axis (does not perform a complete rotation around the axis).

8

Table 1.1

Basic types of links in mechanisms

Name of the link	Symbol	Motion type
pole		*no motion*
crank		*rotation*
connecting rod		*plane-parallel*
crosshead		*progressive*
rocker		*reciprocating rotary*

Kinematic pair (KP) is a movable joint of two contact links.

Kinematic pairs are classified by:

- type of KP elements;
- number of links imposed by KP on the relative motion of links;
- method of link closure in KP.

Kinematic pair elements: surface, line or point by which two movable links join, and which limit the relative motion of these links (Fig. 1.2).
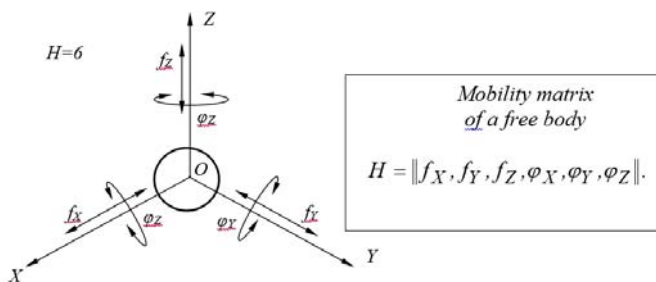
Fig. 1.2. Mobility of a free body

According to the element type (by F. Reuleaux) kinematic pairs are divided into:

- lower KP (element – *surface*);
- higher KP (elements – *line or point*).

According to the number of links (*by I.I. Artobolevski*), imposed by KP on the relative motion of links, kinematic pairs are divided into five classes: *I, II, III, IV, V* (Fig 1.3).

The KP class is defined by the dependency:

$$S_{KP} = 6 - H$$

where S_{KP} is the number of links (*constraints*);

H is the number of degrees of freedom (*pair mobility*).
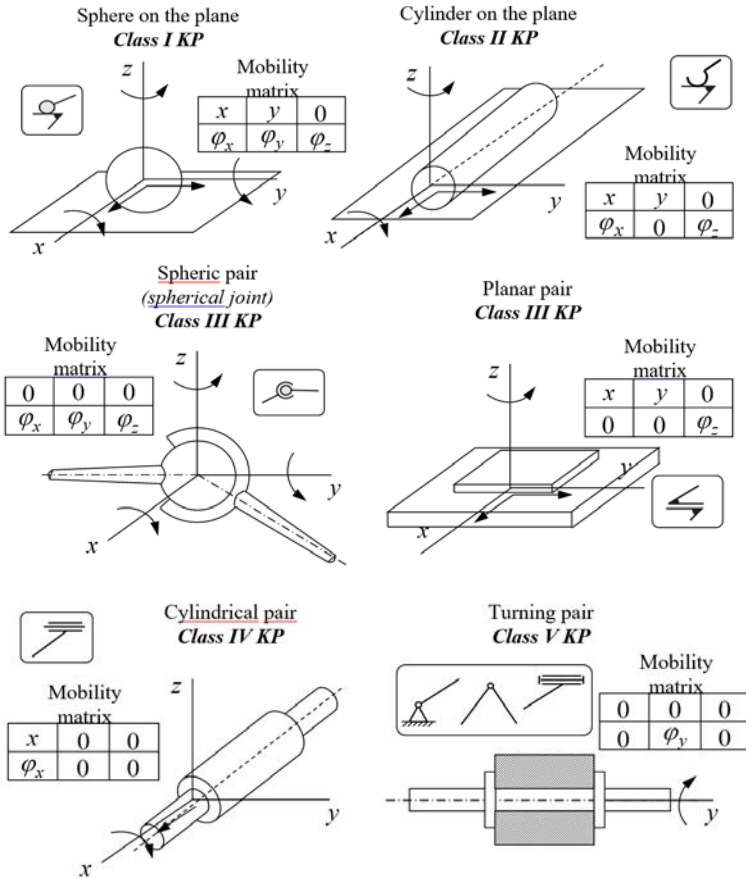
Fig. 1.3. Different classes of kinematic pairs

Types of closure in kinematic pairs

The constant contact of KP elements is provided by geometric or force closure.

Geometric closure is performed by elements of an appropriate form of the KP links or the KP structure.

Force closure is performed by the elasticity forces of springs or the weight of links.

Kinematic chains and joints

Kinematic chain (KC) is a system of links connected by kinematic pairs (Fig. 1.4.).

Kinematic chains are divided into:

- simple and compound:
  simple KC (each link forms no more than two KP).
  compound KC (at least one link forms more than two KP).
- open and closed:
  open KC (at least one chain forms only one KP).
  closed KP (all chains form no less than two KP).
- planar and spatial:
  planar KC (all points move on one plane or parallel planes).
  spatial KC (all points move on various non-parallel planes).
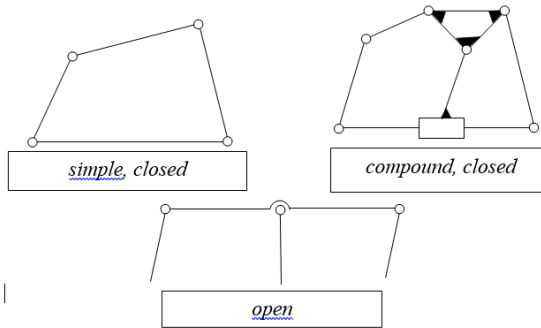
Fig. 1.4. Samples of kinematic chain

In some cases kinematic pairs of classes *I-IV* can be reasonable replaced with the equivalent open kinematic chains (*links of which form only class V KC*) – kinematic joints [69].

Structural formulas of mechanisms

The general patterns in the structure of mechanisms which connect the number of degrees of freedom W with the number of links, and also with the number and type of kinematic pairs, are called structural formulae.

The number of degrees of freedom of mechanism W is the number of degrees of freedom of links in the kinematic chain of a mechanism relative to the pole.

In order to determine W of *spatial mechanisms* Malyshev's structural formula can be applied

$$W = 6 \cdot n - \sum_{i=1}^{5} i \cdot p_i \ ,$$

$$W = 6 \cdot n - 5 \cdot p_5 - 4 \cdot p_4 - 3 \cdot p_3 - 2 \cdot p_2 - p_1,$$

where n is the number of movable links of a mechanism,

$\quad$ i is the KP class,

$\quad$ p_i is the number of KP of the i-th class.

In order to define W of planar mechanisms Chebyshev's structural formula is applied:

$$W = 3 \cdot n - 2 \cdot p_5 - p_4$$

For example, for a crank-and-rod mechanism (Fig. 1.5): 1 – crank, 2 – connecting rod, 3 – crosshead, 4 – pole.

$$W = 3 \cdot 3 - 2 \cdot 4 - 0 = 1$$
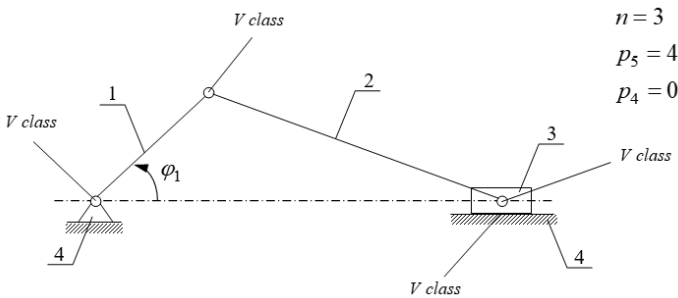
Fig. 1.5. Common scheme of the crank-and-rod mechanism

Generalized coordinate (φ_1) is the coordinate which determines positions of all links of a mechanism. The link, a generalized coordinate corresponds to, is called the initial link.

The degree of freedom of mechanisms is equal to the number of its generalized coordinates.

Classification of mechanisms by structural features

The basic principle of mechanism formation (first formulated by L.V. Assur): most mechanisms can be built by a series connection of structural groups to a class *I* mechanism.

Class I mechanism is connection of the initial link and the pole with a *class V* kinematic pair (for example, *rotary-type mechanisms*).

Structural group (Assur's group) is the kinematic chain which does not change its degree of freedom when its free elements join to other links of the mechanism, and which cannot be divided into simple kinematic chains with zero degree of freedom.

Structural groups of planar mechanisms satisfy the condition:

$$W_{gr} = 3 \cdot n - 2 \cdot p_5 - p_4 = 0 \cdot$$

Structural groups of spatial mechanisms satisfy the condition:

$$W_{gr} = 6 \cdot n - 5 \cdot p_5 - 4 \cdot p_4 - 3 \cdot p_3 - 2 \cdot p_2 - p_1 = 0 \cdot$$

Class of a structural group is defined by the highest class of a loop within the structure.

Class of a loop is defined by the number of kinematic pairs with the chains included (Fig.1.6).

<div align="center">

II   III   IV   V

</div>
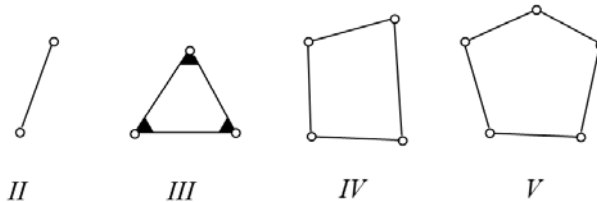
Fig. 1.6. Examples of loop classes

Order of a structural group is defined by the number of elements with which a group joins to the base mechanism (Fig. 1.7).
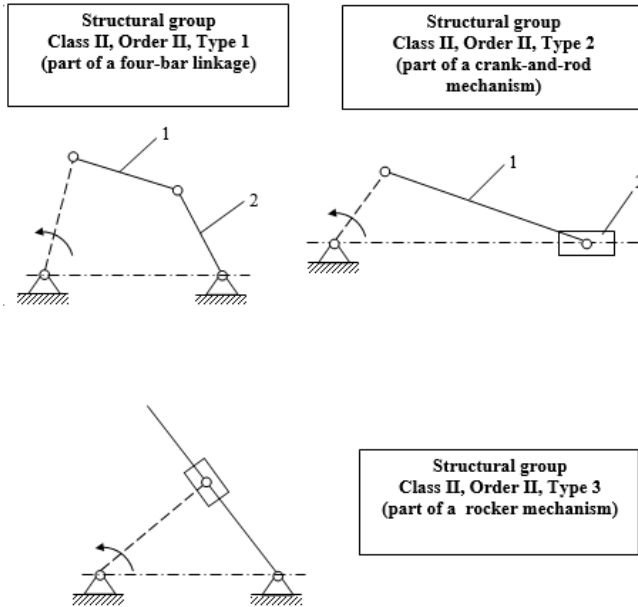
Fig. 1.7. Mechanism class is defined by the highest class
of the structural groups within a mechanism

1.3. Kinematic analysis of mechanisms

Kinematic analysis of mechanisms includes determinations of motion of the links along a prescribed motion of the initial links.

The basic tasks of kinematic research:

- to define positions of the chains of a mechanism,
- to find displacements of certain movable links,
- to build trajectories of certain points of a mechanism, and
- to determine velocities and accelerations of certain movable links and points of a mechanism.

The kinematic analysis of a mechanism begins with the structural group nearest to the initial link (Fig. 1.8).
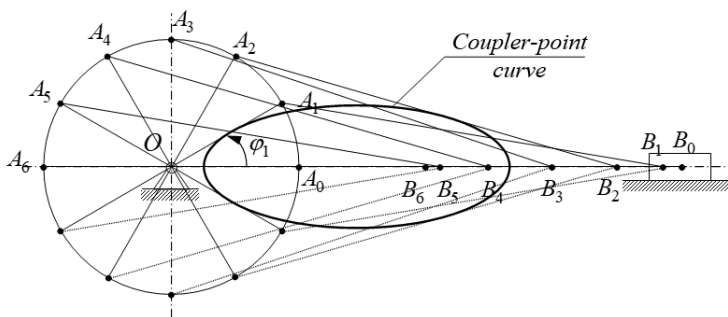
Fig. 1.8. Regarding building the trajectory of points
of a crank-and-rod mechanism

Mechanism plan is a scaled image which corresponds to a certain position of the initial link.

In order to construct the mechanism plan the following should be specified:
- link lengths,
- coordinates of immovable links of a mechanism, and
- generalized coordinate.

Most mechanisms included in the mechanical systems of modern technical facilities are cyclical (gear, cam, etc.), i.e. execute periodic

Cycle of motion is a period of time after which a mechanism returns to its initial position, and its kinematic parameters take on the initial values.
To determine displacements, velocities and accelerations of links and points of a mechanism three methods are used:
- graphical (chord method and tangent method),
- grapho-analytical (plan method), and
- analytical.

Graphical method

The principle of the method:
- with the known values of the link lengths of a mechanism and on the basis of its successive positions, the diagram *s=f (t)* is built;

15

- after two-fold graphical differentiation of the diagram $s=f(t)$ the following diagrams are obtained

$$V = f(t) = \frac{ds}{dt} \quad \text{and} \quad a = f(t) = \frac{dV}{dt} = \frac{d^2s}{dt^2}$$

While making kinematic research it is reasonable to use *analogs of velocities* V_q *and accelerations* a_q, which are only a function of the generalized coordinate φ, and do not depend on the velocity of motion of the initial link.

In this case:
- with the known values of the link lengths of a mechanism and on the basis of its successive positions, the diagram $s=f(\varphi)$ is built;
- after two-fold graphical differentiation of the diagram $s=f(\varphi)$ the following diagrams are obtained

$$V_q = f(\varphi) = \frac{ds}{d\varphi} \; m/rad$$

and

$$a_q = f(\varphi) = \frac{dV}{d\varphi} = \frac{d^2s}{d\varphi^2} \; m/rad^2 \; .$$

The relationship between velocities, accelerations and their analogs:

$$V = V_q \cdot \omega; \qquad a = a_q \cdot \omega^2.$$

Advantages of the graphical method: simplicity, visualization, and possibility to use CAD.

Disadvantages of the graphical method:
- difficult to use for extensive uniform construction;
- impossible to determine accelerations of moving links and points in extreme positions of a mechanism;
- impossible to determine directions of velocities and accelerations of certain points of movable links of a mechanism.

Grapho-analytical method

Grapho-analytical method implies the building of velocity and acceleration vector diagrams to determine values and directions of velocities and accelerations of points of the mechanism's links.

Velocity (acceleration) vector diagram is the scaled image of vectors of the absolute velocities (accelerations) of points of a mechanism, which originate from one point called *the pole*.

Advantages of the grapho-analytical method: possibility to obtain the values and directions of velocities and accelerations of points of a mechanism on the basis of the velocity and acceleration vector diagrams.

Disadvantages of the grapho-analytical method: labor intensity of research into kinematics of the mechanism per motion cycle.

Analytical method
method of closed vector contours, proposed by V.A. Zinoviev

According to Zinoviev's method the analytical dependencies for determination of the basic kinematic parameters can be obtained if an actual mechanism is conditionally replaced with a closed vector contour formed by its links.

Advantages of the analytical method: high accuracy and possibility to use CAD.

Disadvantage of the analytical method: difficult to get analytical formulae for determination of kinematic parameters of complicated mechanisms.

1.4. Power analysis of mechanisms

Power analysis of mechanisms: determination of external forces which provide the motion on the basis of a given law of motion for the initial link of a mechanism.

Tasks of the power analysis of mechanisms
• to determine unknown external forces on the mechanism's links;
• to determine interaction forces in areas where the links contact (reactions in kinematic pairs); and
• to determine the equilibrium force and counterbalance moment of the forces.

Power analysis of a mechanism begins with the link
farthest to the initial link of a structural group.

The axiom of coupling. D'Alambert's principle.
Kinematic chains statistically determined are the chains in which the number of unknown reactions corresponds to the number of static equations [4].

The number of unknown reactions is $2P_5+P_4$.
The number of equilibrium equations is $3n$.
The feature of a statically determined kinematic chain:

$$3n = 2P_5 + P_4, \; 3n - 2P_5 - P_4 = 0 = W \cdot$$

Conclusion: statically determined kinematic chains are structural groups, therefore the power calculation of mechanisms is made separately per structural group beginning with the farthest one from the initial link.

Such individual study of structural groups is conducted on the basis of the axiom of coupling: any constrained link can be considered as free, if it is conditionally separated from the mechanism and the other links are considered as the corresponding reaction.

The theoretical basis of the power calculation of mechanisms is d'Alambert's principle: a movable system of bodies in any moment of time under external forces, constraints and inertial forces is in equilibrium:

$$\sum_{i=1}^{n} \overline{F}_i^{\,ex} + \sum_{j=1}^{k} \overline{R}_j + \sum_{m=1}^{l} \overline{F}_m^{\,in} = 0.$$

The Joukowski Arm

For determination of the equilibrium moment on the initial link of a mechanism without calculating constraints in kinematic pairs, the concept of "the rigid arm of Joukowski" is used; it is based on the principle of virtual displacements: if in some position of a mechanical system the forces applied to it get balanced, for any possible displacement of the system from this position, the amount of work of the set forces is equal to zero.

The Joukowski theorem: if one transfers all given forces, applied to the links of a mechanism at a certain moment, to corresponding points of the velocity vector diagram rotated by 90°, not changing the values and directions of the forces, the sum moment of all these forces including the equilibrium force relative to its pole is equal to 0

And the rotated velocity vector diagram is considered as a rigid arm in equilibrium relative to the pole of the vector diagram under all forces applied. Mathematical notation of the Joukowski theorem:

$$\sum_{i=1}^{n} F_i h_i = 0.$$

Where F_i is the force applied to the *i*-th link of a mechanism; h_i is the arm of a corresponding force (the shortest distance from the pole of the velocity vector diagram to the line where the i-th force is applied).

Classification of effective forces in mechanisms

All effective forces in a mechanism can be conditionally divided into active (prescribed forces) and reactive (reactions in kinematic pairs).

Driving forces F_{dr} are applied to input links; they coincide by direction with the vector of displacement of the point of application, or form an acute angle with it. Work of driving forces is always positive.

Forces of useful resistance $F_{u.r.}$ are applied to output links; they are opposite to the vector of displacement of the point of application, or form an obtuse angle with it. Work of useful resistance forces is always negative.

Forces of parasite resistance $F_{p.r.}$ are the friction forces in kinematic pairs or the environmental resistance. The friction forces in brakes or, for example, in contact areas between locomotive wheels and the rail are not considered as parasite resistance forces, because the friction is useful [41].

Gravity forces *G are applied to the center of mass of links and always directed vertically downwards.*

Inertia forces F_{in} emerge due to irregular motion of the mechanism's links.

The inertia force (Fig. 1.9):

$$\overline{F}_{in} = -m \cdot \overline{a}_S .$$

where m is the link mass, (*kg*);

$\overline{a_S}$ is the acceleration of the mass center of a link, *m/sec²*.
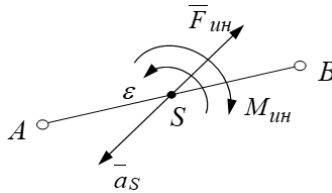
Fig. 1.9. Inertia force at rotational moment

The moment of inertia forces: $\overline{M}_{in} = -I_S \cdot \overline{\varepsilon}$,

Where I_S is the moment of inertia of a link relative to the center of mass, ($kg \cdot m^2$);

$\overline{\varepsilon}$ is the angular acceleration of a link, (rad / sec).

Reaction forces R emerge on the contact areas of links (in kinematic pairs). Like the force, the reaction is characterized by: module, direction, point of application.

Peculiarities of considering reactions in kinematic pairs of planar mechanisms:

1) class 5 kinematic pairs (Fig. 1.10)*:*
    a) turning pair;
    - module and direction are unknown;
    - point of application is known;
    b) sliding pair;
    - module and point of application are unknown;
    - direction is known;
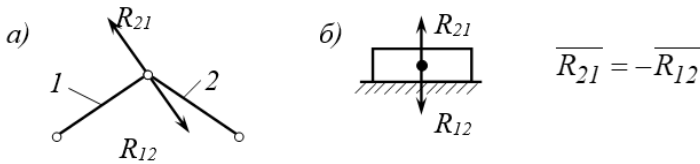
Fig. 1.10. The reactions of class 5 kinematic pairs:
a – turning, *b* – sliding

2) class 4 kinematic pairs (Fig. 1.11)*:*
    $t-t$ tangential;
    $n-n$ normal.
    - module is unknown.
    - point of application and direction are known.
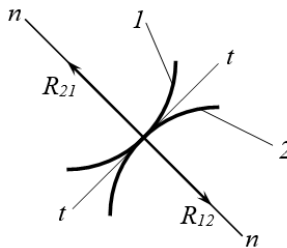
Fig. 1.11. The reactions of class *4* kinematic pairs

1.5. Mechanical transmission

Types of transmissions. Mechanical transmissions.

Transmission is a unit for transferring energy at a distance (Fig. 1.12).
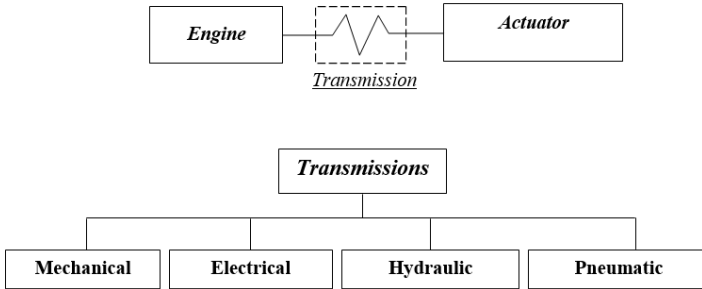
Fig. 1.12. Types of transmissions

Functions of transmissions:
- to distribute energy among mechanisms;
- to increase or decrease the velocities of links;
- to convert the motion;
- to regulate the velocity;
- to start, stop and reverse a machine; and
- to protect machines elements from overloading.

Basic requirements for transmissions:
- reliability and needed service life;
- simple structure;
- portable and small size;
- low resistance to motion (*especially at engine starts*);
- comparatively high accuracy in transmission of motion;
- possibility to obtain the least moment of inertia for rotating links, reduced to the engine shaft;
- noiseless, high vibration resistance, and ease of operation

There are two basic shafts in transmissions (Fig. 1.13)*:*
- input (driver);
- output (driven).
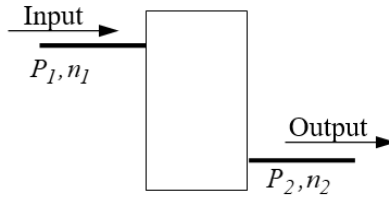
Fig. 1.13. Scheme of interaction of basic shafts in transmissions

In multiple transmissions there are *intermediate shafts* between input and output shafts

Basic characteristics of transmissions:
- *capacity* at input P_1 and output P_2;
- *specific speed* (expressed by rotating frequencies at input n_1 and output n_2, or angular velocities at input ω_1 and output ω_2).

Derivative characteristics of transmissions:
- efficiency:

$$\eta = \frac{P_2}{P_1} \, ,$$

- contact ratio:

$$i = \frac{\omega_1}{\omega_2} = \frac{n_1}{n_2} \, .$$

If rotational directions of two contacting links are equal, $i > 0$, and if they are not equal, $i < 0$.

If $i > 1$, $n_1 > n_2$ is *the reducing* transmission (*reducer*).

The reducer decreases the rotations or angular velocity, but increases the torque moment.

If $i < 1$, $n_1 < n_2$ is *the step-up* transmission (*multiplier*).

The multiplier increases the rotations or the angular speed, but decreases the torque moment.

Mechanical transmission is a machine used to transfer or convert mechanical motion (Fig. 1.14).

22

```
              Mechanical transmissions
     by principle of motion from the driver to the driven shaft

        Friction                              Gear
      Transmission                         Transmission


        Friction                     Friction drive
      Transmission
                                       Belt drive


                                       Gear drive
         Gear
      Transmissions                    Chain drive


                                    Tooth-belt drive


     Transmissions for              Screw - Nut
   transformation of rotary
   motion into progressive
         motion                     Gear - Rack
```
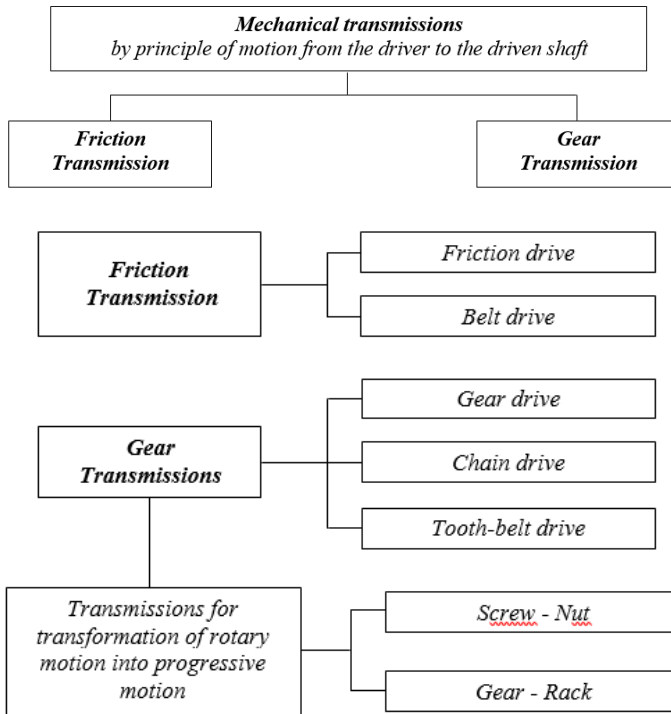
Fig. 1.14. Different types of transmissions

1.6. Design principles for mechanisms
with higher kinematic pairs. Gear

Gear transmissions are mechanisms with higher kinematic pairs, in which transmission and conversion of motion from one link to another are realized with projections (*teeth*) on the surfaces of links (Fig. 1.15) [2, 46].

Advantages of gear mechanisms:
a) high mechanical efficiency,
b) constant gear ratio,
c) portability, and
d) capacity to transmit considerable loads.

Disadvantages of gear mechanisms:
a) high accuracy in manufacture,
b) high rigidity.
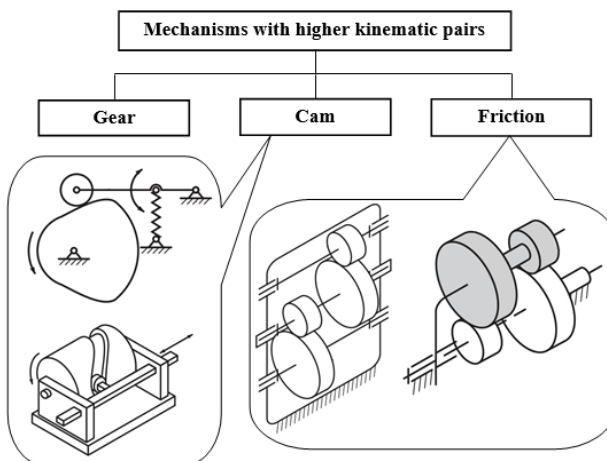
Fig. 1.15. Scheme of gear transmissions (mechanisms)

Gearing is the process of transmission and conversion of motion from one link to another due to pair-wise interaction of the teeth (Fig. 1.16).

1 - pinion (input link)
2 - wheel (output link)
3 - pole
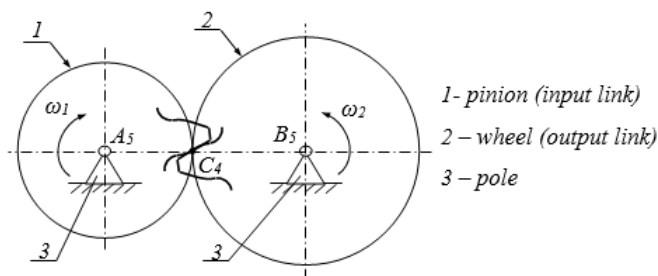
Fig. 1.16. Kinematic diagram of a simple gear mechanism

Gear ratio:

$$i_{1-2} = \pm \frac{\omega_1}{\omega_2}, \quad i_{2-1} = \pm \frac{\omega_2}{\omega_1}.$$

where ω_1, ω_2 are the angular velocities of a pinion and a wheel;

z_1, z_2 the number of the teeth of a pinion and a wheel;

«+» ω_1 and ω_2 are like-directed;

«–» ω_1 and ω_2 are oppositely directed.

The transmission gear wheel with a fewer number of teeth is *called the pinion*.

The transmission gear wheel with a more number of teeth is called *the wheel*.

Classification of gear mechanisms (transmissions) by mutual location of rotation axes of gear wheels

1. Cylindrical – rotation axes are parallel (Fig. 1.17).

Straight   **Helical**   **Double-helical**

External gearing   *Internal gearing*
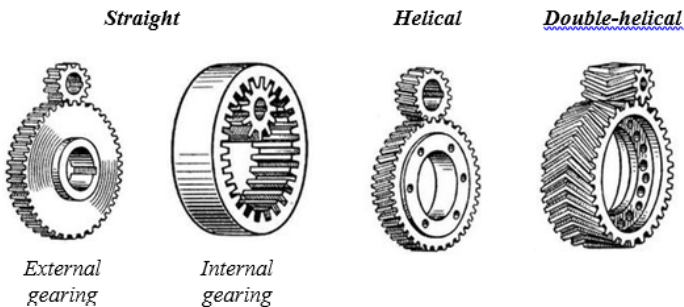
Fig. 1.17. Cylindrical type of gear mechanisms

Advantages and disadvantages of cylindrical straight gear wheels.
Advantages:
- no axial forces;
- possibility to transfer the wheel along the axis in operation.

Disadvantages:
- noisy in operation;
- low operation smoothness;
- low bearing capacity.

Forces in cylindrical straight gear transmissions.

Peripheral force:

$$F_{t12} = \frac{2 \cdot T_2}{d_2},$$

Where T_2 is the torque moment on the second shaft,

d_2 is the diameter of the pitch line of the second wheel.

Radical force (Fig. 1.18)*:*

$$F_{r12} = F_{t12} \cdot \text{tg}\,\alpha \, ,$$

where α is the pressure angle.
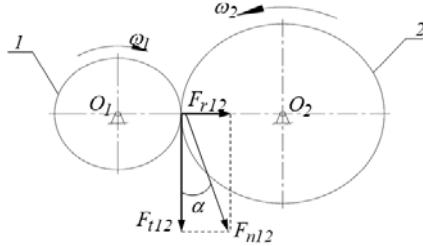
Fig. 1.18. Radical force of cylindrical gear transmissions

Advantages and disadvantages of cylindrical helical gear wheels (Fig. 1.19.)

Advantages:
- high gearing smoothness;
- less noisy;
- high bearing capacity.

Disadvantages:
- axial forces applied to the wheels and, also, to the poles of their shafts or axes.

F_z – *axial force,*
F_n – *normal force,*
F – *peripheral force*
(rotates the wheel),
β – *helix angle.*
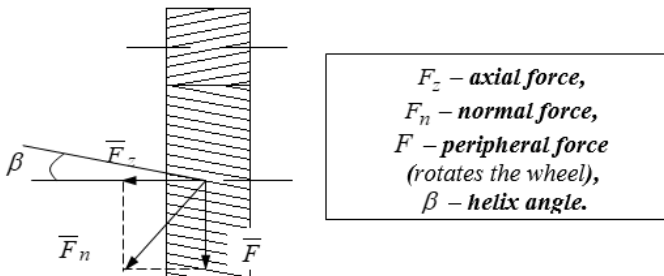
Fig. 1.19. Forces in cylindrical helical gear transmissions

Advantages and disadvantages of gear transmissions with double-helical wheels (Fig. 1.20).

F_z – axial force,
F_n – normal force,
F – peripheral force
(rotates the wheel),
β – helix angle.
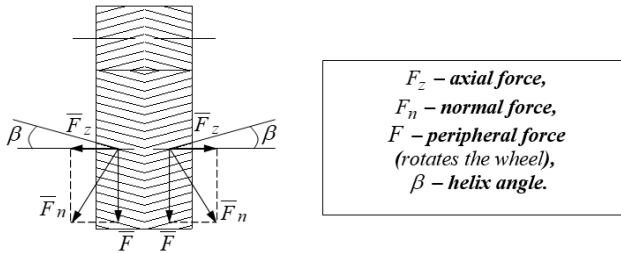
Fig. 1.20. Forces in transmissions with double-helical gear wheels

Advantages:
- no axial forces applied to the wheels and, also, to the poles of their shafts and axes.

Disadvantages:
- difficult in manufacture;
- high cost.

2 Bevel – rotation axes cross.

Advantages and disadvantages of bevel gears (Fig. 1.21).

Straight   **Helical**   **Spiral**
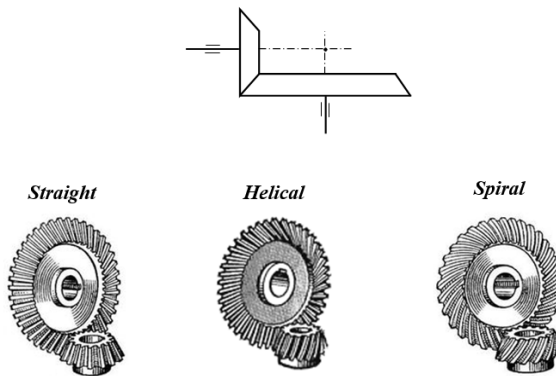
Fig. 1.21. Bevel type of gear mechanisms

Advantages:
- capacity to transmit and convert rotation motion among links with the rotation axes which transverse;
- capacity to transmit motion among links with a variable shaft angle; and
- layout variants for complicated gears and combined mechanisms.

27

Disadvantages:
- complex production and assembly technology of bevel gears; and
- higher axial and moment loads on shafts, especially due to cantilevered position of gears.

3 Hyperbolical – the rotation axes cross.

Advantages and disadvantages of screw gear transmissions (Fig. 1.22).
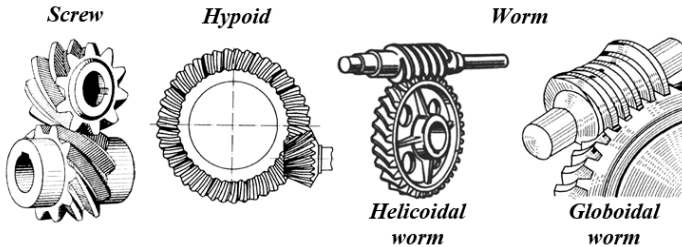
Fig. 1.22. Hyperbolical type of gear mechanisms

Advantages:
- smooth and noiseless operation;

Disadvantages:
- low efficiency; and
- increased wear and scuffing.

Advantages and disadvantages of hypoid gear transmissions.
Advantages:
- smooth and noiseless operation;

Disadvantages:
- low efficiency;
- increased wear and scuffing, and
- high requirements for accuracy in manufacture and assembly.

Advantages and disadvantages of worm gears transmissions.
Advantages:
- high values of the gear ratio;
- noiseless and smooth operation;
- increased kinematic accuracy; and
- self-braking (at low efficiency).

Disadvantages:
- low efficiency;
- increased wear and scuffing; and
- high requirements for accuracy in assembly.

> *The gear–rack transmission (<u>rack gearing</u>) is one of the transmissions where <u>rotation motion transforms into progressive motion</u>.*
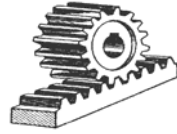
Basic theorem of planar gearing (R. Willis, 1841)

    Basic theorem of planar gearing (Willis's theorem): in gearing the base normal in the contact point of mating profiles should run through the pitch point, which position is determined by a specified relative motion of links on the common perpendicular (Fig. 1.23).

O_1, O_2 – centers of rotation of gears;
O_1-O_2 – common perpendicular;
P – pitch point;
A – point of contact of mating profiles;
n - n – base tangent;
α_W – pressure angle;
$O_1P = r_{W1}$; $O_2P = r_{W2}$ – radii of pitch circles (centroid).
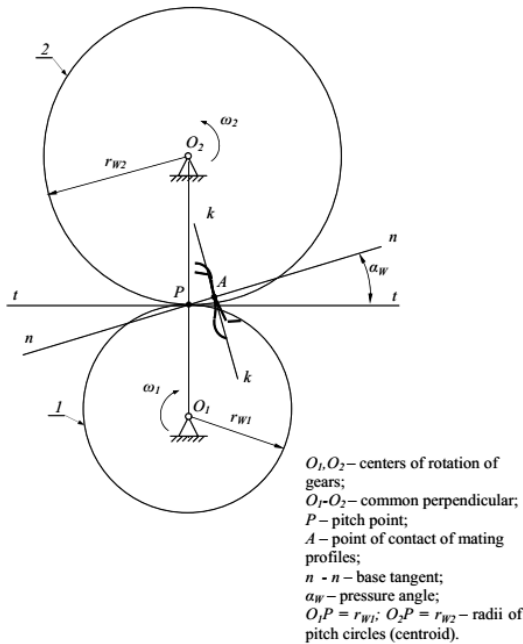
Fig. 1.23. Basic theorem of planar gearing

Consequences of the basic theorem of gearing (Willis's theorem)
- *contact ratio:*

$$i_{1-2} = \pm \frac{\omega_1}{\omega_2} = \pm \frac{O_2P}{O_1P} = \pm \frac{r_{w2}}{r_{w1}},$$

- *gear ratio:*

$$u_{1-2} = \frac{r_{w2}}{r_{w1}} = \frac{p_W \cdot z_2 / (2\pi)}{p_W \cdot z_1 / (2\pi)} = \frac{z_2}{z_1} = |i_{12}|,$$

where p_W is the gear pitch along pitch circles;

z_1, z_2 the number of teeth of a pinion and a wheel.

Gear ratio of simple gearing:

$$u = \frac{z_\kappa}{z_{ui}} \geq 1,$$

where z_k, z_{ui} are the number of teeth of a wheel and a pinion.

The condition $i_{1-2} = const$ is provided by the form (*configuration*) of mating profiles.

By side tooth profile there are:

❖ *involute gearing* (proposed by Leonhard Euler): The side tooth profile is described with an involute;

Advantages and disadvantages of involute gearing.

Advantages:

- insensibility to a change in the center distance; and
- easy in manufacture.

Disadvantages:

- low contact and bending resistance,
- undercuting of dedendums in rolling manufacture, and
- increased wear of teeth in the moment of approach and recess actions.

❖ *circular gearing* (*Novikov's gearing,* Fig. 1.24): The tooth side profile is described with a circular arc. Besides, one wheel has convex teeth, and the other wheel has concave teeth;

Advantages and disadvantages of Novikov's gearing.

Advantages:

✓ higher loading capacity by contact stability (about 1.5…1.7 times higher than that of a similar one by size and material of involute helical gearing).

Disadvantages:

✓ higher sensitivity to change in the center distance; and

✓ comparatively compound basic rack profile.

❖ *cycloid gearing:* The side tooth profile is described with a cycloid.

Advantages and disadvantages of cycloid gearing.

Advantages:
- ✓ lower wear of tooth profiles (in comparison with involute gearing);
- ✓ higher contact ratio than that in similar involute gearing; and
- ✓ lower velocity of tooth profile slip.

Disadvantages:
- ✓ more compound profile of the cutting tool;
- ✓ high production cost; and
- ✓ sensibility to assembly defects in terms of the center distance.

Fig. 1.24. Novikov's gearing

Involute and its properties

Involute is the curve generated by a point which rolls along the base circle without slip (Fig. 1.25).
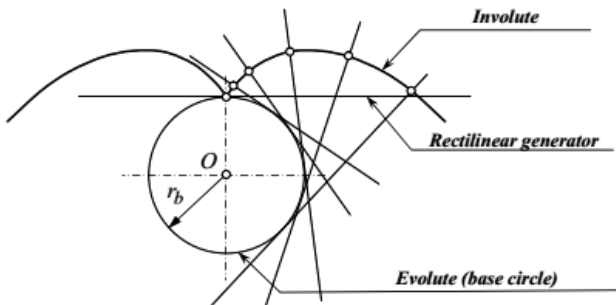
Fig. 1.25. Involute

Basic features of an involute:
- • rectilinear generator is always normal to the involute;
- • involute is a curve without bends;
- • involute shape depends only on the radius of the base circle;

- involute starts on the base circle and always locates beyond its limits;
- radius of curvature in the involute origin (on the base circle) is equal to zero.

Roll angle of an involute (Fig. 1.26):

$$v = \angle KOA = \frac{\cup KA}{r_b},$$

Considering that

$$\cup KA = AM$$

and

$$AM = r_b \cdot tg\,\alpha,$$
$$v = tg\,\alpha,$$

where α is the pressure angle of an involute.
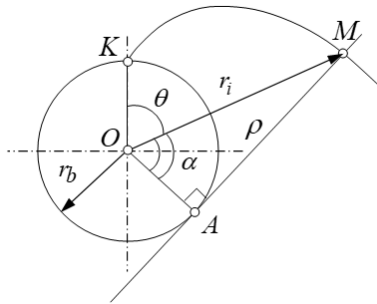
Fig 1.26. Roll angle of an involute

Radius of curvature of an involute:

$$\rho = AM = r_b \cdot tg\,\alpha.$$

Current radius vector of an involute point:

$$r_i = OM = \frac{r_b}{cos\,\alpha}.$$

Involute polar angle:

$$\theta = v - \alpha = tg\alpha - \alpha = inv\alpha \text{,}$$

where *invα* is the involute of angle α.

Geometric calculation of standard gearing (Fig. 1.27)
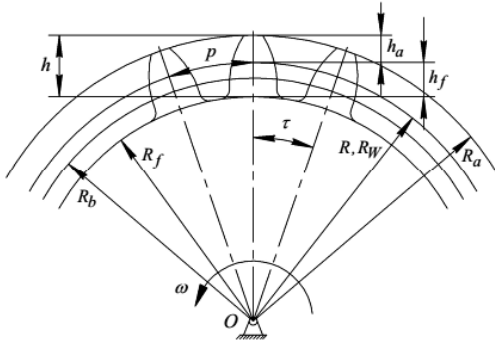
Fig. 1.27. Geometric calculation of standard gearing

- r_i is the radius of a pitch line:

$$r_i = \frac{m \cdot z_i}{2},$$

where *m* is the tooth modulus (*mm*), $m = \frac{p}{\pi}$ where *p* is the circular reference

pitch.

- r_{bi} is the radius of the base circle: $r_{bi} = r_i \cdot cos\,\alpha_0$,

where α₀ is the angle of the basic rack profile of a cutting tool ($\alpha_0 = 20^0$).

- r_{Wi} is the radius of the pitch circle: $r_{Wi} = r_i$.
- r_{ai} is the radius of the top circle: $r_{ai} = r_i + h_a$,

where h_a is the addendum, $h_a = h_a^* \cdot m$,

h_a^* is the addendum coefficient ($h_a^* = 1$).

- r_{fi} is the radius of the dedendum circle: $r_{fi} = r_i - h_f$,

33

where h_f is the dedendum, $h_f = h_f^* \cdot m$,

h_f^* is the dedendum coefficient ($h_f^* = 1.25$).

- α_w is the pressure angle: $\alpha_w = \alpha_0$.
- h is the tooth depth: $h = (2 \cdot h_a^* + c^*)m$ or $h_i = r_{ai} - r_{fi}$

where c* is the dedendum clearance coefficient ($c^* = 0.25$).

- c is the dedendum clearance: $c = c^* \cdot m$.
- τ_i is the tooth pitch angle: $\tau_i = \dfrac{360^\circ}{z_i}$.

- a_w is the center distance (distance $O_1 O_2$):
$a_W = a = \dfrac{m \cdot z_\Sigma}{2}$, where a is the reference center distance,

z_Σ is the total number of teeth of a pinion (Z_1) and a wheel (Z_2),

$$z_\Sigma = z_1 + z_2.$$

Basic elements of the involute gearing geometry

1. Theoretical line of action $N_1 N_2$
2. Active (working) line of action $B_1 B_2$
3. Active tooth profiles *are profile sections contacting in gearing.*
4. Initial arc of action *CD* and overlap angle φ_α

QUALITY RAITINGS OF GEAR TRANSMISSIONS

1) The overlap ratio ε considers continuity and smoothness of gearing, and shows the number of tooth pairs simultaneously in action (Fig. 1.28).

$$\varepsilon = \frac{\varphi_{\alpha 1,2}}{\tau_{1,2}} = \frac{\cup cd}{p_W}.$$

$$\varepsilon \geq [\varepsilon] = 1.1; \qquad \varepsilon \to \varepsilon_{max}$$
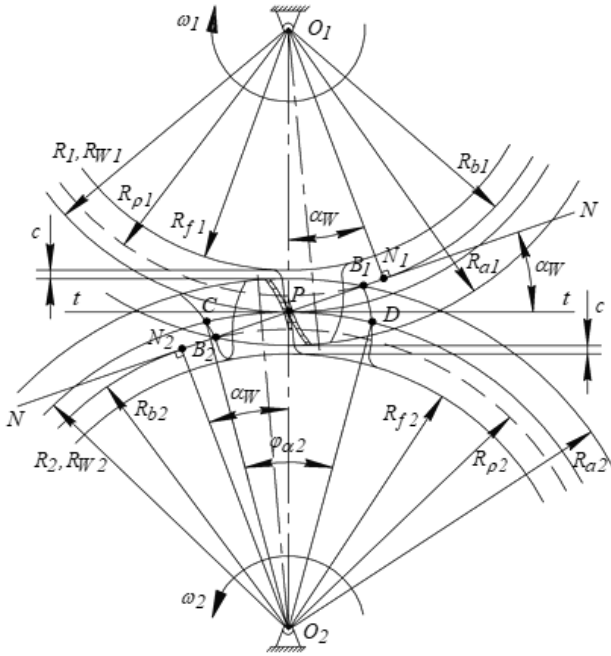
Fig. 1.28. Geometric calculation of the overlap ratio

2) Coefficients of specific sliding λ_1, λ_2 evaluate the intensity of tooth wear (Fig. 1.29).

$$\lambda_1 = 1 + i_{2-1} - \frac{W}{x} \cdot i_{2-1} \ ;$$

$$\lambda_2 = 1 + i_{1-2} - \frac{W}{W - x} \cdot i_{1-2} \ .$$

Dedendums suffer more from wear than addendums.

3) The coefficient of specific pressure υ characterizes the contact strength of a tooth.

$$\upsilon = \frac{m}{\rho} \ ,$$

35

where ρ is the reduced radius of curvature of involute profiles in a contact point,

$$\rho = \frac{\rho_1 \cdot \rho_2}{\rho_1 \pm \rho_2}.$$
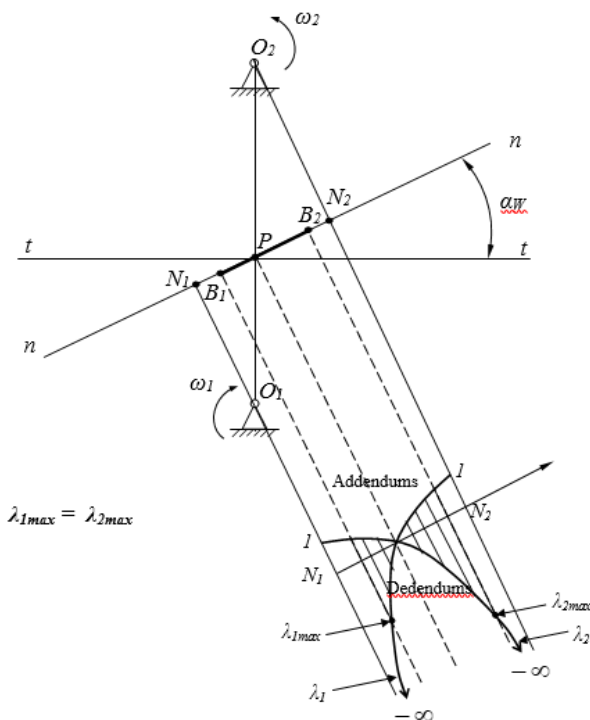
Fig. 1.29. Diagrams of specific sliding

4) The coefficients of the tooth shape Y_{F1}, Y_{F2} evaluate the bending resistance of teeth.

Tooth gears are made of steel, cast iron and plastics.

- *Steel* is used to manufacture tooth gears for high-loaded transmissions.
- *Cast iron* is used to manufacture large-capacity low-speed wheels, and also for open tooth transmissions.

- *Plastic* is used to manufacture wheels for low-capacity and kinematic transmissions.

Modern methods in gear manufacturing

Coping method is based on the fact that the configuration of a cutting tool surface corresponds to the root form between two adjacent teeth. Cutting tool is disk and involute end mills (Fig. 1.30).
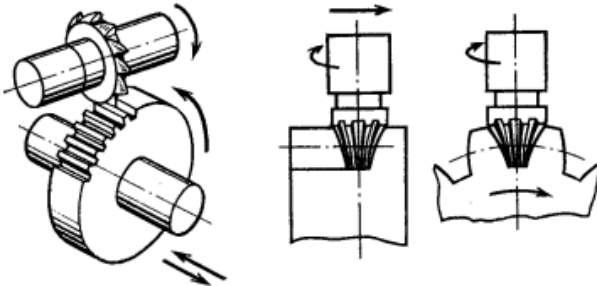
Fig. 1.30. Cutting tool for the coping method

Advantages of the method:
  1) possibility to cut teeth with general milling equipment.
Disadvantages of the method:
  1) need to have a number of cutting tools (for various combination of m, z),
  2) low efficiency, and
  3) poor quality of the tooth surface.
Rolling method realizes the machine gearing: the surface of tool tips (*generating flat*) and the cutting tooth surface have the same relative motion as the tooth links in gearing.
Cutting tools are gear cutters, rack-type tools, hob gears.
Advantages of the method:
  1) high quality of the tooth surface, accuracy of manufacture,
  2) possibility to use one tool to cut involute wheels with different number of teeth, and
  3) high efficiency.
Disadvantages of the method:
  1) high labor capacity of the technological process.
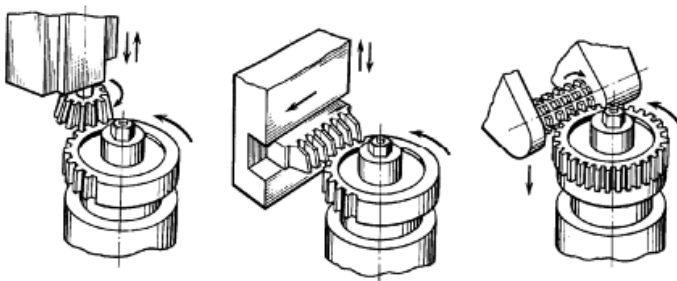
Fig. 1.31. Cutting tool for the rolling method

Cutting tool is shaped on the basis of the basic rack profile.

Basic rack profile is characterized:
- pressure angle of the basic rack profile is $\alpha_0=20^0$,
- coefficient of addendum $h_a^*=1$,
- coefficient of dedendum clearance $c^*=0.25$,
- radius of the fittet curve at the dedendum $\rho=0.4m$.

The following should be considered in choosing the basic rack profile:
- increased angle α_0 causes a higher loading capacity, but intensifies the danger of teeth pointing (Fig. 1.32);
- increased angle α_0 and decreased coefficient h_a^* cause lower relative slip, and, therefore, teeth wear;
- a decrease of angle α_0 accompanies an increase of overlap ratio ε;
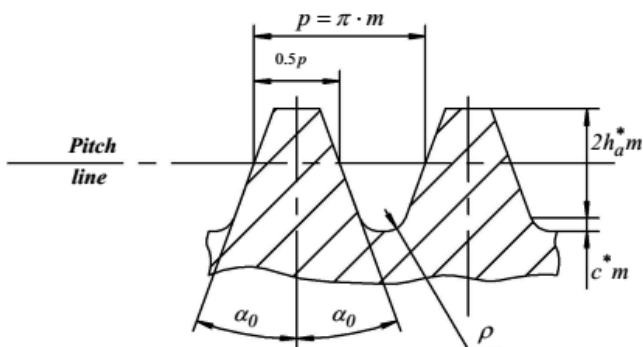
Fig. 1.32. Increased the pressure angle of the basic rack profile

- increased h_a^* leads to increased contact ratio ε, better smooth operation and increased contact strength;
- decreased h_a^* lessens the danger of a tooth undercut.

Tooth undercut in gear manufacturing

- for gear cutters (Fig. 1.33)

$$z_{min} = \frac{4 \cdot h_a^*}{(2 - i_{2-1}) \cdot sin^2 \alpha_0},$$

where $i_{2-1} = \omega_2 / \omega_1$; $h_a^* = 1.0$; $\alpha_0 = 20^0$.

1) $z_1 > z_{min}$ **2)** $z_1' < z_{min}$

Fig. 1.33. Tooth undercut in gear cutters manufacturing

- for rack-type tool ($i_{2-1} = 0$)

$$z_{min} = \frac{2 \cdot h_a^*}{sin^2 \alpha_0} \quad \Rightarrow \quad z_{min} = 17.$$

Displacement of cutting tools in gear manufacture (Fig. 1.34)

Absolute displacement of a gear cutting tool: $l = m \cdot x$,
where x is the coefficient of displacement.
Types of gears:

Zero: $l = 0 : x = 0$.
Positive: $l > 0, x > 0$.
Negative: $l < 0, x < 0$.
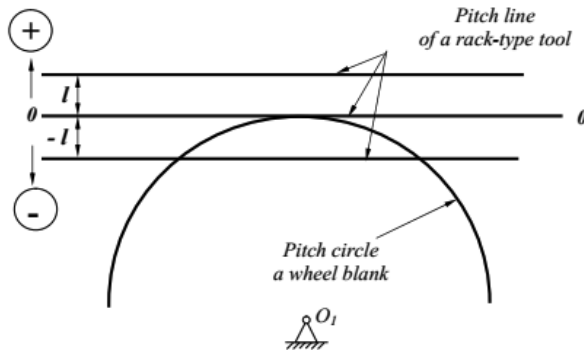
Fig. 1.34. Displacement of cutting tools

Systems for selection of coefficients of displacement

1 GOST 16532 – 70.

2 Kudriavtsev's system is the choice of x_1 and x_2 by condition of the least specific pressures v.

3 The system of the Central Design Bureau of Reducer Production (ЦКБР) is the choice of x_1 and x_2 by equalizing the maximum specific sliding at dedendums $\lambda_{1max} = \lambda_{2max}$.

4 The system of limiting contours is the choice of x_1 and x_2 with complex consideration of most requirements for the gear design.

Types of gear transmissions
(according to given coefficients of displacement)

1 Zero gear transmission - $x_1 = x_2 = 0$.

Center distance $\quad a_W = a = \dfrac{m \cdot (z_1 + z_2)}{2};$

Pressure angle $\alpha_W = \alpha_0 = 20^0$.

2 Equidisplaced gear transmission - $x_1 = -x_2$, $x_\Sigma = x_1 + x_2 = 0$.

Center distance $\quad a_W = a = \dfrac{m \cdot (z_1 + z_2)}{2};$

Pressure angle $\alpha_W = \alpha_0 = 20^0$.

3 Positive gear transmissions $x_\Sigma = x_1 + x_2 > 0$.

40

Center distance $a_W > a = \dfrac{m \cdot (z_1 + z_2)}{2}$;

Pressure angle $\alpha_W > \alpha_0 = 20^0$.

4 Negative gear transmission $x_\Sigma = x_1 + x_2 < 0.$

Center distance $a_W < a = \dfrac{m \cdot (z_1 + z_2)}{2}$;

Pressure angle $\alpha_W < \alpha_0 = 20^0$.

1.7. Polyarticular mechanisms

When there is a need to realize greater values of a gear ratio, compound (polyarticular) gear mechanisms are used. They are divided into two basic types:

1) with fixed axes:
- ordinary, and
- stepped.

2) with movable axes:
- with two or more degrees of freedom ($W \geq 2$) – differentials, and
- with one degree of freedom ($W = 1$) – planetary.

1. Kinematic analysis of a polyarticular mechanism with fixed rotation axes.

The general formula to determine values and a sign of the gear ratio of such polyarticular mechanisms:

$$i_{1-n} = \underbrace{(-1)^k}_{Sign} \cdot \underbrace{i_{1-2} \cdot i_{2-3} \cdot i_{3-4} \cdot \ldots \cdot i_{(n-1)-n}}_{Value},$$

where $i_{1-2}, i_{2-3}, \ldots, i_{(n-1)-n}$ are the gear ratios of levels of a polyarticular

mechanism;

k is the number of levels of external gearing.

For an ordinary gear mechanism (Fig. 1.35)

$$i_{1-3} = i_{1-2} \cdot i_{2-3} = \left(-\frac{z_2}{z_1} \right) \cdot \left(-\frac{z_3}{z_2} \right) = \frac{z_3}{z_1},$$

$$i_{1-j} = (-1)^k \cdot \frac{z_j}{z_1}.$$

Intermediate gears, which do not influence the value of the total gear ratio, are called idle gears (idlers).

For a stepped gear mechanism (Fig. 1.35)

$$i_{1-6} = i_{1-2} \cdot i_{3-4} \cdot i_{5-6} = \left(-\frac{z_2}{z_1}\right) \cdot \left(-\frac{z_4}{z_3}\right) \cdot \left(-\frac{z_6}{z_5}\right).$$

$$i_{1-j} = (-1)^k \cdot \frac{\prod z_{out}}{\prod z_{in}}.$$
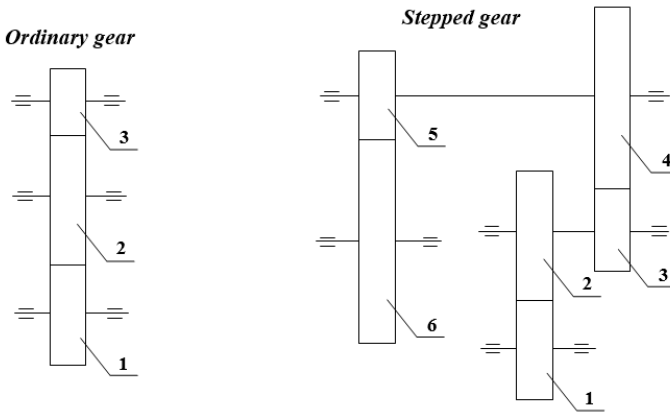
Fig. 1.35. Ordinary and stepped gear mechanisms

2. Kinematic analysis of a polyarticular mechanism with movable rotation axes.

Differential mechanisms

Degree of freedom of a mechanism

$$W = 3n - 2p_5 - p_4 = 3 \cdot 3 - 2 \cdot 3 - 1 = 2.$$

By applying the method of reversibility (*inversion*) of motion (Fig. 1.36): *all links of a mechanism receive an additional angular velocity relative to axis O_H which is equal to ω_H of carrier H by value, but oppositely directed,* we can obtain values of angular velocities for

42

- gear 1: $\omega_1^{(H)} = \omega_1 - \omega_H$;
- gear 2: $\omega_2^{(H)} = \omega_2 - \omega_H$;
- carrier H: $\omega_H - \omega_H = 0$.
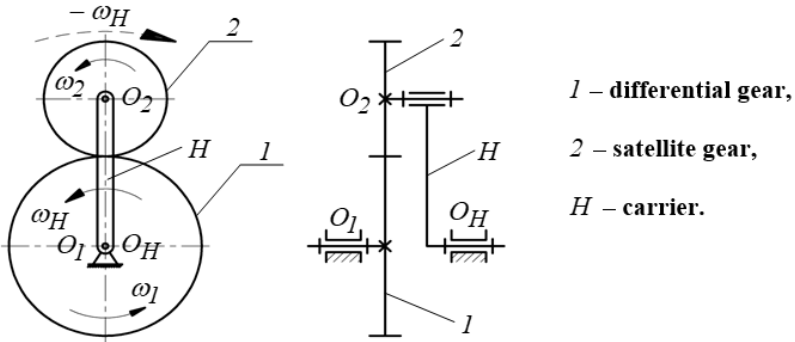
Fig. 1.36. Inversion of motion with the differential mechanisms

1 – differential gear,

2 – satellite gear,

H – carrier.
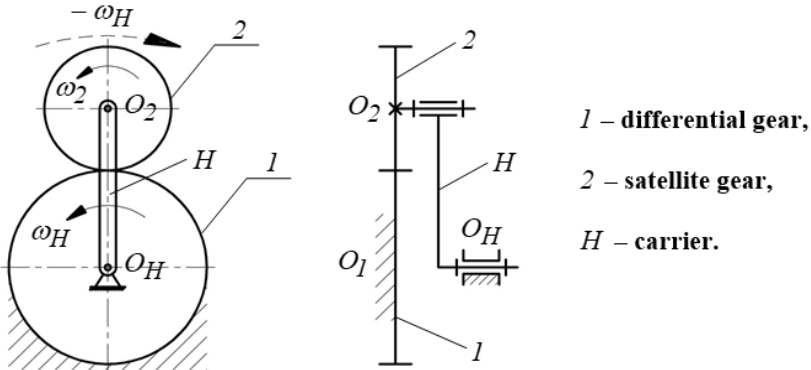
Fig. 1.37. Inversion of motion with the planetary mechanisms

1 – differential gear,

2 – satellite gear,

H – carrier.

The gear ratio of a differential mechanism (the Willis formula)

$$i_{1-2}^{(H)} = \frac{\omega_1^{(H)}}{\omega_2^{(H)}} = \frac{\omega_1 - \omega_H}{\omega_2 - \omega_H} = -\frac{z_2}{z_1}.$$

Planetary mechanisms (Fig. 1.36)

Degree of freedom of a mechanism

$$W = 3n - 2p_5 - p_4 = 3 \cdot 2 - 2 \cdot 2 - 1 = 1 \cdot$$

Gear ratio of a planetary mechanism (the Willis formula), at $\omega_1 = 0$.

$$i_{1-2}^{(H)} = \frac{-\omega_H}{\omega_2 - \omega_H} = -\frac{z_2}{z_1} \cdot$$

1.8. Cam mechanisms

CAM MECHANISMS (Fig. 1.38) are the mechanisms with intermittent motion of an output link which include a higher kinematic pair, one element of which is formed with a surface of variable curvature (Fig. 1.39-1.40).

0 – pole;
1 – cam (*input link*);
2 – follower (*output link*);
3 – roller;
r_0 – radius of working profile.

Cam lobe

Degree of freedom (*by Chebyshev's formula*): $n = 3$, $p_5 = 3$, $p_4 = 1$

$W = 3n - 2p_5 - p_4 = 3 \cdot 3 - 2 \cdot 3 - 1 = 2$.

Cam heel
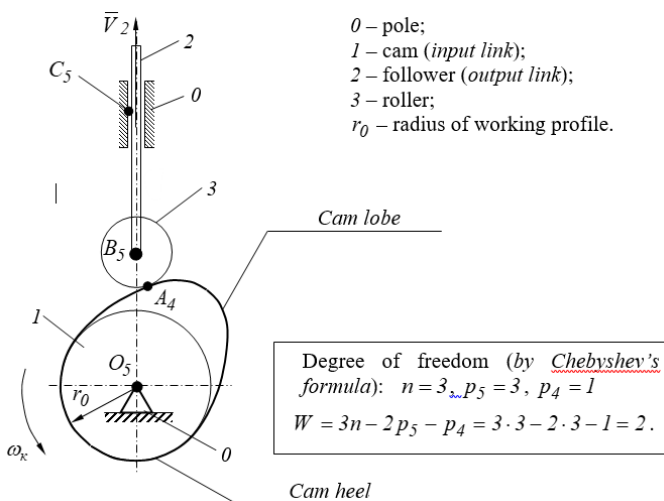
Fig. 1.38. Cam mechanisms

Cam is the link with an element of the higher kinematic pair, which is formed with a surface of variable curvature (Fig. 1.41).

Advantages of cam mechanisms:
- Possibility to provide a complicated and theoretically accurate law of motion for a follower.

44

- Portability.
- Possibility to transmit considerable efforts.
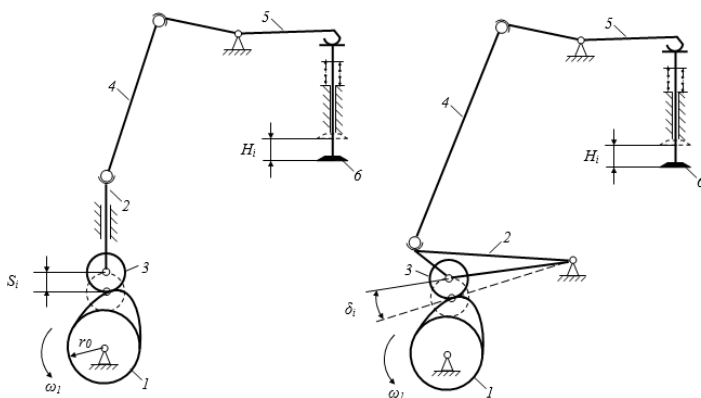
Fig. 1.39. Kinematic schemes of cam mechanisms in gas distribution systems
of diesel locomotive engines:
1 - cam; *2* – follower; 3 – cam roller; 4 – rod; 5 – lever;
6 – valve with a valve spring set
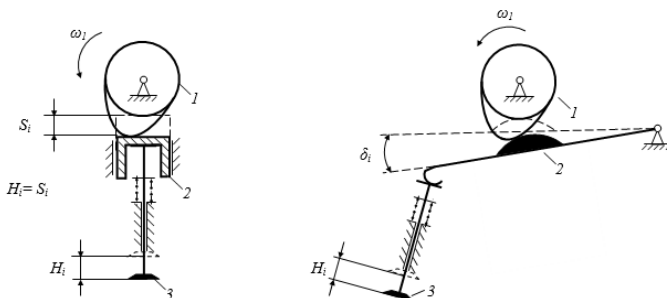
Fig. 1.40. Kinematic schemes of cam mechanisms in gas distribution systems
of high-speed engines:
1 – cam; 2 – follower; 3 – valve with a valve spring set

Disadvantages of cam mechanisms (needed to be considered in design):
- Complicated cam manufacturing technology.
- Necessity to organize closure in a higher kinematic pair.
- Considerable specific loads in elements of a higher kinematic pair
  (a need for materials of high mechanical characteristics).

1) Cam – rotation motion.
Follower – progressive motion.
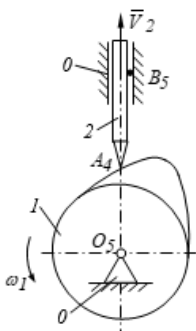
2) Cam and follower – rotation motion.
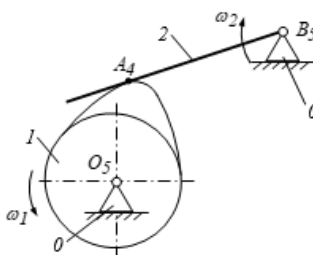
3) Cam and follower – progressive motion.
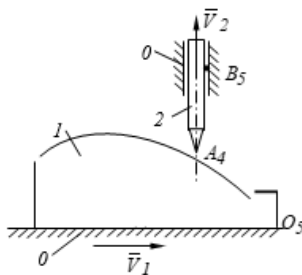
4) Cam – progressive motion.
Follower - rotation moment.
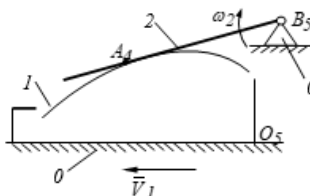
Fig. 1.41. Classification of planar cam mechanisms by type relative to the motion of cam and follower

Cam mechanism with a knife follower (*the element of a kinematic pair is a point*): used at low velocities to transfer low loads due to decreased wear resistance of elements of a higher kinematic pair (Fig. 1.42).

Cam mechanisms with a flat and spherical follower (*the element of a kinematic pair is a line*): have high load capacity, but in transfer of considerable loads their work can accompany intensive wear of the contact surfaces due to sliding friction in the higher kinematic pair "*cam-follower*".

In order to eliminate sliding friction in a higher kinematic pair, an intermediate link, a roller, which forms a rotating class V kinematic pair with the follower, is introduced into the structure of the kinematic pair.
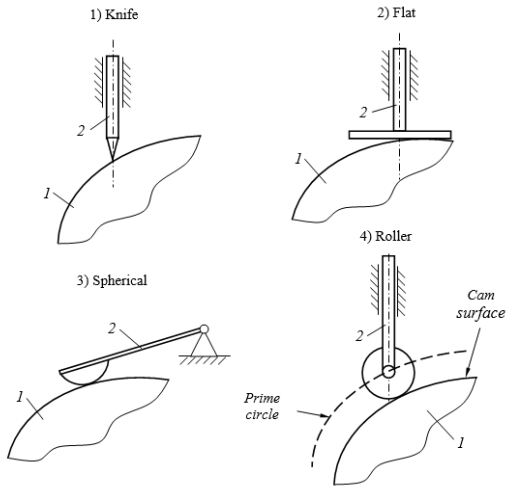
Fig. 1.42. Types of followers

Types of closures in cam mechanisms (Fig. 1.43)
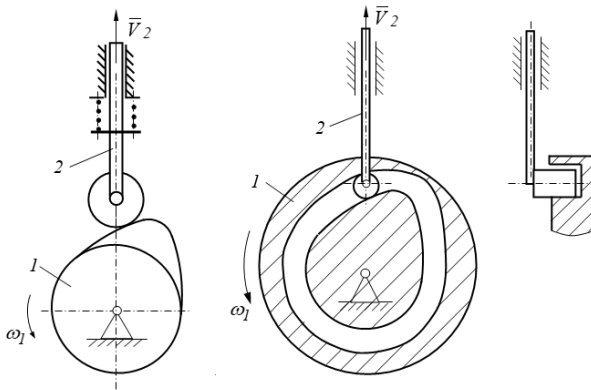
Fig. 1.43. Different types of closures in cam mechanisms

Disadvantages of force closure with a spring:
- elastic force of spring F_{sp} creates additional loads on links of a cam mechanism;

47

- rotating speed of the cam ω_1 is limited by values of the inertia forces $F_{in\,2}$ tending to break the contact in a higher kinematic pair, conditioned by negative accelerations of the follower ($\alpha_2 < 0$). In order to provide closure at any position of a cam, the following condition should be fulfilled: $F_{np} + F_{uh2} > 0$;

- slight displacement of the spring at the maximum pressure determines the corresponding limits of the maximum displacement of the follower.

Efficiency of a cam mechanism with geometric closure is provided by a fixed gap between a roller and one or the other slot side. But, in operation, the inertia forces influencing the follower can change and cause deformation of the slot and increase of the gaps. It may cause failures with the follower, and the required laws of motion will not be followed.

Phases in motion of a follower (Fig. 1.44)
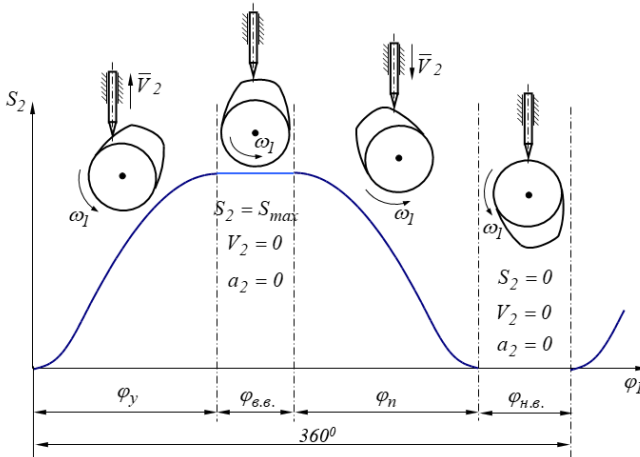
Fig. 1.44. Phases in motion of a follower

Phase angles:
φ_y is the distance angle; $\varphi_{в.в.}$ is the upper dwell angle;
φ_n is the angle of approach; $\varphi_{н.в.}$ is the lower dwell angle.

48

Consideration of pressure angles in the cam mechanism design

$$\overline{F}_n = \overline{F}_B + \overline{F}_\Gamma, \qquad F_B = F_n \cdot cos\,\beta,$$

$$F_\Gamma = F_n \cdot sin\,\beta \cdot$$

Pressure angle β of the cam on the follower is equal to the angle between normal *n-n* to the working or theoretical profile of the cam and the linear velocity vector of the follower (Fig. 1.45):

$$\beta_{max} = \frac{V_{q2max}}{R_0 + S_2}.$$

The higher *β* is, the greater the follower is pressed to the guides, and the higher the friction in them is, as well as the wear. And an increase in the friction force leads to a needed increase in driving force $F_{\partial e}$, thus increasing torsion and contact stresses in links of a mechanism.
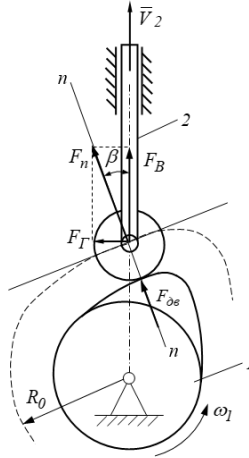
Fig. 1.45. Consideration of pressure angle β in the cam mechanism design

When *β* is high, the friction force increases to the value when the follower scuffs in the guides and stops despite an increase of the moving force, and the mechanism cannot operate. The pressure angle at which scuffing occurs is called the decalage.

When the pressure angle increases, the sizes of a mechanism decreases due to decreased sizes of its links.

1. For a cam mechanism with progressing roller followers (Fig. 1.46)

$$[\beta_{max}] = 30^0.$$
Design condition: $\beta_{max} \leq 30^0$.

2. For a cam mechanism with spherical roller followers

$$[\beta_{max}] = 45^0.$$
Design condition: $\beta_{max} \leq 45^0$.

3. In a cam mechanism with flat followers pressure angles $\beta = 0$.

Impacts in cam mechanisms

Impacts in cam mechanisms are momentary changes of values and directions of inertia forces due to corresponding changes in accelerations of the follower $\overline{F}_{uH} = -m \cdot \overline{a}$.

Fig. 1.46. Limits of maximum pressure angles in the cam mechanism design

According to the character of changes in accelerations of a follower per cycle the following working conditions of cam mechanisms are distinguished:

- work of a cam mechanism with "rigid impacts" (Fig. 1.47.a): presence in the cycle of the cam mechanism an instant change of the follower's acceleration by an infinite value, which can cause opening a higher kinematic pair formed by the follower and the cam, as well as their collision. Therefore, such cam mechanisms can operate only at low rotation frequencies of a cam $n_1 \leq 50$ *rev/min.*

- work of cam mechanisms with "soft impacts": presence in the cycle of cam mechanisms an instant change in the follower's accelerations by a finite value (Fig. 1.47.b). Besides, work with soft impacts corresponds to changes in accelerations of the follower by a cosine curve (Fig. 1.47.c) [1, 24]. For such cams $n_1 \leq 1200$ *rev/min;*

- non-impact character of work of cams is characterized by absence of instant changes in accelerations of the follower per cycle. The example of such mechanisms is cams in which acceleration of the follower is changed by trapezoidal (Fig. 1.47.d) and sinusoidal (Fig. 1.47.e) curve.

Fig. 1.47. Different working conditions of cam mechanisms

1.9. Dynamic analysis of mechanisms

Dynamics of mechanisms: The forces applied to the mechanism links are prescribed and the law of motion for the initial link should be determined [30].

The basic task of dynamic analysis of a mechanism is determination of actual law of motion of their links (*considering the masses and inertia moments of all links of a mechanism, as well as all forces and couples of forces applied to its links*) [12, 44]. In order to facilitate the tasks of dynamic analysis, actual mechanisms are replaced with *dynamic models* of the same inertia and force characteristics like the mechanism to be replaced.

For example (Fig.1.48): the initial link of a rotary-type mechanism, the inertia properties of which are equivalent to those of the whole mechanism (characterized by a reduced inertia moment J_{np}), which undergoes the loads equivalent to all forces and couples of forces applied to its links (characterized by a reduced moment of forces M_{np}) is taken as a dynamic model of the mechanism.

For determination of parameters of this dynamic model (reduced moment of forces M_{np} and reduced inertia moment J_{np}) the methods of reduced forces and reduced masses are used.

The mechanism link to which a reduced force (*a reduced moment*) is applied is called *the reduction link*, and its point of application is the reference point. As a rule, the initial link of a mechanism is taken as the reduction link.
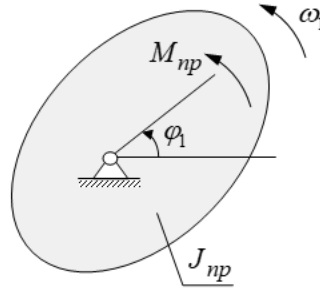
Fig. 1.48. Scheme
of the dynamic model

Reduction of forces is based on *the elementary work equivalence*, i.e. the elementary work of each force on a possible displacement of the point of application or moment on a possible angular displacement of the link, on which it is applied, should be equal to the elementary work of a reduced moment on a possible angular displacement in the dynamic model:

$$A(M_{np}) = \sum A(F_i, M_i),$$

$$M_{np} \cdot \omega_1 = \sum_{i=1}^{n}(F_i \cdot V_i \cdot cos\,\alpha_i + M_i \cdot \omega_i)$$

where $\omega_1 = \dfrac{d\varphi_1}{dt}$ is the angular velocity of a reduction link,

φ_1 is the rotation angle of a reduction link,
F_1, M_1 are the force and the moment of force applied to the *i*-th link,
$V_i = \dfrac{ds_i}{dt}$ is the speed of a point of application F_i,

ds_i is the elementary displacement of a point of application F_i,
α_i is the angle between the directions of vectors F_i and V_i,
$\omega_i = \dfrac{d\varphi_i}{dt}$ is the angular velocity of the *i*-th link,

φ_i is the rotation angle of the link to which moment M_i is applied.

$$M_{np} = \sum_{i=1}^{n}\left(\frac{F_i \cdot V_i}{\omega_1} \cdot cos\,\alpha_i + M_i \cdot \frac{\omega_i}{\omega_1}\right)$$

Reduction of masses is based on *the kinetic energy equivalence*, i.e. the kinetic energy of reduced mass m_{np} or reduced inertia moment J_{np} in corresponding positions of the mechanism should be equal to the sum of kinetic energies of all links of the mechanism.

Reduced mass m_{np} is called a conditional mass concentrated in the reference point at which the kinetic energy in this point equals to the sum of kinetic energies of all links of the mechanism.

Reduced inertia moment J_{np} is called the parameter of a dynamic model, the kinetic energy of which equals to the sum of kinetic energies of actually moving links [12].

Kinetic energy equality condition:

$$T\left(J_{np}\right) = \sum_{i=1}^{n} T\left(m_i, J_{S_i}\right),$$

$$J_{np} \cdot \frac{\omega_1^2}{2} = \sum_{i=1}^{n}\left(m_i \cdot \frac{V_{S_i}^2}{2} + J_{S_i} \cdot \frac{\omega_i^2}{2}\right),$$

where m_i is the mass of the *i*-th link,

V_{Si} is the centre-of-mass velocity (*gravity*) of the *i*-th link,

J_{Si} is the inertia moment of a link relative to the axis running through its center of mass (*gravity*),

ω_i is the angular velocity of the *i*-th link.

$$J_{np} = \sum_{i=1}^{n} m_i \cdot \left(\frac{V_{S_i}}{\omega_1}\right)^2 + \sum_{i=1}^{n} J_{S_i} \cdot \left(\frac{\omega_i}{\omega_1}\right)^2$$

As is seen from the equation, reduced masses and inertia moments depend only on ratios of speeds, which, in turn, depend on positions of a reduction link, and always take positive values.

Determination of kinetic energies:

- for progressive motion: $T = \dfrac{m \cdot V^2}{2},$

- for rotation motion: $T_i = \dfrac{J_i \cdot \omega_i^2}{2},$

Where J_i is the inertia moment of the i-th link relative to its rotation axis,

- for plane motion:

$$T_i = \frac{m_i V_{S_i}^2}{2} + \frac{J_{S_i} \cdot \omega_i^2}{2},$$

where V_{S_i} is the speed of the center of mass of the i-th link,

J_{S_i} is the inertia moment of the i-th link relative to the axis running through the center of mass.

Equations of motion for a mechanism

In order to define the law of motion for the initial link of a mechanism, the equation of motion written in energy or differential form is used.

The basis for composing the equation of motion for a mechanism is the kinetic energy theorem according to which a change in the kinetic energy of a mechanical system at some period equals to the sum of work of all applied forces to the system during this period of time, i.e.

$$\Delta T = \sum_{i=1}^{n} A_i \qquad T - T_0 = A_{\partial.c.} - A_{c.c.}$$

where T, T_0 are the kinetic energy of a mechanic system in the end and beginning, of the period (*displacement*) under study, respectively,

$A_{\partial.c.}$, $A_{c.c.}$ are the work of moving and resistance forces on the displacement under study.

The equation of motion of a mechanism in energy form (*energy integral*) at progressive motion of a reduction link

$$T = \frac{m_{np} \cdot V_{np}^2}{2}, \qquad T_0 = \frac{m_{np0} \cdot V_{np0}^2}{2},$$

$$\frac{m_{np} \cdot V_{np}^2}{2} - \frac{m_{np0} \cdot V_{np0}^2}{2} = A_{\partial.c.} - A_{c.c.},$$

where m_{np}, m_{np0} are the reduced masses of a mechanism at the end and beginning of the given period (*displacement*) under study, respectively,

V_{np}, V_{np0} the velocities of the reference point in the end and beginning of the period (*displacement*) under study, respectively,

The equation of motion of a mechanism in energy form (*energy integral*) at rotation moment of a reduction link

$$T = \frac{J_{np} \cdot \omega^2}{2}, \qquad T_0 = \frac{J_{np0} \cdot \omega_0^2}{2},$$

$$\frac{J_{np} \cdot \omega^2}{2} - \frac{J_{np0} \cdot \omega_0^2}{2} = A_{\partial.c.} - A_{c.c.},$$

where J_{np}, J_{np0} are the reduced inertia moments of a mechanism in the end and beginning of the period (*displacement*) under study, respectively,

ω, ω_0 are angular speeds of a reduction link in the end and beginning of the period (*displacement*) under study, respectively,
Considering that

$$\sum_{i=1}^{n} A_i = \int_{\varphi_0}^{\varphi} M_{np} d\varphi$$

previous equation is written as follows

$$\frac{J_{np} \cdot \omega^2}{2} - \frac{J_{np0} \cdot \omega_0^2}{2} = \int_{\varphi_0}^{\varphi} M_{np} d\varphi,$$

where φ is the generalized coordinate (*the rotation angle of a reduction link*),
φ_0 is the value of angle φ in the beginning of motion,
$M_{np} = M_{np\,\partial.c.} - M_{np\,c.c.}$ is the reduced moment presented as a

difference between reduced moments of moving and resistance forces.
The equation of motion of a mechanism in differential form is obtained by differentiating equation by coordinate φ

$$d\left(\frac{J_{np} \cdot \omega^2}{2}\right) = M_{np} d\varphi \ , \qquad \frac{d}{d\varphi}\left(\frac{J_{np} \cdot \omega^2}{2}\right) = M_{np} \ .$$

Let us determine the derivative in the left part of equation (ω and J_{np} are variable values)

$$\boxed{\dfrac{d\varphi}{dt}}$$

$$\Uparrow$$

$$\frac{d}{d\varphi}\left(\frac{J_{np}\cdot\omega^2}{2}\right)=J_{np}\cdot\omega\cdot\frac{d\omega}{d\varphi}+\frac{\omega^2}{2}\cdot\frac{dJ_{np}}{d\varphi}=J_{np}\cdot\frac{d\omega}{dt}+\frac{1}{2}\cdot\frac{dJ_{np}}{d\varphi}\cdot\omega^2$$

whence

$$J_{np}\cdot\frac{d\omega}{dt}+\frac{1}{2}\cdot\frac{dJ_{np}}{d\varphi}\cdot\omega^2=M_{np}$$

is the equation of motion in differential form.

1.10. Basic periods in the motion of machines (Fig. 1.43)
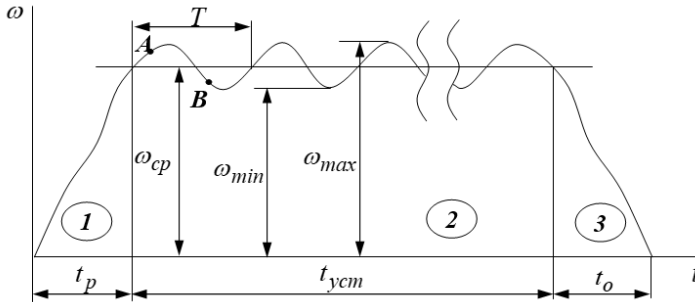
Fig. 1.43. Periods in the motion of machines

I period: machine acceleration during a machine acceleration t_P the velocity of travel of the initial link increases from zero to average value ω_{cp}

$$A_{\mathcal{A}}>A_C,\quad A_C=A_{\Pi.C.}+A_{B.C.},$$

where $A_{\mathcal{A}}$ is the work of driving forces,

A_C is the work of resistance forces,

$A_{\Pi.C.}$, $A_{B.C.}$ is the work of useful and parasite resistance forces.

The surplus of $A_{\mathcal{A}}$ over A_C is consumed by an increase in the kinetic energy of a machine.

In order to reduce the start-up time of a machine useful load $A_{П.C.} = 0$, should be eliminated, and the motion of a machine without useful load is called the idle run.

II period: steady motion the basic stage of motion (time t_{ycm}).

The initial link velocity (of the mainshaft of the machine motion ω) changes periodically (during the period of cycle change T).

Causes of periodical vibrations of speed ω are periodical changes in the forces applied to the links of a mechanism.

Per cycle $\omega - A_{ΣД} = A_{ΣC}$.

Inside the cycle ω:
- including A: $\quad A_Д > A_C \Rightarrow \omega \rightarrow \omega_{max}$ the accelerated motion of a machine,
- including B: $\quad A_Д < A_C \Rightarrow \omega \rightarrow \omega_{min}$ the decelerated motion of a machine,

III period: machine lockup (run-out) for time t_0. At this stage the work of driving forces is $A_Д = 0$, and the stored energy goes to overcome the work of resistance forces.

In practice, in order to reduce the lockup time of a machine the parasite resistance forces are frequently artificially increased by installing brakes.

Control of the angular speed of motion for a mechanism

Control of the angular speed of the mechanism's motion is aimed to decrease vibrations of the angular speed of the driving link to the values admitted by the requirements for the technological process.

The causes of angular speed vibrations ω:

1) Causes of short-term periodic vibrations (periodic vibrations of rotating and resistance moments conditioned are caused by working processes in the engine cylinders, the structure of the mechanism or technological processes). Here, at a steady periodically-irregular motion of the mechanism, the angular speed of its driving link is controlled with the flywheel of high inertia moment.

2) Causes of long-term non-periodic vibrations do not depend on the structure of the mechanism (for example, an increase or a decrease in the useful load for a long period). In this case for non-periodic long-term disballances in forces special regulating devices (regulators) are used.

Coefficient of irregular motion of a machine

The intensity of periodic vibrations of the angular speed at a steady-state motion is evaluated by *the coefficient of irregular motion δ*

$$\delta = \frac{\omega_{max} - \omega_{min}}{\omega_{cp}}, \quad \text{where } \omega_{cp} = \frac{\omega_{max} + \omega_{min}}{2}.$$

Negative consequences of periodic vibrations of the angular speed at a steady-state motion:
1. Disfunction of the working process of a machine.
2. Additional dynamic loads in mechanisms.

Limitation of the coefficient of irregular motion δ for some machines:
1. Turbo generators $\delta \leq 1/200$.
2. AC electro generators $\delta = 1/200....1/300$.
3. Internal combustion engines $\delta = 1/80....1/100$.
4. Compressors $\delta = 1/50....1/100$.
5. Pumps $\delta = 1/5....1/30$.

Regulation of periodic vibrations of the angular speed at steady-state motion

Equation of motion in energy form for the rotor *dynamic model*

$$\frac{J_{\Pi P\kappa} \cdot \omega_\kappa^2}{2} - \frac{J_{\Pi P\mu} \cdot \omega_\mu^2}{2} = \int\limits_{\varphi_H}^{\varphi_K}(M_{\Pi P\partial} - M_{\Pi Pc})\,d\varphi = A_\Sigma.$$

Basic assumptions:

$$J_{\Pi P\kappa} = J_{\Pi P\mu} = J_{\Pi P}. \quad \omega_\mu = \omega_{min}; \quad \omega_\kappa = \omega_{max}.$$

From equation: $\quad J_{\Pi P}\dfrac{(\omega_{max}^2 - \omega_{min}^2)}{2} = A_\Sigma.$

$$J_{\Pi P}\frac{(\omega_{max} + \omega_{min})}{2} \cdot \frac{(\omega_{max} - \omega_{min}) \cdot \omega_{cp}}{\omega_{cp}} = A_\Sigma$$

$$J_{\Pi P} \cdot \delta \cdot \omega_{cp}^2 = A_\Sigma.$$

$$\boxed{\delta = \frac{A_\Sigma}{J_{\Pi P} \cdot \omega_{cp}^2}}$$

$\Longrightarrow$ increase $J_{\Pi P}$ due to installation of *a flywheel*.

As far as velocity vibrations conditioned by periodic influence of forces cannot be completely eliminated, their intensity should be reduced, thus, the

coefficient of irregularity δ should be acceptably small. This can be achieved by fixation on the main shaft of a machine an additional mass (*in the form of a disc or rim with spokes*), of larger inertia moment called *the flywheel*. Its inertia moment should be equal to the value at which the irregularity of motion of the flywheel does not exceed the specified limits.

By selecting the inertia moment of the flywheel, $J_{\Pi P}$ can obtain the value at which the shaft of the reduction link rotates with an allowable degree of irregularity. The main function of a flywheel is to limit the angular speed of the main shaft of a machine within the range defined by the coefficient of irregularity δ.

Regulation of non-periodic vibrations of the angular velocity

Speed regulator is the device used to maintain a constant velocity of continuous motion or a constant average velocity of periodic motion. The speed regulator automatically eliminates the difference between values of driving forces and resistance forces (due to some reasons) in a mechanism.

Transient process is characterized by disfunction of the work balance cycle $A_{\Sigma \Pi} = A_{\Sigma C}$:

    1. $A_{\Sigma \Pi} < A_{\Sigma C}$ decreasing ω (risk of machine lockup).

    2. $A_{\Sigma \Pi} > A_{\Sigma C}$ increasing ω (risk of reaching the point of breakage for an engine).

Modern systems of automatic velocity regulation (Fig. 1.43) are used to eliminate a transient process due to direct influence on work $A_{\Sigma \Pi}$ or work $A_{\Sigma C}$.

In devices the rotation frequency (angular velocity) of working axes is stabilized through application of the brake centrifugal shaft speed governor.

1 – axis with two clutches – immovable *2* and movable *6* with brake disk *7*. Flyweights *4* are articulated to the clutches with rods *3* and *5*. Between the clutches there is compression spring *9*. When the governor shaft rotates the flyweights
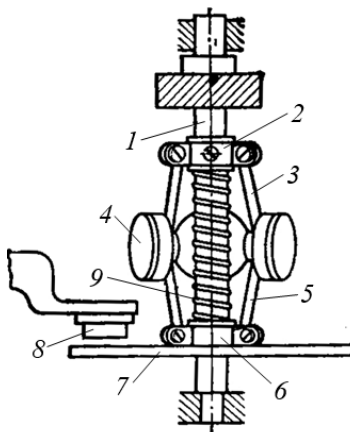
Fig. 1.43. Modern systems of automatic velocity regulation

59

go apart, and the movable clutch rises by squeezing the spring. If the angular speed of a governor exceeds the nominal speed, brake disk *7* rests against immovable stop *8* and creates a brake torque.

In energy machines the velocity of axis is regulated through direct influence on work $A_{\Sigma Д}$ by changing the intensity of power supply (*petrol, diesel fuel, etc,* Fig. 1.44).

1 - regulating object (engine);
2 - external source of non-periodic oscillations *ω* (working machine actuated by an engine);
3 – sensor;
4 – regulator.
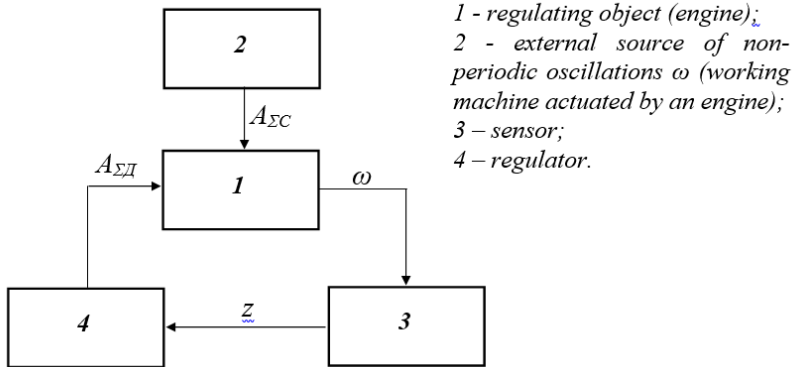
Fig. 1.44. Functional diagram of an automatic control system of closed contour

*Automatic control regulation diagram of a unit
with a centered speed governor*

The governor is actuated from the initial link of an engine with a pair of bevel gears. When the initial link of an engine rotates with angular speed ω_1 the governor rotates with angular speed $\omega_p = \omega_1/i_{1p}$, where i_{1p} is the gear ratio from the initial link to the governor. At various angular speeds ω_1 of the initial link the clutch occupies various positions. The clutch is connected with a leverage which increases or decreases the supply of driving energy (*e.g. steam or gas*) to the engine consisting of links *OR* and *RT*, and the damper. Pin *M* belonging to link *OR* slides along the guides of the clutch (Fig. 1.45).

Let us assume that due to a decrease in resistance forces in the working machine the angular speed of the governor increases. Then, the spheres under the centrifugal forces go away from the rotation axis and the clutch goes upwards. And link *RT* acts to the damper, which, while going downwards, decreases the channel section along which the working substance (*steam, gas, etc*) supply to the engine. Then, the driving forces and angular speed ω_P

decrease, and the clutch begins to go downwards, and, consequently, the damper transfers upwards by increasing the channel section. After an increase in supply of driving energy, the process can be repeated again. Thus, the work of the governor is *an oscillation process*. The governor automatically responds to a change in the angular speed of the initial link and supplies needed energy for a transfer of the regulating body.
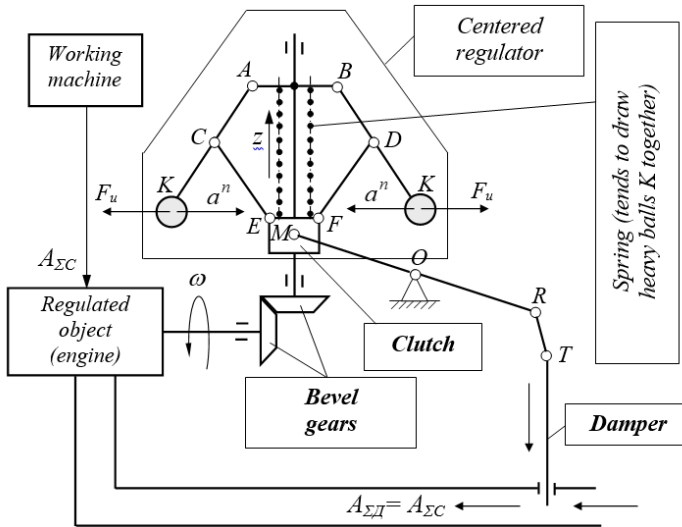
Fig. 1.45. The mechanism of the regulator

1.11. Friction in mechanisms

Friction is the resistance to a relative displacement, which emergs between two bodies on their contact surface areas (Fig. 1.46).

By kinematic features there are:

Fig. 1.46. Friction in mechanisms

- ✓ sliding friction (*type 1 friction*) emerges when one body slides along the surface of another body (*e.g. travel of piston in a cylinder*);
- ✓ rolling friction (*type 2 friction*) emerges when one body rolls on the surface of ano-ther body (*e.g. rolling of a wheel along the rail*).

61

According to lubrication between interacting surfaces there are:
- ✓ dry friction – with no lubricants,
- ✓ fluid friction – interacting surfaces are divided with a lubricant layer,
- ✓ boundary friction – interacting surfaces are divided with a very thin lubricant layer (0.1 mkm and less),
- ✓ half-floating friction – combination of dry and boundary friction,
- ✓ semi-fluid friction – combination of fluid and boundary friction.

With prevalence of dry friction (a larger part of the contact surfaces is not covered with a lubricant), the friction is considered as half-floating, and with the prevalence of fluid friction (a larger part of contact surfaces is covered with a lubricant), the friction is considered as semi-fluid.

SLIDING friction

Sliding friction is conditioned by two factors (Fig. 1.47):
- surface roughness, and
- intermolecular interaction forces between the interacting bodies.

Friction laws (by Amonton and Coulomb):

1) friction force, at other conditions being equal, does not depend on sizes of contacting surfaces.

2) maximum value of the static friction force is directly proportional to the normal pressure (*normal reaction*) of one body on the other in the moment when they begin their relative motion, i.e.

$$F_{max} = f_0 \cdot N,$$

where f_0 is the coefficient of static friction (dimensionless quantity experimentally determined and depends on the substance of interacting bodies and the condition of the surfaces: character of treatment, temperature, moisture, lubrication, etc.).

Fig. 1.47. Sliding friction

3) friction force increases with an increase of time of previous contact of the interacting surfaces.

And the modulus of friction force during motion is determined as

$$F_{mp} = f_\partial \cdot N,$$

where f_∂ is the coefficient of kinetic friction.

The dependency of fiction force on normal pressure is

$$F_{mp} = f \cdot N + A,$$

where f is the friction coefficient determined experimentally and taken as a constant (dimensionless quantity),

A is the constant which considers the intermolecular interaction forces.

$$F_{mp} = f \cdot N \quad \textit{Amonton-Coulomb's law}$$

The coefficient of sliding friction depends on:
- material,
- lubrication,
- relative velocity (its increase causes a decrease in the friction coefficient),
- specific pressure (its increase causes an increase in the friction coefficient).
- ▪ The sliding friction force emerges only with presence of a shifted force.
- ▪ The modulus of the sliding friction force for a body in equilibrium can take values not exceeding the maximum ones, i.e. the condition $F_{mp} \leq F_{max}$ should be fulfilled.
- ▪ The friction force always directs oppositely to the relative speed.
- ▪ When the velocity of motion increases, the friction force decreases.
- ▪ When a specific pressure increases, the friction force increases.
- ▪ When a period of previous contact extends, the friction force increases.

ROLLING friction

Rolling friction emerges when one body rolls over the other (Fig. 1.48).

The equation of moments of forces affecting the roller relative to point A:

$$\sum_{i=1}^{n} M_A(F) = N \cdot k - F \cdot h = 0,$$

whence $N \cdot k = F \cdot h$
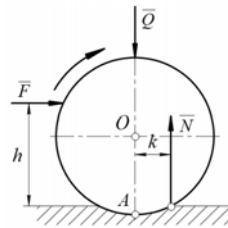
Fig. 1.48. Rolling friction

where $M_{\kappa} = N \cdot k$ is the rolling friction moment,

    k [mm, sm] is the coefficient of rolling friction,

    $F \cdot h$ is the rotary (*driving*) moment.

    Coefficient of rolling friction depends on elastic properties of materials of the interacting bodies, condition of the surfaces, and the radii of curvature.

    Force *F* which should be applied to the roller for its regular rolling on the plane is

$$F = \frac{k}{h} \cdot Q.$$

where $\dfrac{k}{h} = f'$ is the reduced (conditional) coefficient of rolling friction

(conditional dimensionless quantity).

    As far as in practice rolling friction accompanies sliding friction, it is important to consider the conditions of this friction:

- $\dfrac{k}{h} < f$ is the pure rolling.

- $\dfrac{k}{h} > f$ is the pure sliding.

- $\dfrac{k}{h} = f$ is the combination of rolling and sliding.

Friction in kinematic pairs
Friction in a planar crosshead
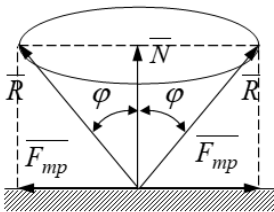
Fig. 1.49. the friction angle

Maximum angle φ, by which, due to friction, complete reaction $\overline{R}$ of the supporting surface is declined from the normal, is called *the friction angle.*

$$tg\varphi = \frac{F_{mp}}{N} = f.$$

$$F = F_{mp} = N \cdot f = G \cdot f.$$

    If a body moves relative to the supporting surface in different sides, the line of action of reaction $\overline{R}$ describes a conical surface called *the friction cone*.

Friction in a wedge crosshead

Body *1* with force $\overline{Q}$ applied to it moves uniformly along horizontal guide *2* under force $\overline{F}$. The crosshead presses against the guide with the side surfaces, on which friction forces F_{mp1} and F_{mp2} emerge (Fig. 1.50).
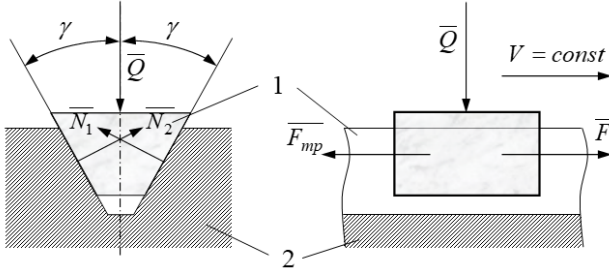
Fig. 1.50. Friction in a wedge crosshead

$$F = 2 \cdot F_{mp} = 2 \cdot f \cdot N, \quad \text{where } F_{mp} = F_{mp1} = F_{mp2},$$
$$N = N_1 = N_2, \quad f = f_1 = f_2.$$

Reactions N_1, N_2 are determined from the triangle of forces if we take equation $\overline{Q} + \overline{N_1} + \overline{N_2} = 0$. By considering that $N = N_1 = N_2$ we can get the following from the diagram of forces
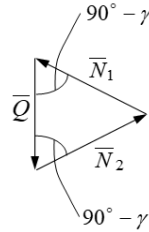
Fig. 1.51. Diagram of forces

$$N = \frac{Q}{2 \sin \gamma}$$

$$F = \frac{f}{\sin \gamma} \cdot Q = f' \cdot Q, \quad \text{whence} \quad f' = \frac{f}{\sin \gamma},$$

where f' is the reduced (*conditional*) friction coefficient of a wedge pair.

As far as angle $\gamma < 90°$ (*always*), $f' > f$ is the friction coefficient of a planar rectilinear pair.

Friction in a turning kinematic pair   (in a friction bearing)
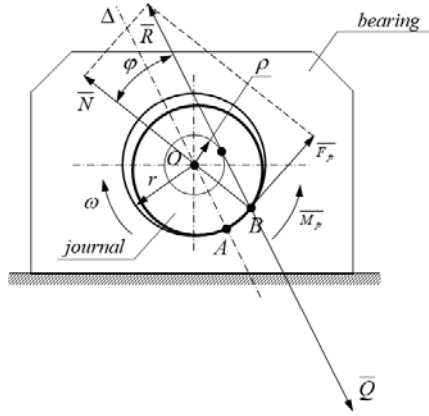
Fig. 1.52. Friction in friction bearing

Complete reaction (directed along the tangent to the friction circle)

$$\overline{R} = \overline{N} + \overline{F}_{mp}, \qquad \overline{R} = -\overline{Q},$$

where R is the complete reaction of a bearing,

Q is the resultant of the external loads,

F_{mp} is the friction force.

The friction circle radius

$$\rho = r\,sin\,\varphi = r\frac{f'}{\sqrt{1+(f')^2}},$$

where r is the radius of a journal,

φ is the deviation angle of a complete reaction from the normal (*friction angle*),

f' is the friction coefficient in a bearing.

At low values of friction coefficient f'

$$\rho = \frac{r\cdot f'}{1+\dfrac{f'^2}{2}} = r\cdot f'\left(1-\frac{f'^2}{2}\right)$$

At $f' \ll 1; \Rightarrow \rho = r\cdot f'$.

Frictional moment in a turning pair

$$M_{mp} = F_{mp} \cdot r = R \cdot \rho = f' \cdot Q \cdot r^{\cdot}$$

The friction coefficient is determined experimentally for different working conditions for a turning pair, and depends on distribution of the pressure across the contact surface between the journal and the bearing.

For unrun-in journals (*by Weisbach*): $f' = \dfrac{\pi}{2} f$.

For run-in journals (*by Reie*): $f' = \dfrac{4}{\pi} f$,

where *f* is the friction coefficient of corresponding plane surfaces, all other things being equal.

1.12. Wear in mechanisms

Wear is the process of deterioration and detachment of material off the surface of a solid body manifesting in a gradual change in the size and form of a body.

Wear decreases strength of details and accuracy of mechanisms, increases loads on bearings, leads to an increase in vibrations and noise. (Fig. 1.53)

Wear curve

t_1 – initial wear period.

t_2 – steady wear period.

t_3 – intensive (emergence) wear period. *The wear speed increases rapidly and the machine requires repairing.*
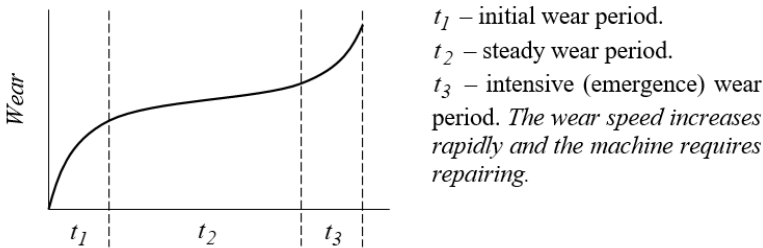
Fig. 1.53. Wear period

Types of wears:

1) Type I seizure. It occurs in rolling and sliding friction.

The basic cause is an actual load exceeding a permissible load.

Elastic deformations on the friction surface turning into plastic.

The top layer of material tears off and gets spread on the surface.

2) Type II seizure. It occurs in sliding friction.

The basic cause is high temperatures in the friction area.

The top layer of material tears off and gets spread on the surface.

3) Pitting wear. It occurs at rolling friction.

The basic cause is considerable specific loads changing by a cyclic law.

The particles of material tear off the surface of a detail where pits appear.

4) Abrasive wear. It occurs at sliding friction.

The basic cause is sand and dust into the contact area.

5) Oxidation wear.

It occurs in moist conditions.

Wear (measured in units of length, volume or mass) decreases the strength of details, changes the character of their mating, increases gaps in movable joints, and produces noise.

There exist:

- limiting wear – the wear corresponding to the limiting state of a product (or its part); and
- permissible wear – the wear at which a product keeps its workability.

1.13. Mechanical efficiency

Mechanical efficiency: $\eta = \dfrac{A_{n.c.}}{A_{\partial.c.}} < 1$,

$$\eta = \frac{A_{\partial.c.} - A_{в.c.}}{A_{\partial.c.}} = 1 - \frac{A_{в.c.}}{A_{\partial.c.}} = 1 - \psi,$$

where ψ is the mechanical loss factor,

$$\psi = \frac{A_{в.c.}}{A_{\partial.c.}},$$

$A_{в.c.}$ is the work of parasite resistance forces;

$A_{\partial.c.}$ is the work of moving forces;

$A_{n.c.}$ is the work of useful resistance forces;

General efficiency of mechanisms connected in series
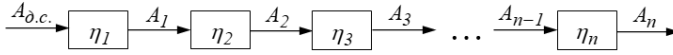
$$\eta_1 = \frac{A_1}{A_{\partial.c.}}, \quad \eta_2 = \frac{A_2}{A_1}, \quad \eta_3 = \frac{A_3}{A_2}, \quad \ldots, \quad \eta_n = \frac{A_n}{A_{n-1}}.$$

$$\eta_{общ}^{посл} = \eta_1 \cdot \eta_2 \cdot \eta_3 \cdot \ldots \cdot \eta_n = \frac{A_n}{A_{\partial.c.}}.$$

General efficiency of mechanisms connected in parallel
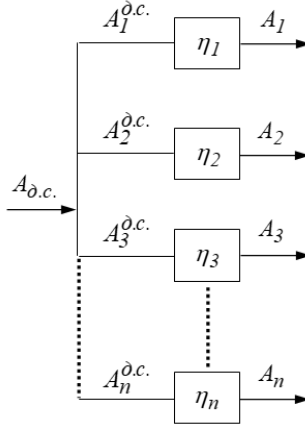
General efficiency of mechanisms connected in parallel

$$\eta_1 = \frac{A_1}{A_1^{\partial.c.}}, \quad \ldots \quad \eta_2 = \frac{A_2}{A_2^{\partial.c.}},$$

$$\eta_3 = \frac{A_3}{A_3^{\partial.c.}}, \quad \ldots \quad \eta_n = \frac{A_n}{A_n^{\partial.c.}},$$

$$\eta_{общ}^{пар} = \frac{A_{n.c.}}{A_{\partial.c.}} = \frac{\sum\limits_{i=1}^{n} A_i}{\sum\limits_{i=1}^{n} A_i^{\partial.c.}} = \frac{\sum\limits_{i=1}^{n} A_i^{\partial.c.} \cdot \eta_i}{\sum\limits_{i=1}^{n} A_i^{\partial.c.}}$$

$$\eta_{общ}^{пар} = \frac{A_1^{\partial.c.} \cdot \eta_1 + A_2^{\partial.c.} \cdot \eta_2 + A_3^{\partial.c.} \cdot \eta_3 + \ldots + A_n^{\partial.c.} \cdot \eta_n}{A_1^{\partial.c.} + A_2^{\partial.c.} + A_3^{\partial.c.} + \ldots + A_n^{\partial.c.}}.$$

69

When determining the general mechanical efficiency of complex engineering units the mechanical efficiencies of modules, as well as the character of their connection are considered.

For instance, for a combined connection of modules of engineering units, the general mechanical efficiency is defined as follows.

The efficiencies of modules *3-7* equal:
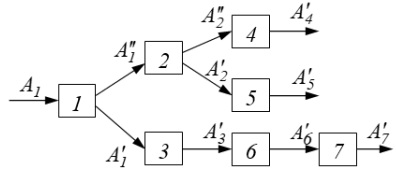
$$\eta_3 = \frac{A_3'}{A_1'}; \ \eta_4 = \frac{A_4'}{A_2''}; \ \eta_5 = \frac{A_5'}{A_2'}; \ \eta_6 = \frac{A_6'}{A_3'}; \ \eta_7 = \frac{A_7'}{A_6'}.$$

When modules are connected in parallel their total efficiency is determined as the product of efficiencies of these modules:

$$\eta_{3,6,7} = \frac{A_7'}{A_1'} = \frac{A_3'}{A_1'} \cdot \frac{A_6'}{A_3'} \cdot \frac{A_7'}{A_6'} = \eta_3 \cdot \eta_6 \cdot \eta_7 \ .$$

When modules are connected in parallel the power flow is divided, and the total work is distributed by flows:

$$\eta_{4,5} = \eta_4 \cdot \nu_4 + \eta_5 \cdot \nu_5 \ ,$$

where ν_4 and ν_5 are the coefficients of distribution of the work by flows *4* and *5*.

It should be mentioned that the sum of distribution coefficients for several modules connected in parallel is *1*:

$$\nu_1 + \nu_2 + ... + \nu_n = 1 \ .$$

By applying the dependencies obtained, the equation for defining the overall mechanical efficiency of a compound engineering unit can be written:

$$\eta = \eta_1 \cdot \left[\nu_2 \cdot \eta_2 \left(\nu_4 \cdot \eta_4 + \nu_5 \cdot \eta_5 \right) + \nu_3 \cdot \eta_3 \cdot \eta_6 \cdot \eta_7 \right]$$

1.14. Functional analysis of universal gondola domestic production

Rail transport is a leader in addressing the needs of the production sector and the public in transportation is an important factor for social and economic growth of Ukraine, development of foreign economic relations [37, 54-55]. Transport Strategy of Ukraine for the period until 2020, which was approved by the Cabinet of Ministers of Ukraine on 20 October 2010, the rail transport put forward demands for improvement of transportation technology, infrastructure modernization and renewal of rolling stock. To date, the largest share of railways rolling stock falls on truck fleet of cars, which integrates universal, specialized and closed their types [29, 63, 79, 81, 104].

The most common among truck fleet cars are universal gondola. The majority of them are operated on the edge of the designated lifetime, which determines the need to replace them. The majority of designs Freight park, which made domestic and international carriage works were designed according to traditional methods and approaches that do not provide full use of their structural features [86-90]. The above justifies the urgency of the deployment of R & D activities in order to solve scientific and applied tasks - development of new approaches and methods for the design of freight cars [28]. But the analysis of relevant scientific and technical domestic and foreign literature showed a lack of meaningful information from the solution of functional analysis is nappivahoniv. This substantiates the relevance of functional analysis universal gondola [78, 80].

The paper presents a new approach to identify and use the authors proposed a functional analysis of universal gondola by using a systematic approach and block-modudnoho design principles and design an algorithm working bodies gondola. Functional analysis study of complex technical systems (TS) which is universal gondola carried by the following algorithm. In the first stage universal gondola division into functional modules for which we use a new approach to the formal description of the construction of railway freight. Further carried out using division as a hierarchical information model gondola with two levels of hierarchy Figure 1 [53].

Second stage determine the functions of each element. To describe the functions of TS use form which formalized may submit three components:

$$F=(D,G,H),$$

wherein D- indication of produced considered TS leads to the desired result;

G- indication of the object to which the action aims D

H- indication of specific conditions and limitations under which the action is performed D

The third stage is constructed hierarchical TS functional interaction between elements (modules) (Fig. 1.54)
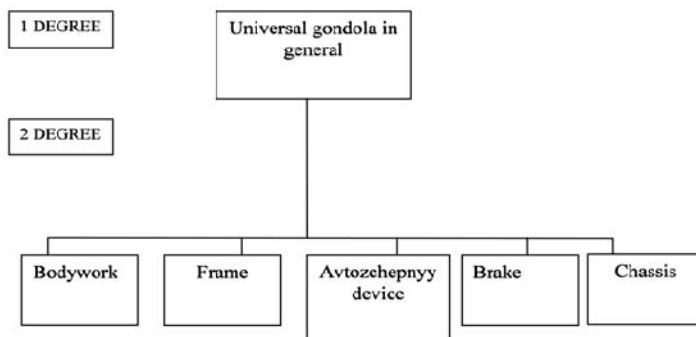
Fig. 1.54. The distribution of the elements (modules) of the first
and second levels of the design of universal gondola

In functional analysis TS user is the principle of selection and examination of the structures of the two rivnyavoyu hierarchy. According to this principle first defined the main function (function) of the considered TS, which represent the top level of the hierarchical structure of the TS. After defining the main function set functional elements to ensure its implementation, which in turn, form the first hierarchical level. Further, each functional element of the first level is considered as an independent TC, which will highlight the elements of the second level, the operation of the elements of the first level. Similarly, the division is made on the functional elements of the third and subsequent levels. Depth separation TC determined in this case, the nature and requirements of the problem being solved. Table 1 shows the results of the analysis functions universal gondola model 12-9745 [21, 97].

Considered TC (Table 1.2) is divided into functional elements of the first and second level, while the second level features provide the elements of the first level, and the latter, in turn, functioning TS in general. Items marked by the first level E_i, the function of these elements - through F_i with 0, 1, 2 ... n, and the elements of the second level and function - respectively through E_{i-k} and F_{i-k} where I = 0, 1, 2 ... n; where to k = 1, 2, ... m.

Some elements considered gondola perform more than one function and marked for the first and the second level respectively through F'_i, F''_i and Objects directed action considered TC through its elements are marked by V_i; i = 1, 2. .. 1,, with objects Vi sovpadayut component of G in the description of F by the formula.

Table 1.2

Analysis functions universal gondola model 12-9745

The item (module)	Functions element (module)
E- universal gondola V_1 - railroad V_2 - goods V_3- other cars or locomotive	F'- Shipping
E_0- Body	F_0'- stowage F_0''-the cargo in the transportation F_0'''- Providing discharge under the influence of gravitational forces
E_1 - Frame	F_1- Locating (E0), (E2), (E3), (E4),(E5)
E_2- Avtozchepnyy device	F_2- providing traction wagon with another wagon or locomotive (element V3), as well as perception, transmission and amortization efforts peredovanyemyh from other cars or locomotive
E_3 - Brake	F_3- creating artificial resistance movement wagon, and also for on-site car
E_4- Chassis	F_4- traffic safety car on track with the need to smooth stroke (smallest dynamic impact on freight transportation and elements path) and lowest resistance movement

Table 1.2 of hierarchically arranged elements of TC obtained in its constructive division, and functions performed by these elements, allows you to build functional structure TS gondola. She will present a graph of functional interaction elements TC and objects. Vertices functional interactions are functional elements and objects. Tops - functional elements - are located in the graph in a hierarchical order. The upper horizontal row is the top-elements belonging to the first hierarchical level, in the second row - each top-level II. Constructive relationship between the elements shown in the graph by dashed lines. Features elements are represented as edges of the graph, and they come from the tops of whose functions are described and included in the top-elements, which they provide rabotosposobnist, or top-objects which interact. Key-elements nodes, vertices and edges of objects on the graph conform to Table 1.2 (Fig. 1.55) [11-12].

The proposed conditional functional and constructive gondola division into separate subsystems can be used in its construction have developed techniques used in the design of freight cars and elements of creative design and search methods zabespechyuchyh a new technical solution to a set of executable navpivvahona his job function (Fig. 1.56).
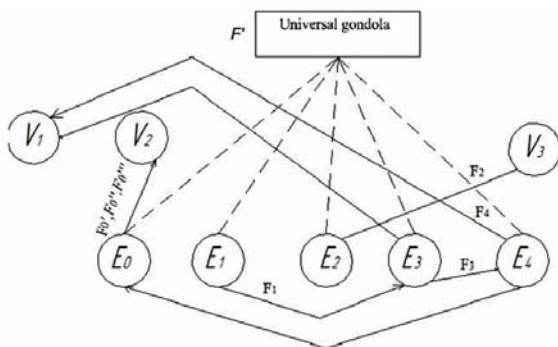
Fig. 1.55. Functional structure of universal gondola model 12-9745

To create bodywork gondola used method of automated design of freight cars designed. Fig. 3 shows the algorithm for the design of working gondola designed using elements of design methods developed K.Rotom, based on the dismemberment process of designing several phases of individual work steps each. At first (zero) phase analyzes the relationship gondola with navkolyschnym environment (cargo transported, railway and so on.).

Analysis of the environment is carried out in the working steps "necessary functioning", "technical requirements". The analysis formed the criteria for selecting analog.

On the next (first) phase developed the concept of operation. In the first step of this phase of the selection of the closest analogue to the projected wagon required for a given operation. This step includes the construction of functional structures wagon counterpart. In the second step compares the available options with the right, and the third is made defining the required additional elements (working groups) carriers trebuyemyh Export functions. Formation of products begins on the second phase of "formation" to develop constructive working scheme of the vehicle provides the necessary operation [15].

This step analyzes the many options constructive schemes of work in an existing database or applied new technical solutions. To improve the quality of the designed products (a necessary operation) working step "function" (comparison of available functions necessary) where repeated several times. Made drawing elements (modules) forming working bodies into database-aided design of freight cars [28].

Task

0 Phase formuvannya zavdannya

0.1 Problem, analysing interactions wagon Environment

Necessary operation

Technical requirements

1 Phase functioning

1.1 Finding the necessary counterpart to functioning

1.2 Function

Comparison of available functions necessary

1.3 Determining the required additional elements (operating authority) carrier required functions

2. Phase formation product

2.1 Formation konstruktyvnoyshemy working of providing the necessary operation

2.2 Function

Comparison of available functions necessary

Result

Production of working drawings of car

Fig. 1.56. Algorithm design work of the gondola

The proposed conditional functional division gondola into separate subsystems that can be used in its construction have developed techniques used in the design of freight cars and elements of creative design and search methods zabezchyvayuchyh a new technical solutions. The algorithm design working bodies gondola should be used in improving existing and designing new cars and other means of transport engineering.

One of the important stages of the research and determine trends, current and future level of performance cars is to analyze patent search [61]. The patent research regulated by the state standard GOST 3575-97 in Ukraine. It sets out the basic terms and procedures for patent research. The patent research is important for budget institutions or partially financed from the state budget. Mathematical methods of calculation and analysis of the patent fund allow assessment of trends object technology. Using these methods defined areas of structures, including long-term trends and who have exhausted their potential. The relevance of the chosen research topic is determined by the fact that the prediction of gondola structures can decide in the direction of search and research, upgrades designs of cars in general.

THE PURPOSE OF THE ARTICLE

The article presents an analysis of the dynamics of patenting designs gondola body for the past 20 years and prospects for their development. The analysis conducted in the study of the dynamics of patenting designs gondola in leading countries [12].

MAIN CONTENT

The patent information is most valuable material for the prediction of construction technical system which is the body gondola because of its specificity, novelty, accuracy, concentration, completeness of information about the technical nature.

Analysis of the entire array of patent information allows us to trace not only the evolution of structures, but also to determine the status for a given period and identify prospects. To identify existing structures of gondola body patent search conducted in the following countries: Germany, U.S., EU, China, Canada, Ukraine and Russia. There was the search of technical information in journals, newsletters, directories listed industrial countries. The depth patent search was defined research objectives: determine trends and identify the most promising developments. Using patent information is based on the fact that the patent application is implemented in 10-12 years in the first sample and another 8 years - in mass production. The analysis revealed that the average time of development in the production of patented technical solutions to improve the gondola is 17-20 years.

The distribution of patent search by countries (Fig. 1.57) [17].
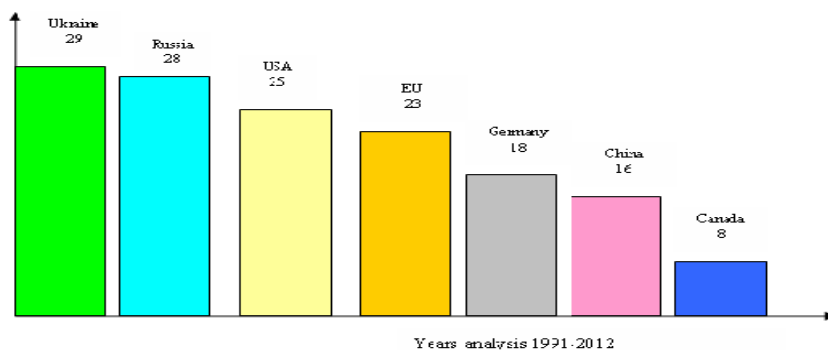
Fig. 1.57. The distribution of patent fund by country

76

The distribution of patent search is valuable information but it gives only a generalized notion of patenting by country patent search and more valuable information is the direction of body structures from patents (Fig. 1.58).
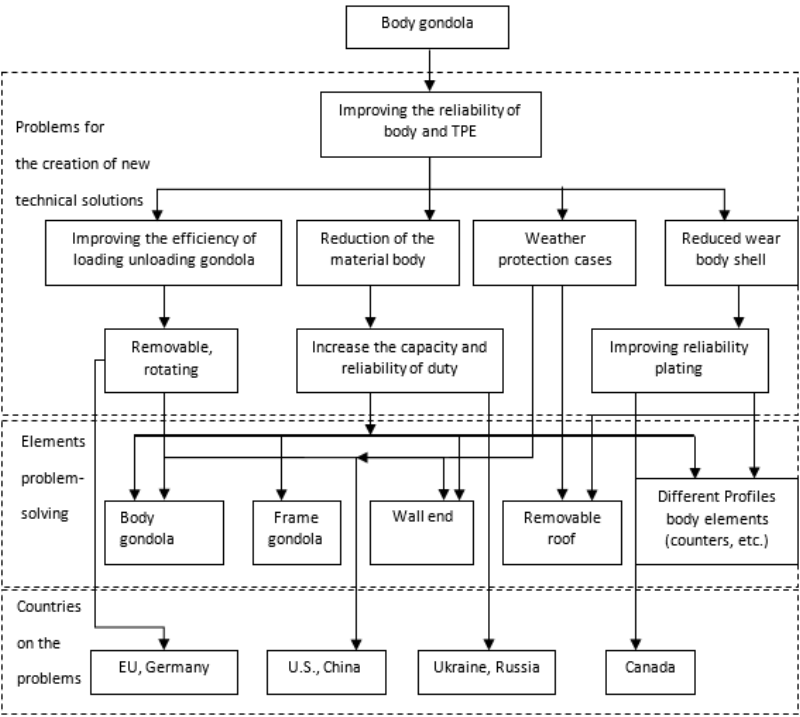
Fig. 1.58. Distribution of the patent fund issues

The Distribution Patent Foundation on issues of patent search by countries.

Analyzing the problem areas are the main structural elements to be baskets gondola upgrades are: a wall socket, frame, removable roof sheathing. This dramatically upgraded body gondola through the introduction of various forms of profiling in Russia and Ukraine. Directions for searching of solutions to implement new profiles with ample roof are prevalent in the United States and Chinese. Development of reverse body has evolved in Europe [70, 75]. Covering improvement is engaged by scientists in Canada.

The analysis of the patent was based on the so-called patent numbers that show the distribution of patent documents in time. Generally, the study of the dynamics of patenting is conducted for each selected direction for the region as a whole, separately for each country search. In addition, the dynamics of patenting is determined separately for domestic security document and in general, the "global" data. Determining the quantitative characteristics of the dynamics of the study area can be done by various methods, the most famous of which is to compute the so-called coefficient of dynamic (dynamic curves), the value of which characterizes the intensity of a particular area. Method of calculating dynamic coefficients is rather complicated and time-consuming. The prospect of technical areas revealed by regression analysis selected array of inventions, consistently developing specific technical solution or signs. The criteria adopted by the prospects of the dynamics of patenting rates offered by N.M. Timofeevoy [12, 66].

$$N_i = N_0 \cdot e^{в t_i}$$

where N_i – The number of applications per year t_i

N_0 – The number of patents per year at beginning point;

e – base of natural logarithms;

в – coefficient of prospects;

$t_i = \tau_i - \tau_0$ – number of years;

τ_i – current year;

τ_0 – year of origin.

Year of the origin; we obtain a linear relationship, which is solved by the method of least squares.

$$\ln N_i = \ln N_0 \cdot в t_i \quad,$$

Let , $\ln N_i - y_i$,a $\ln N_0 - a$, and get $y_i = a + в t_i$ or

$$y_i = \overline{y} + в\left(t_i - \overline{t}\right)$$

Where $\overline{t} = \dfrac{\sum\limits_{i=1}^{k} t_i}{K}, \overline{y} = \dfrac{\sum\limits_{i=1}^{k} y_i}{K}$ k-number of points on axis «t»

Prospect coefficient $в$ is given by formula

$$в = \frac{\sum\limits_{i=1}^{K}\left(y_i - \overline{y}\right)\left(t_i - \overline{t}\right)}{\sum\limits_{i=1}^{K}\left(t_i - \overline{t}\right)^2}$$

For the mode of assessment of the reliability of the regression slope coefficient in having random variation, was conducted in relation to the value of this quantity standard deviation of the experimental points (Sb). Thus test the significance of the slope coefficient (per Student) was determined from the equation

$$ t_\alpha = \frac{6}{S_6} $$

Where $\quad S_{\text{в}} = \sqrt{\dfrac{S^2}{\sum\limits_{i=1}^{K} (t_i - \bar{t})^2}} \quad$ standard deviation for the prospect

coefficient

$\quad S = \sqrt{\dfrac{\sum\limits_{i=1}^{K} (\bar{y} - y_i)^2}{K - 2}}$ - standard deviation for the regression line

For existing tables so-called Student's distribution $\dfrac{6}{S_6}$ for the ratio and

the number of degrees of freedom defined width of the confidence interval. Were selected for analysis only those values in, for which bilateral confidence probability was at least 90%.

Figure 3 graphs the regression dynamics patenting gondola body on the countries and technical areas of the body structures (Fig. 1.59) [12].
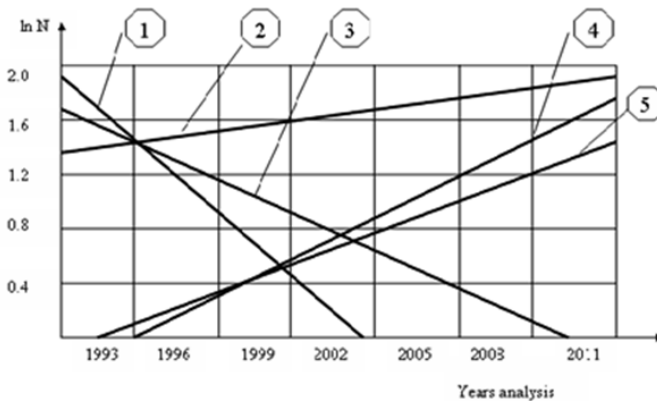
Fig. 1.59. The dynamics of patenting body gondola Country Patent Search

79

1. Canada (b=-0,181,S_b=0.087, =2,08)
2. US and Germany (b=0,032,S_b=0.031, =1,03)
3. the USA and China (b=-0,142, S_b=0.072, =1,92)
4. Ukraine (b=0,315S_b=0,12, =2,625)
5 Russia (b=0,304,S_b=0.15, =2,03)

The analysis of patenting trends in technical development and improvement of gondola body should be complemented by statistical studies [82, 85, 91]. The most significant inventions in each direction patented in many countries. This so-called "patent-analogues", they are sometimes 60% of the total amount of patents. The practical value of such inventions confirmed production experience in priority countries.

Therefore latitude extent of patenting and patent solutions also allow for a comparative assessment of the prospects of individual inventions and various technical areas.

2. FUNDAMENTALS OF EVALUATION CALCULATION FOR STRUCTURAL ELEMENTS

2.1. General information

Strength is the capacity of a structure and its elements to bear certain loads without decay.

Rigidity is the capacity of a structure and its elements to resist deformation (*change in form and size*) under external loads.

Stability is the capacity of a structure and its elements to maintain a certain initial form of elastic equilibrium.

*Basic forms of structural elements
used in buildings and machines*

Bar (rod) is the body in which one size (*length*) considerably exceeds the other two (*lateral*) sizes. Bars are divided into: *rectilinear*, *curvilinear*, *prismatic* (*of uniform and variable section*) and *thin-walled* (Fig. 2.1)
/
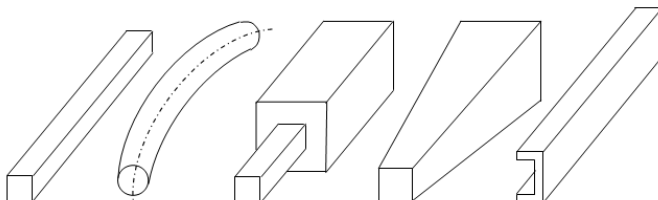
Fig. 2.1. Different shell's shapes

Shell is the body limited with curved surfaces located close to each other.

*The surface dividing the shell-wall thickness into
equal parts is called the midline.*

By form of the middle surface there are *cylinder*, *conical*, *spherical* and *toroidal* shells (Fig. 2.2).
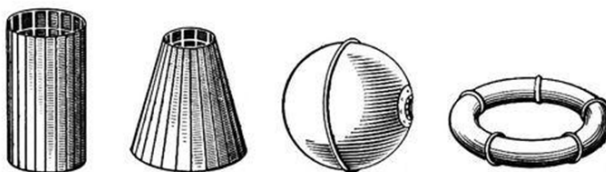
Fig. 2.2. Different form of the middle surface

Plate is the shell, the middle surface of which is a plane (Fig. 2.3).

Solid body is the body, in which all three dimensions are of the same order (Fig. 2.4).
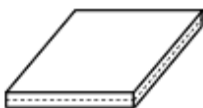
Fig. 2.3. Different plate's forms   Fig. 2.4. Solid body
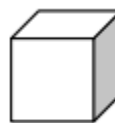
Loads The loads applied to the structure (and taken by details of machines and structures in operation) are the external loads.

Loads on the element of a structure can be:
- applied to sections of its surface (surface loads); and
- distributed by volume (volumetric loads).

Surface loads are divided into:
- *concentrated* – the loads applied on a very small area in comparison with the overall dimensions of a detail and conditionally considered as applied in one point.

The dimension of concentrated loads is N.

- *distributed* – the loads applied to areas of a detail or a larger structure area and which, while building a design model, cannot be replaced with concentrated loads.

The dimension of distributed loads:
-        by length N/m,
- by area of the element of a structure N/m^2,

Volumetric loads are forces applied to each particle of the material of a detail (*proper weight, inertia forces*) [72].

$$\text{The dimension of volumetric loads is } N/m^3.$$

By lifetime loads are divides into:
- *permanent* – the loads applied to a structure during its whole lifetime (*proper weight of a structure*).
- *temporary* – the loads applied to a structure during a limited period (*train weight*).

By pattern of influence on a structure, loads are divided:
- *static* – the loads which increase slowly from zero to the limited values, and then maintain constant.
- *dynamic* – the loads which cause high accelerations in a structure or its certain elements, which cannot be neglected in calculations.

Dynamic loads are divided into:
- *instantaneous* – the loads which rapidly achieve a certain value (*pressure of a locomotive wheel while entering a bridge*);
- *impact* – the loads applied during a very short time period;
- *intermittent-fluctuating* – the cyclically changing loads.

The external forces on structural elements include not only loads, active forces, but also constant reactions, reactive forces.

Internal forces (method of sections)

When external forces are applied to actual bodies or temperature changes, the internal interaction forces (intermolecular interaction forces) appear in these bodies; the internal forces counteract the external forces and try to return the particles to their pre-deformation position.

Determination of internal forces emerging due to loading a body is the basic task of strength calculation.

For determination of internal forces the method of sections is used.

The method is based on a sequence of the following operations:

- a detail is conditionally cut in the place where the internal forces are determined;
- one of two parts of the detail dissected is conditionally cast out;
- effect of the part neglected is replaced with the internal forces (*balanced with external forces applied to the remaining part*).

- unknown internal forces are determined from the equilibrium equations.

Generally, for a spatial task, the system of internal forces is reduced to main vector of forces $\vec{R}$ applied to the center of figure, and main moment $\vec{M}$ which are resolved into constituents along the coordinate axis (internal power factors in the section) (Fig. 2.5):

$$\vec{R} = \vec{N}_x + \vec{Q}_y + \vec{Q}_z, \quad \vec{M} = \vec{T}_x + \vec{M}_y + \vec{M}_z.$$
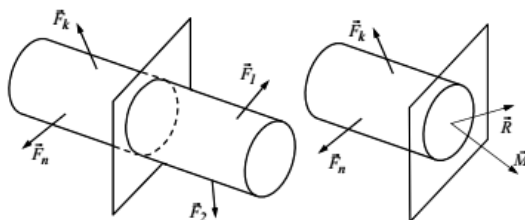
Fig. 2.5. The main vector of forces applied to the center of figure

Internal power factors in the section (Fig. 2.6):

$\vec{N}_x$ longitudinal (normal) force;

$\vec{Q}_y, \vec{Q}_z$ lateral (crosscutting) forces;

$\vec{T}_x$ torque moment;

$\vec{M}_y, \vec{M}_z$ flexure moment.
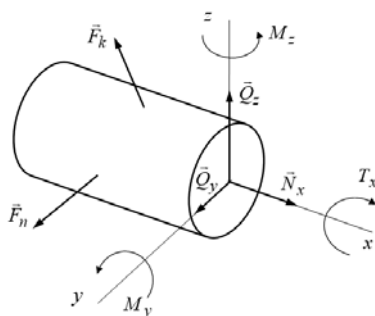
Fig. 2.6. Internal power factors in the section

In order to determine the unknown internal power factors six static equilibrium equations are used:

$$\begin{cases} \sum_{i=1}^{n} F_{ix} = 0 \; ; \quad \sum_{i=1}^{n} F_{iy} = 0 \; ; \quad \sum_{i=1}^{n} F_{iz} = 0 \; ; \\ \sum_{j=1}^{k} M_{jx} = 0 \; ; \quad \sum_{j=1}^{k} M_{jy} = 0 \; ; \quad \sum_{j=1}^{k} M_{jz} = 0. \end{cases}$$

Mechanical stresses and deformations

Stress is the local measure of internal forces; it characterizes their intensity on a dimensionless area of the section [10, 84].

> The dimension of tension is
> Pascal $(1 \; Pa = 1 \; N/m^2)$.

Combined stress in a point on area ΔA (Fig. 2.7):

$$\vec{p} = \lim_{\Delta A \to 0} \frac{\Delta \vec{R}}{\Delta A} \,,$$

where $\Delta \vec{R}$ is the resultant of the internal forces on dimensionless area ΔA.
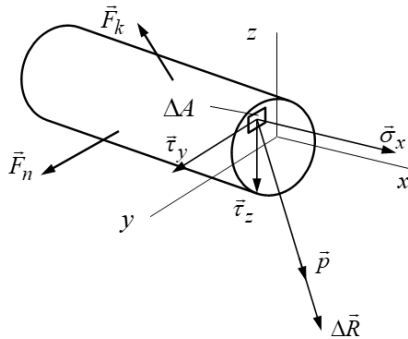
Fig. 2.7. Mechanical stress in a point on area

$$\Delta \vec{R} = \Delta \vec{N}_x + \Delta \vec{Q}_y + \Delta \vec{Q}_z \,,$$

85

where $\Delta\vec{N}_x$ is the normal component,

$\Delta\vec{Q}_y, \Delta\vec{Q}_z$ are the tangential components.

Mechanical stresses:
- normal:

$$\sigma_x = \lim_{\Delta A \to 0} \frac{\Delta\vec{N}_x}{\Delta A},$$

- tangential:

$$\tau_y = \lim_{\Delta A \to 0} \frac{\Delta\vec{Q}_y}{\Delta A},$$

$$\tau_z = \lim_{\Delta A \to 0} \frac{\Delta\vec{Q}_z}{\Delta A}.$$

The modulus of a combined stress on area ΔA: $\quad p = \sqrt{\sigma^2 + \tau^2}$,

where $\sigma = \sigma_x$ is the normal stress in the plane perpendicular to the section and characterizes the intensity of the pryout or compressive forces to the particles of the structural element located on both sides from the section;

$\tau = \sqrt{\tau_y^2 + \tau_z^2}$ is the combined tangential stress in the plane of the section and characterizes intensity of forces which shift particles of the structural component in the plane of the section under study.

Deformation is the change in form and size of a detail or structure under the external forces or thermal effect.

Deformation is the quantitative characteristic of distortion.

Geometrical deformation is divided into:

- *linear deformations* (ε) characterize the specific extension or shortening of a dimensionless line which is conditionally put along a corresponding direction from a specified point.
- *angular deformations* (γ) characterize the change in the initial right angles.

Elastic deformation is the deformation disappearing after termination of the forces causing this deformation (the detail returns to its initial form and size).

Residual deformation is the deformation which does not disappear after termination of the forces causing this deformation (the detail does not return to its initial form and size). And the residual deformation without deterioration is called *the plastic deformation*.

Basic types of deformations:

- *Extension* or *compression* is characterized by *lengthening* or *shortening* of a bar.
- *Shift (cut)* is characterized by a relative parallel shift of two adjacent transversal sections.
- *Torsion* is characterized by the angle of mutual twisting of sections relative to the bar axis.
- *Flexure* is accompanied by curving the bar axis and characterized by the deflection value and rotation angle in each section.

A combination of several basic types of deformations is called a complex deformation.

Basic hypotheses and assumptions

1. Hypothesis on material continuity. The material is supposed to completely (*without hollows*) fill the body shape.

2. Hypothesis on homogeneity and isotropy. The material properties in any volume and in any direction are supposed to be similar. *(*If physical and mechanical characteristics of the body material are equal along all directions, the body is called isotropic; and if they are not equal it is called anisotropic).

3. Hypothesis on infinitesimality of deformations. The deformations of a body are supposed to be so small in comparison with the size of a deformed body that they do not influence the mutual location of stresses.

4. Principle of independent effect of stresses (principle of superposition). The result of a system of stresses on the structure is supposed to be equal to the sum of all stresses separately [10].

5. Saint-Venant's principle. It is supposed that if within some area of an elastic body a system of forces is applied, at distances which considerably excess the specific dimensions of this area, stresses and deformations are virtually equal for all static equivalent systems of forces.

6. Hypothesis of plane sections (Bernoulli's hypothesis). It is supposed that lateral sections of a bar, plane and perpendicular to its axis before deformation, remain plane and perpendicular to its axis after deformation.

2.2. Strangth calculations for deformations "tension-compression" (law of huke)

Axial tension or compression of a bar is the simple loading at which only one internal power factor, *internal longitudinal force N*, emerges in its lateral sections, but all other forces are equal to zero (Fig. 2.8).
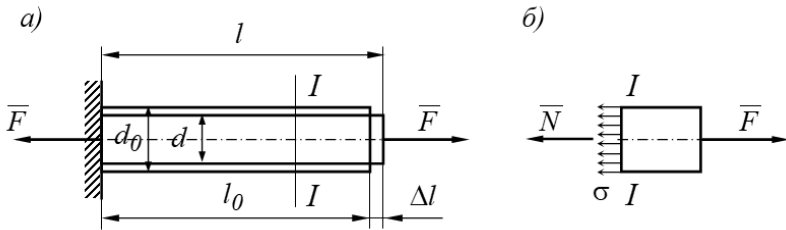
Fig. 2.8. Axial tension or compression of a bar

By applying the section method: $|N| = |F|$, $\overline{N} = -\overline{F}$.

> *Longitudinal force N in the cross section of a bar is numerically equal to the algebraic sum of projections of external forces to its axis. located at one side from the section.*

Law of signs:
- $N > 0$, if it extends (*directed from the section*);
- $N < 0$, if it compresses (*directs to the section*).

In cross sections only evenly distributed normal stresses σ act:

$$\sigma = \frac{N}{A}, \quad \text{where } A \text{ is the area of a section.}$$

The bar under extension is being deformed by changing its longitudinal and lateral dimensions at corresponding values:
- for tension: $\Delta l = l - l_0 > 0$, $\quad \Delta d = d - d_0 < 0$;
- for compression: $\Delta l = l - l_0 < 0$, $\quad \Delta d = d - d_0 > 0$.

Relative deformations:

longitudinal: $\varepsilon = \dfrac{\Delta l}{l_0};$ lateral: $\varepsilon' = \dfrac{\Delta d}{d_0}.$

Coefficient of lateral deformation (Poisson's ratio): demonstrates the dependency between longitudinal and lateral deformations of an element, and characterizes the elastic properties of materials.

$$\mu = \left| \frac{\varepsilon'}{\varepsilon} \right| .$$

- $0 \le \mu \le 0,5$ for isotropic materials;
- $\mu \approx 0,3$ for structural materials;
- $\mu = 0$ for cork;
- $\mu \approx 0,5$ for rubber and liquid.

Hooke's law: the normal stresses are directly proportional to the relative longitudinal deformation:

$$\sigma = E \cdot \varepsilon ,$$

Where E is the modulus of elongation, the modulus of type I elasticity, Young's modulus (dimension is Pascal).

Modulus E characterizes the properties of material to resist elastic deformation, i.e. the higher is the modulus, the less the material becomes deformed.

Absolute tension of a bar:

$$\Delta l = \frac{N \cdot l_0}{E \cdot A},$$

where $E \cdot A$ *is the rigidity at tension.*

The formula can by used for the section of a bar, within which N and A remain constant.

Strength condition at tension (compression) (Fig. 2.9):

$$\sigma_{max} = \frac{N_{max}}{A} \leq [\sigma],$$

where $[\sigma]$ is the permissible stress (*the safest*),

$$[\sigma] = \frac{\sigma_{on}}{[n]}$$

where σ_{on} is the unsafe stress (*at which there appears a possibility to break the detail or disturb its functionality*); $[n]$ is the normative safety factor $[n] = 1.5 \div 5$. It depends on working conditions, accuracy of calculation methods, material properties and purpose of the structure);

N_{max} is the maximum value of a normal force.

On taking into account the dead weight in tension let us consider a uniform section bar of weight G and length l clamped with its top side and loaded with its dead weight.
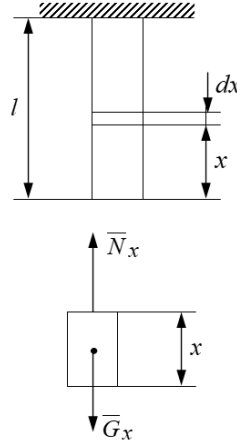
Fig. 2.9. Strength at tension

According to the method of sections

$$\sum x = 0, \quad N_x - G_x = 0, \quad N_x = G_x,$$

where G_x is the dead weight of the cross-section of length x,

$$G_x = \gamma \cdot A \cdot x,$$

where γ is the specific weight of the material of a bar,

A is the cross section area.

Stress in the longitudinal section:

$$\sigma = \frac{N_x}{A} = \frac{\gamma \cdot A \cdot x}{A} = \gamma \cdot x,$$

$$\sigma_{max} = \gamma \cdot l.$$

Absolute extension of the element of the bar of length dx

$$\Delta x = \varepsilon \cdot dx = \frac{\gamma \cdot x}{E} dx \cdot$$

Complete extension of the bar:

$$\Delta l = \frac{\gamma}{E} \int_0^l x dx = \frac{\gamma \cdot l^2}{2E}.$$

By multiplying the denominator and numerator in the formula by cross sectional area A, we obtain:

$$\Delta l = \frac{\gamma \cdot l \cdot A \cdot l}{2 \cdot E \cdot A} = \frac{G \cdot l}{2 \cdot E \cdot A}.$$

2.3. Mechanical characteristics of materials

In order to determine mechanical characteristics of materials (modulus of elasticity, Poisson's coefficient, plasticity, solidity, etc.) special tests are made, the simplest of them is the elongation test.

Special *cylindrical* or *prismatic* (*plane*) test-pieces are made of the material under study (Fig. 2.10):

long

$$l_0 = 11{,}3\sqrt{A_0};$$
$$(l_0 = 10d_0);$$

short

$$l_0 = 5{,}65\sqrt{A_0};$$
$$(l_0 = 5d_0).$$
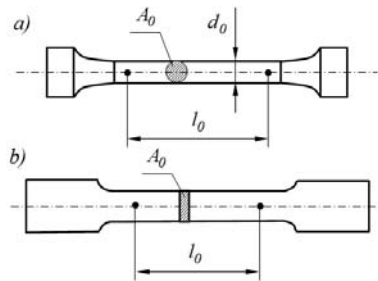
Fig. 2.10. Special cylindrical and prismatic test-pieces

The test piece is mounted in clamps and extended with a special machine, which automatically measures load F, absolute tension Δl and write

stress-strain curve $F = f(\Delta l)$, with subsequent reconstructing it into the coordinate system $\sigma = f(\varepsilon)$ ($\sigma = \dfrac{F}{A_o}, \varepsilon = \dfrac{\Delta l}{l_o}$) (Fig. 2.11) [38, 39].
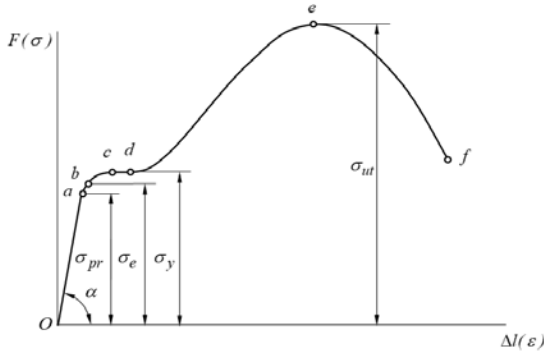
Fig. 2.11. Strain-stress curve for low-carbon steel

Section Oa is *the zone of proportionality* $\Delta l(\varepsilon)$

Proportional limit $\sigma_{pr} = \dfrac{F_a}{A_0}$ is the boundary stress, to which the material follows Hooke's law ($tg\alpha = \sigma / \varepsilon = E$).

Section ab is *the zone of elasticity.*

Elastic limit $\sigma_e = \dfrac{F_b}{A_0}$ is the boundary stress to which the material gets deformed elastically. Points a and b on the curve practically coincide. (Hooke's law is not followed with adequate accuracy).

A further increase in the load after point b produces residual deformations.

Horizontal section cd is *the zones of yield.*
Yield limit $\sigma_y = \dfrac{F_d}{A_0}$ is the stress at which deformation of the test-piece goes at a constantly extending load.

92

Yield is an increase in deformation without an increase in loading. Here, the crystal lattices reconstruct and the material hardens. Besides, slant lines (the Chernov-Lüders bands) at an angle of 45˜ to the axis of the test-piece emerge on the surface.

Cold hardening is the process of increasing elastic properties of material through plastic pre-deformation (*used for hardening details*).

Section de is *the zone of hardening.*

Ultimate stress or ultimate resistance $\sigma_{ut} = \dfrac{F_{max}}{A_0}$.

After running through yield, the material gets harder; it again acquires the capacity to resist tension.

Section ef is *the zone of local yield.*

When the test-piece reaches point *e* on the curve, *a neck* emerges. And deformations are concentrated only at the neck, which rapidly becomes thin, and, consequently, the stress and conventional stress fall. In point *f* the test-piece breaks.

The tension tests also define *the characteristics of plasticity*:
- *Relative residual elongation in breakage*

$$\delta = \frac{l_p - l_0}{l_0} \cdot 100 \ \%,$$

where l_p is the effective length of the test-piece after breakage.

Value δ depends on the ratio of length to cross sectional dimensions of the test-piece.
- Relative residual constriction in breakage

$$\psi = \frac{A_0 - A_{ш}}{A_0} \cdot 100 \ \%,$$

where $A_{ш}$ is the area of the smallest cross section of a neck after breakage.

Value ψ characterizes the plasticity of material more precisely than δ, because it depends less on the shape of the test-piece.

> In accordance with a relative residual elongation
> in breakage all materials are divided into *plastic* and *brittle*.

Plasticity is the property of material to acquire more residual deformations without damages.

Brittleness is the property of material to break without visible residual deformations.

- $\delta > 5\ \%$ for *plastic* materials (*copper, aluminum, brass, low-carbon steel, lead*);
- $\delta < 5\ \%$ for *brittle* materials (*hardened steel, cast iron, glass, stone, concrete*).

Unsafe stress for plastic materials is taken as limit of fluidity σ_y, and for brittle materials – ultimate tensile strength σ_{ut}^{+} (for tension) and σ_{ut}^{-} (for compression).

Ultimate tensile stress of a brittle material at compression several times higher than that for tension, and a brittle material compresses well and extends poorly.

At high temperatures *the creep* is of considerable importance, it implies a growth of plastic deformation in time at a constant stress which does not cause plastic deformations at short loads.

A decrease in stresses in time due to creep in a loaded detail at its complete steady deformation is called *relaxation*.

Solidity test is used to access the value of ultimate tensile strength.

Solidity is the property of material to resist intrusion of a more solid body – *indenter* – into its surface.

In order to determine solidity the following methods are used: the Brinell scale, the Rockwell scale and the Vickers hardness test.

Brinell Hardness Number *HB* is the ratio of the load with which a steel hardened sphere presses on the surface of a test-piece to the spherical indentation area obtained (m^2):

$$HB = \frac{2F}{\pi \cdot D \cdot \left(D - \sqrt{D^2 - d^2} \right)}$$

where F is the applied load, N;

    D is the diameter of the sphere, m ;

    d is the diameter of the indentation, m
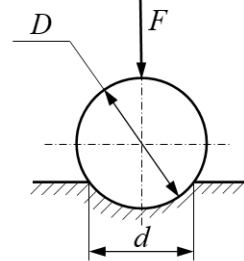
Fig. 2.12. Determination of solidity by the Brinell scale

94

When using the Rockwell scale, a sharp diamond cone (*HRC*) indents in the surface of a test-piece, and for the Vickers hardness test a diamond pyramidion (*HV*) is used.

2.4. Strength calculations for deformation "shear"

Shear is the simple deformation of a bar at which only *internal lateral force* ($Q \neq 0$) acts in the cross section.

It is the type of resistance at which a bar is loaded with two equal oppositely-directed and infinitely closely spaced forces which cause shear of the area between them.

Pure shear is the plane stressed state at which only tangential stresses act on the edges of a rectangular element (Fig. 2.13).
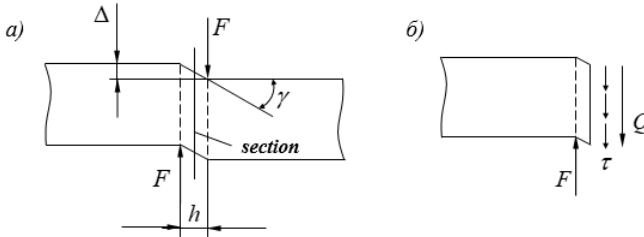
Fig. 2.13. Pure shear

According to the equilibrium state in the left side of a bar (*applying the method of sections*) *the lateral force*:

$$Q = \int \tau dA = F.$$

Considering that the shearing stresses are evenly distributed on the cross section, we can obtain:

$$\tau = \frac{F}{A}.$$

The following values characterize the shear:
- Δ absolute shear; anc
- Δ/h relative shear (measure of the direct angle shift of on element).

Angle of shear: $\Delta/h = tg\gamma \approx \gamma$.

Hooke's law at shear (shearing stresses are directly proportional to angular deformations):

$$\tau = G \cdot \gamma,$$

where G is *the type II modulus of elasticity* or *the modulus of shear* (*Pa*).

The ratio between modulus of shear G, Young's modulus E and Poisson's coefficient μ is expressed by the formula:

$$G = \frac{E}{2(1+\mu)}.$$

Taking that $\tau = const$: $\tau = Q/A.$

By substituting τ and γ in Hooke's law we obtain the formula for determination of the absolute shear:

$$\Delta = \frac{Q \cdot h}{G \cdot A},$$

where $G \cdot A$ is *the rigidity at shear*.

Strength condition at shear:

$$\tau_{max} = Q_{max}/A \le [\tau_{cp}].$$

where $\lfloor \tau_{cp} \rfloor$ is the safe load for shear.

2.5. Geometric characteristics of plane sections

In strength and rigidity calculations under *tension and shear* one characteristic of a plane section, *the area*, is used. For *torsion and flexure* the following *geometric characteristics of plane sections* are used.

Statistic moments of the section relative to axes x and y are the integrals (Fig. 2.14):

$$S_x = \int\limits_A y dA, \quad S_y = \int\limits_A x dA.$$

On the basis of the theorem on the moment of a resultant force:

$$S_x = A \cdot y_c, \quad S_y = A \cdot x_c,$$

where x_c, y_c are the coordinates of the center of gravity of the section.

The static moments of sections relative to the central axes (axes going through the center of gravity of the section) equal to zero.

The dimension of static moments of a section is sm³ or m³.

Axial (equatorial) moments of inertia of the section relative to axes x and y are integrals of the type (Fig. 2.15):

$$I_x = \int\limits_A y^2 dA, \quad I_y = \int\limits_A x^2 dA.$$

The dimension of axial moments of inertia of the section are *sm⁴* or *m⁴*.

Polar moment of inertia of the section relative to a given point (pole O) is an integral of the type:

$$I_\rho = \int\limits_A \rho^2 dA,$$

where ρ is the distance from an element area to the coordinate origin.

$$As \qquad \rho^2 = x^2 + y^2, \quad I_\rho = I_x + I_y.$$
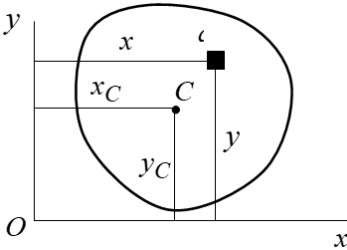
Fig. 2.14. Statistic moments
of the section relative to axes x and y
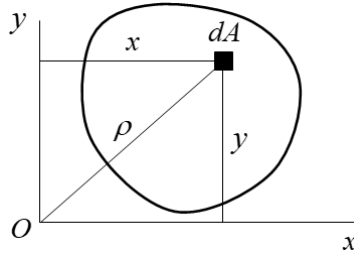
Fig. 2.15. Axial moments of the section
relative to axes x and y

The dimension of the polar moment of inertia of the section is *sm⁴* or *m⁴*.

Centrifugal moment of inertia of the section is an integral of the form

$$I_{xy} = \int\limits_A xy \, dA.$$

The dimension of the centrifugal moment of inertia of the section is sm^4 or m^4.

According to the position of the axes the centrifugal moment of inertia can be positive or negative, and also equal to zero.

The axes, relative to which the centrifugal moment is zero, are called *the principal axes of inertia*.

All mutually perpendicular axes, at least, one of which is the axis of symmetry of a figure, are its *principal axes*.

The principal axes, running through the center of gravity of the section, are called *the centroidal principal axes*.

2.6. Strength calculations in deformation "torsion"

Torsion is the simple load at which only *internal torque moment* ($T_x \neq 0$) acts in the cross section of a bar.

The bar (rod) acting for torsion, regardless the form of its section, is called *the shaft*.
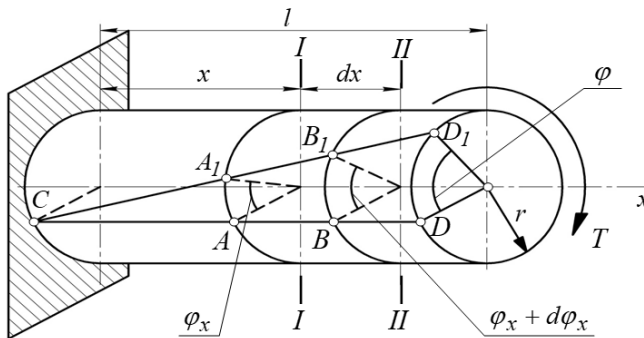
Fig. 2.16. Torsional deformation

It is taken that in torsional deformation (Fig. 2.16):
- shaft axis remains rectilinear;
- cross sections of the shaft remain plane and rotate around its axis relative to each other at an angle called *the torsion angle* (φ);
- distances between cross sections of the shaft do not change;
- rectilinear generatrices turn into helical lines, (e.g. *generatrix CD into helical line CD_1*); and

98

- radii of the sections remain rectilinear.

Considering the all above-mentioned, *torsion of a cylindrical bar* can be taken as the result of shears due to mutual turn of the cross sections. Therefore in cross sections of the shaft only shearing stresses occur, but normal stresses are equal to zero (Fig. 2.17).
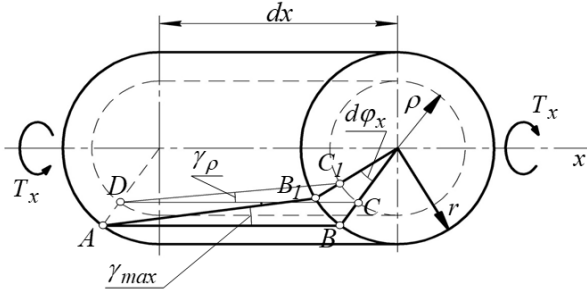
Fig. 2.17. Torsion of a cylindrical bar

Relative torsion angle: $\quad \theta = \dfrac{\varphi}{l} = \dfrac{d\varphi_x}{dx} = const$,

Where l is the shaft length,
$d\varphi_x$ is the torsion angle on a section of the shaft of length dx.

Angle of relative shear:

$$\gamma_{max} = \frac{BB_1}{AB} = \frac{r \cdot d\varphi_x}{dx} = r \cdot \theta \qquad \gamma_\rho = \frac{CC_1}{DC} = \frac{\rho \cdot d\varphi_x}{dx} = \rho \cdot \theta.$$

On the basis of Hooke's law at shear *shearing stresses in a section of the shaft* are:

$$\tau_{max} = G \cdot \gamma_{max} = G \cdot \frac{d\varphi_x}{dx} \cdot r \qquad \tau_\rho = G \cdot \gamma_\rho = G \cdot \frac{d\varphi_x}{dx} \cdot \rho.$$

Complete moment of internal forces (torsion moment):

$$T_x = \int_A \tau_\rho \cdot \rho \cdot dA = \int_A G \cdot \frac{d\varphi_x}{dx} \cdot \rho \cdot \rho \cdot dA =$$

$$= \int_A G \cdot \theta \cdot \rho^2 \cdot dA = G \cdot \theta \cdot \int_A \rho^2 \cdot dA = G \cdot \theta \cdot I_\rho,$$

where I_ρ is the polar moment of inertia of the cross section of a bar (*for a round solid bar*):

$$I_\rho = \int_A \rho^2 dA = \int_0^{d/2} 2\pi\rho^3 d\rho = 2\pi\frac{(d/2)^4}{4} = \frac{\pi \cdot d^4}{32}, \text{ where } dA = 2\pi\rho d\rho).$$
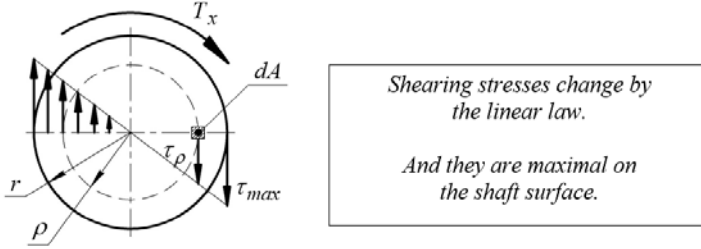
Fig. 2.18. Shear shearing stresses in a section of the shaft

Relative torsion angle:

$$\theta = \frac{T_x}{G \cdot I_\rho},$$

where $G \cdot I_p$ is the rigidity of the cross section at torsion.

Complete torsion angle (measured in radians):

$$\varphi = \int_0^l \frac{T_x}{G \cdot I_\rho} dx.$$

If $T_x = const$ *and* $I_\rho = const$, the complete torsion angle is *presented as* Hooke's law at torsion:

$$\varphi = \frac{T_x \cdot l}{G \cdot I_\rho}.$$

If the shaft has several sections distinguishing by the size of sections and values of torsion moments, the complete torsion angle equals the algebraic sum of torsion angles of these sections.

Shearing stresses in an arbitrary point of the section of the shaft are:

$$\tau = \frac{T_x \cdot \rho}{I_\rho}.$$

Maximum shearing stresses take place on the surface of the shaft at $\rho = r$:

$$\tau_{max} = \frac{T_x \cdot r}{I_\rho} = \frac{T_x}{W_\rho},$$

where $W_\rho = \frac{I_\rho}{r}$ is the polar moment of resistance at torsion (m^3).

For a solid round section: $W_\rho = \frac{\pi \cdot d^3}{16}$.

Strength condition at torsion:

$$\tau_{max} = \frac{T_{xmax}}{W_\rho} \le [\tau],$$

where $[\tau]$ is the permissible shearing stress at torsion.

The minimal diameter of a shaft (by strength condition)

$$d_{min} = \sqrt[3]{\frac{16 \cdot T_{\kappa p\,max}}{\pi \cdot [\tau]}}.$$

Rigidity condition at torsion: $\quad \theta_{max} = \frac{T_{xmax}}{G \cdot I_\rho} \le [\theta],$

where $[\theta]$ is the permissible relative torsion angle.

Internal torsion moment T_x in an arbitrary section is equal to the algebraic sum of external torsion moments located at one side from the section.

2.7. Strangth calculations under deformations "flexure"

Flexure is the deformation at which bending moments M_z appear is the cross sections of a beam (*due to which the beam axis curves*).

Pure flexure is the deformation at which only the bending moment appears in the section of a beam.

Lateral flexure is the deformation at which the bending moment along with lateral force (Q_y) act in the section of a beam.

Beam is a straight-line bar working for flexure. A distance between the rests of a beam is called *the span*.

simple, one-span,
two-support

framework

cantilever
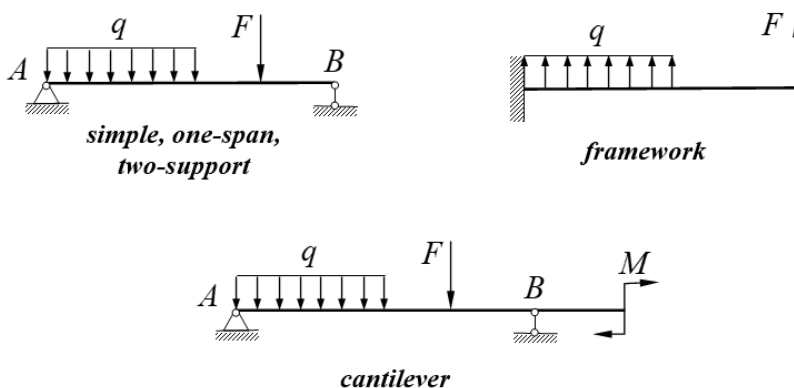
Fig. 2.19. Different type of flexure deformation

Lateral force and bending moment

For a given design diagram the strength and rigidity calculations at flexure begin with determination of support reactions, and then, with the method of sections, one should analyze dependencies by which the internal power factors change (lateral force Q_y and bending moment M_z) and build their diagrams.

Calculation rules for Q_y and M_z (Fig. 2.20):

- *lateral force Q_y* is numerically equal to the algebraic sum of the external forces acting on the detached part of a beam;

- *bending moment M_z is numerically equal to the algebraic sum of moments from the loads applied to the detached part of a beam relative to the centroidal principal axis of the section.*

Rules of signs for Q_y and M_z:

a)

$Q > 0$

$Q < 0$

b)

$M > 0$

$M < 0$
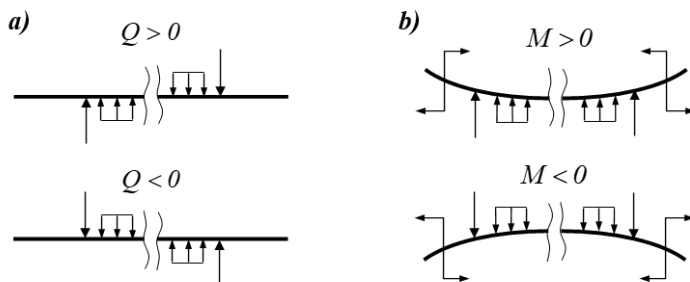
Fig. 2.20. The strength and rigidity calculations at flexure

Lateral force is positive, if its vectors try to rotate parts of a dissected beam clock wise, and negative if vice versa.

Bending moment is positive, if it causes compression in upper fibers of a beam, and negative if vice versa.

When building diagrams of lateral forces and bending moments the following rules are followed:

- positive values of Q_y are put from the basis horizontal line upwards, and negative – downwards;
- moment diagram M_z is built from the side of stretched fibers, i.e. positive values of bending moments are put from the basis horizontal line downwards, and negative – upwards.

Construction of diagrams (Fig. 2.21)

Support reactions (from the static equilibrium conditions):

$$R_A = q \cdot l, \quad M_A = \frac{q \cdot l^2}{2}.$$

Analytical expressions for the lateral force and the bending moment:

$$Q_y = q \cdot l - q \cdot x$$

(the equation of line)

103

$$M_z = q \cdot l \cdot x - \frac{q \cdot x^2}{2} - \frac{q \cdot l^2}{2}$$

(the equation of square parabola)
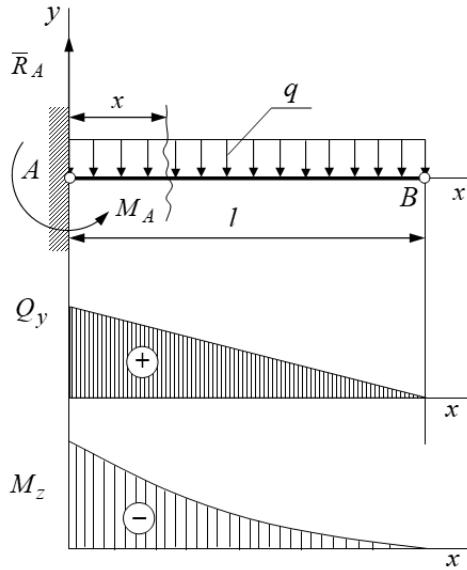
Fig. 2.21. Construction of diagrams support reactions and analytical expressions

Differential dependencies at flexure

The differential dependencies between bending moment, lateral force and distributed load (*by prof. Zhuravskii*)

$$Q_y = \frac{dM_z}{dx}, \quad q = \frac{dQ_y}{dx}, \quad q = \frac{d^2 M_z}{dx^2}.$$

The correctness of the diagrams of lateral forces and bending moments built is controlled with the following statements (Fig. 2.22)*:*

➢ if in a given section concentrated force *F* is applied perpendicularly to the beam axis, the value of lateral force Q_y in this section changes in discrete steps by the value of applied force *F*;

- if in a given section the external moment of couple of forces M is applied, the value of bending moment M_z in this section changes in discrete steps by the value of applied moment M;
- the larger is lateral force Q_y by absolute value, the steeper is the line limiting diagram M_z;
- on a beam section with the constant value of a lateral force, the diagram of bending moments M_z is limited with a direct slanting line;
- if on a beam section lateral force Q_y is positive, bending moment M_z on this section increases, and if Q_y is negative, M_z decreases;
- on sections with uniformly distributed load q, lateral force Q_y changes by a linear dependency, and bending moment M_z changes by a quadratic dependency in which the convexity faces the side of action of distributed load.

A neutral layer is the fiber layer, which bears neither tension nor compression.
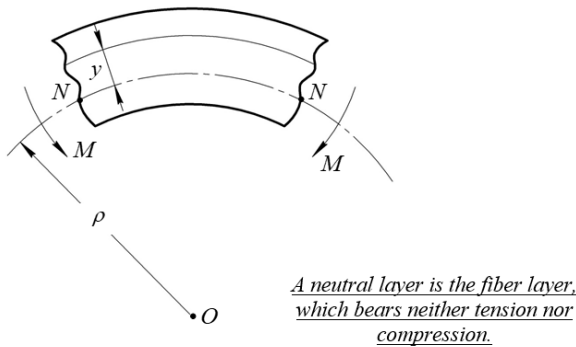
Fig. 2.22. Normal and tangential stresses at flexure

In order to determine normal stresses at a pure flexure the following dependencies are used:

$$\sigma = E \cdot \frac{y}{\rho},$$

where ρ is the radius of curvature of the neutral layer (*line NN*),

y is the distance from the neutral layer.

Stresses in the cross section of a flexed beam change proportionally to the distance from the neutral layer.

According to the equilibrium condition the sum of all elementary moments of internal elastic forces are equal to the external moment (Fig. 2.23):

$$M_z = \frac{E}{\rho} \int\limits_A y^2 \cdot dA = M \,,$$

where $\int\limits_A y^2 \cdot dA = I_z$ is the inertia moment relative to the neutral axis.
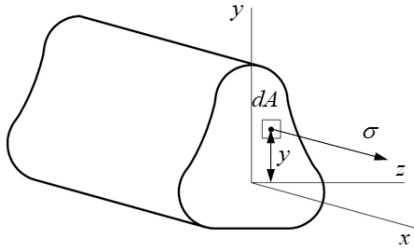
Fig. 2.23. The inertia moment relative to the neutral axis

On the basis of the above-mentioned formula we can obtain:

$$\frac{1}{\rho} = \frac{M_z}{E \cdot I_z} \,,$$

where $\dfrac{1}{\rho}$ is the curvature of the flexed axis of the beam (characterizes the value of deformation at flexure);

$E \cdot I_z$ is the rigidity of the beam at flexure.

Normal stresses at flexure:

$$\sigma = \frac{M_z \cdot y}{I_z} \,.$$

Maximum normal stresses (in the farthest points from the neutral layer):

$$\sigma_{max} = \frac{M_z \cdot y_{max}}{I_z} = \frac{M_z}{W_z} \,.$$

where $\dfrac{I_z}{y_{max}} = W_z$ is the axis moment of resistance of the section of a beam.

For example: for a round section at $y_{max} = d/2$ the axis moment of resistance of the section of a beam is $W_z = \dfrac{\pi \cdot d^3}{32}$.

In the cross sections of a beam at lateral flexure *the tangential stresses* appear together with the normal stresses (*determined by Zhuravski's formula*):

$$\tau = \frac{Q_y \cdot S_z}{b \cdot I_z},$$

where Q_y is the lateral force acting across the section,

S_z is the static moment of the section relative to the neutral axis,

I_z is the inertia moment of the section relative to the neutral axis,

b is the width of the section on the level of a point where stresses are determined.

The tangential stresses in the upper and lower layers equal *0*, and in fibers of the neutral layer they gain the maximum values.

As are as tangential stresses are not considerable in comparison with normal stresses, they can be neglected in the strength calculation. Then, *the strength condition at flexure deformation* looks like:

$$\sigma_{max} = \frac{M_{z\,max}}{W_z} \le [\sigma].$$

Differential equation of the elastic line of a beam

The axis of a beam deformed under loads is a smooth curve called *the elastic curve* (Fig. 2.24).

While calculating the normal stresses the following formula is obtained

$$\frac{1}{\rho} = \frac{M_z}{E \cdot I_z} \quad \Rightarrow \quad \rho = \frac{E \cdot I_z}{M_z}.$$

Mathematics has it that the radius of curvature of a curve in point *A* with coordinates *x, y* is determined by the formula:

$$\rho = \frac{[1+(y')^2]^{3/2}}{y''},$$

where $y' = \dfrac{dy}{dx} = tg\varphi$ (where φ is the angle formed with the tangent to the elastic line of a beam with the positive direction of axis$_x$); $y'' = \dfrac{d^2y}{dx^2}.$
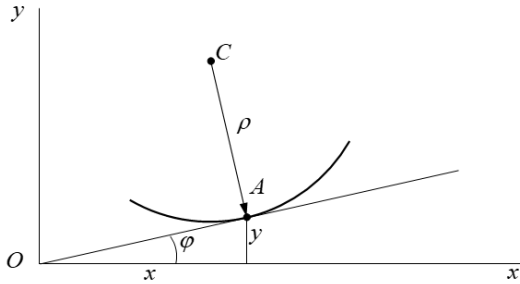
Fig. 2.24. The elastic curve
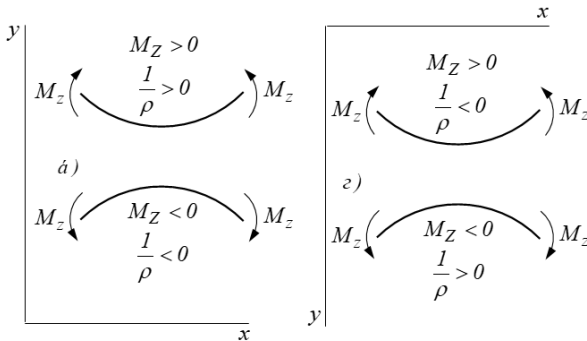
Fig. 2.25. Definition of the sign of curvature

Due to infinitesimality of $\dfrac{dy}{dx}$ in the equation, expression $(y')^2$ can be neglected. Thus, *the radius of curvature of the elastic line of a beam:*

$$\rho = \frac{1}{y''}.$$

108

Considering the above-mentioned formulae we can obtain the *differential equation of the elastic line of a bar in general form*:

$$y'' \cdot E \cdot I_z = M_z.$$

As the figures below demonstrate, according to the coordinate axes and the sign of the bending moment we can define the sign of curvature (Fig. 2.25).

2.8. Basics of theory of stressed and deformed state

Stress state in a point

By studying the stress state in point A, let us allocate an element in the form of an infinitely small parallelepiped near it. It is considered that the stresses at each side are uniformly distributed (Fig. 2.26).
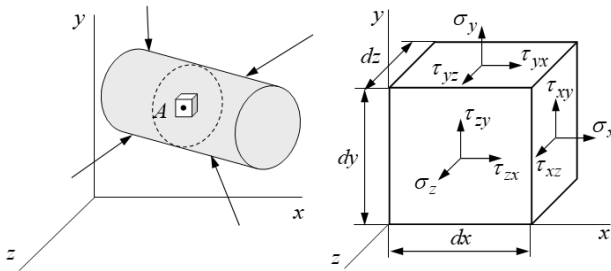
Fig. 2.26. The stress state in point A

The complete stresses at the edges are normal σ and tangential τ components – the projections of complete stresses on the coordinate axes.

The index at σ corresponds to the direction of the normal to the area.

The first index at τ corresponds to the direction of the normal to the area, and the second – to the direction of the stress.

The set of stresses applied to various areas across a point, is called *the stress state in a point*. This set of stresses, presented as a square matrix, is called *the stress tensor*.

The areas with no tangential stresses are called the principal cross-sections, and the normal stresses on these areas – the principle stresses.

$$\begin{Bmatrix} \sigma_x & \tau_{xy} & \tau_{xz} \\ \tau_{yx} & \sigma_y & \tau_{yz} \\ \tau_{zx} & \tau_{zy} & \sigma_z \end{Bmatrix}$$

The principal stresses are indicates as σ_1, σ_2 and σ_3, and the inequality $\sigma_1 > \sigma_2 > \sigma_3$ is satisfied. (Fig. 2.27).

| **Linear** | **Plane** | **Volumetric** |
| (*single-axis*) | (*biaxial*) | (*triaxial*) |
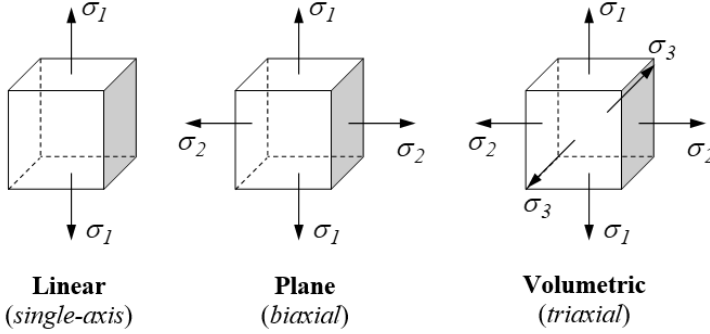
Fig. 2.27. The principal stresses

In the points of a stressed body we can distinguish elementary parallelepipeds, on the edges of which only *normal stresses* act, they are *the principal stresses*. And the following stress states are called: *linear, plane* and *volumetric* [57].

Reciprocity law for tangential stresses: the tangential stresses on two mutually perpendicular areas directed perpendicular to the cross line of these areas are equal by value:

$$\tau_{xy} = \tau_{yx}, \quad \tau_{xz} = \tau_{zx}, \quad \tau_{yz} = \tau_{zy}.$$

For the volumetric stress state the dependency between linear deformations and principal stresses is expressed by the generalized Hooke's law:

$$\begin{cases} \varepsilon_1 = \dfrac{1}{E} \cdot [\sigma_1 - \mu \cdot (\sigma_2 + \sigma_3)]; \\[2mm] \varepsilon_2 = \dfrac{1}{E} \cdot [\sigma_2 - \mu \cdot (\sigma_3 + \sigma_1)]; \\[2mm] \varepsilon_3 = \dfrac{1}{E} \cdot [\sigma_3 - \mu \cdot (\sigma_1 + \sigma_2)]. \end{cases}$$

Strength theories

• Theory of the largest normal stresses (*the I strength theory*) – unsafe condition of material when any principal stress reaches an unsafe value.

Strength condition:

$$\sigma_{\textit{экв}} = \sigma_{max} = \sigma_1 \leq [\sigma].$$

where $\sigma_{\textit{экв}}$ is the equivalent stress (*the stress under which the material in a simple stress-strain condition is in an equally unsafe state as if for the given complex stress*).

This strength theory is experimentally confirmed only for some very brittle materials (stone, brick, ceramics, etc.).

• Theory of the largest linear deformations (*the II strength theory*): structural failure for a general stress state occurs when the greatest relative linear elongation reaches its unsafe value (*at tension and compression*).

Strength condition:

$$\left|\varepsilon_{max}\right| \leq [\varepsilon],$$

using the generalized Hooke's law:

$$\sigma_{\textit{экв}} = \sigma_1 - \mu \cdot (\sigma_2 + \sigma_3) \leq [\sigma].$$

This theory is experimentally confirmed only for some brittle materials (alloy iron, high-strength steel).

• Theory of the largest tangential stresses (*the III strength theory*): the material reaches its limiting state when the highest tangential stress reaches an unsafe value (*the Tresca – St.-Venant theory*).

Strength condition:

$$\tau_{max} \leq [\tau],$$

or with *principle stresses*: $\sigma_{\textit{экв}} = \sigma_1 - \sigma_3 \leq [\sigma]$,

and, besides, for *torsion with flexure*: $\sigma_{\textit{экв}} = \sqrt{\sigma^2 + 4\tau^2}$.

This strength theory is well proved by tests for materials similarly working for tension and compression.

• Theory of the largest potential distortion energy (*the IV strength theory*) – an unsafe state (*yield*) for a general stress state occurs when the specific potential distortion energy reaches its limiting value (*determined at a simple torsion in the moment of yield*) (*energy, theory of Huber-von-Mises-Hencky*).

Strength condition:

$$u_\phi \le \lfloor u_\phi \rfloor,$$

or with *principle stresses*:

$$\sigma = \sqrt{\sigma_1^2 + \sigma_2^2 + \sigma_3^2 - \sigma_1\sigma_2 - \sigma_1\sigma_3 - \sigma_2\sigma_3} \le [\sigma],$$

and, besides, for *torsion with flexure*:

$$\sigma = \sqrt{\sigma^2 + 3\tau^2}.$$

The tests confirm the forth theory for plastic materials, equally working for torsion and compression. Moreover, the forth theory is describes appearance of small plastic deformations in the material more accurately than it does the third theory.

2.9. Stability calculations

Stable and unstable elastic equilibrium

The elastic equilibrium is *stable*, if, at small deviation from the equilibrium state, the system, after termination of the forces causing this deviation, returns to its initial state (Fig. 2.28).
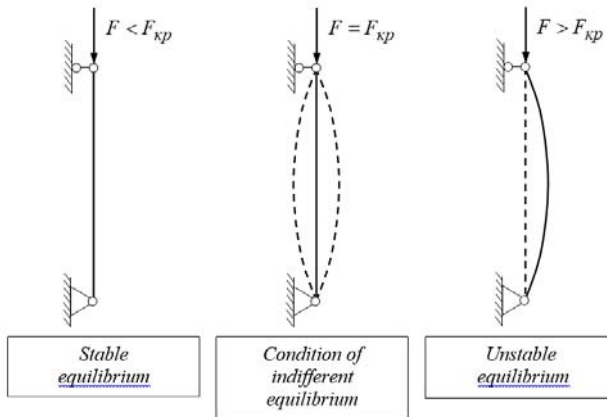
Fig. 2.28. Stable and unstable elastic equilibrium

The elastic equilibrium is *unstable*, if the system, after termination of the forces causing the deviation, does not return to its initial state and deviates more.

Between these two equilibrium states there exists a transient state, called *critical*, at which a deformed body is in an indifferent equilibrium: *it can keep its initial shape and it can even lose it because of a minor disturbance*.

Basic task of stability calculations: to determine the critical value of external forces at which the working elastic system may lose its stability.

Condition to provide a certain stability margin:

$$F \le [F],$$

where F is the acting load,

The load, an excess of which causes a loss of stability in the initial shape of a body, is called the critical force ($F_{\kappa p}$).

$[F]$ is the permissible force providing strength and durability,

$$[F] = \frac{F_{\kappa p}}{k},$$

where $F_{\kappa p}$ is the critical force;

k is the safety factor.

Euler's formula for determination of the critical force

The critical force is determined by Euler's formula and depends on a fixation method for bars (Fig. 2.29).
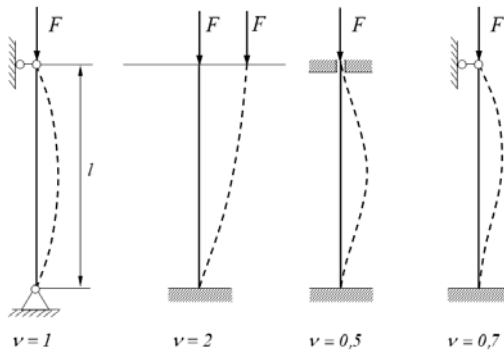
Fig. 2.29. The critical force is determined by Euler's formula

113

Euler's formula in a general view:

$$F_{\kappa p} = \frac{\pi^2 E I_{min}}{(v \cdot l)^2} = \frac{\pi^2 E I_{min}}{l_{np}^2},$$

where E is the modulus of elasticity of the material of a bar (*Young's modulus*);

I_{min} is the smallest axial moment of inertia of a section;

l is the length of a bar;

v is the coefficient of a reduced length (*depends on the method of bar fixation*);

l_{np} is the reduced length of a bar ($l_{np} = v \cdot l$).

Application limits for Young's formula

Euler's formula is used when Hooke's law is true, i.e. when *the critical strength* (*the compression stress corresponds to the critical force*) does not exceed the limit of proportionality.

$$\sigma_{\kappa p} = \frac{F_{\kappa p}}{A} = \frac{\pi^2 \cdot E \cdot I_{min}}{(v \cdot l)^2 \cdot A} = \frac{\pi^2 \cdot E}{\lambda^2} \leq \sigma_{pr},$$

where $\lambda = \dfrac{v \cdot l}{i_{min}}$ is the elasticity of a bar (dimensionless quantity which

characterizes the sizes and methods of bar fixation);

$i_{min} = \sqrt{\dfrac{I_{min}}{A}}$ minimal radius of inertia of the cross sections of a bar.

Limiting value of elasticity:

$$\lambda_{np} \geq \pi \sqrt{\frac{E}{\sigma_{pr}}}.$$

When elasticity of a bar is less than limiting ($\lambda < \lambda_{np}$), *the critical stress* is determined by *Jasinski's empirical dependency*:

$$\sigma_{\kappa p} = a - \epsilon \lambda \cdot$$

where a and ϵ are the coefficients depending on the properties of the material (*determined experimentally*).

114

Jasinski's formula is used for bars of low-carbon steel at an elasticity of $\lambda = 40.....100$. At an elasticity of $\lambda = 0.....40$ the critical stresses are considered approximately constant and equal to the yield strength.

Stability condition

$$\sigma_{max} = \frac{F}{A} \leq \left[\sigma_{ycm}\right],$$

where $\left[\sigma_{ycm}\right]$ is the permissible stress at stability calculations,

$$\left[\sigma_{ycm}\right] = \frac{\sigma_{\kappa p}}{n_{ycm}},$$

where n_{ycm} is the safety factor (*depends on the material and elasticity of a bar*). *For steel* $n_{ycm} = 1,8.....3,0$; *for iron cast* $n_{ycm} = 5,0.....5,5$.

2.10. Strength of materials at cyclic stresses

Concept of fatigue failure of the material

Cyclic loads are the loads which cause periodically changing stresses in cross sections.

At stress fluctuations microcracks appear in the material of a detail which gradually penetrate deep in the detail and considerably weaken the section, thus leading to failures of a detail [10, 23].

Fatigue failure is the failure of material due to stress fluctuations.

Fatigue of material is the process of gradual accumulation of failures in the material due to stress fluctuations which lead to crack development in the material and its damage.

Durability is the capacity of material to resist fatigue failure.

Cycles of stresses

Stress cycle is a set of all values of stress fluctuations per cycle.

Period (T) is the time of a single stress measurement (Fig. 2.30).

A cycle of stress fluctuations is characterized by the following parameters:

• *maximum stress* (σ_{max} or τ_{max});

115

- *minimum stress (σ_{min} or τ_{min});*
- *mean stress (σ_m or τ_m) can be both positive and negative*

$$\sigma_m = \frac{\sigma_{max} + \sigma_{min}}{2}, \quad \left(\tau_m = \frac{\tau_{max} + \tau_{min}}{2}\right);$$
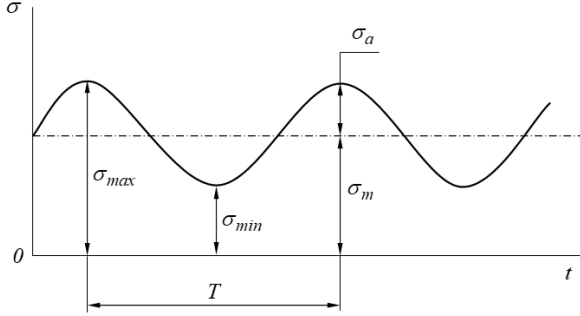
Fig. 2.30. Cycle of stress

- cycle amplitude (σ_a or τ_a) is always positive

$$\sigma_a = \frac{\sigma_{max} - \sigma_{min}}{2}, \quad \left(\tau_a = \frac{\tau_{max} - \tau_{min}}{2}\right).$$

Coefficient of cycle asymmetry: $R_\sigma = \dfrac{\sigma_{min}}{\sigma_{max}}, \quad \left(R_\tau = \dfrac{\tau_{min}}{\tau_{max}}\right).$

The most unsafe cycle in terms of strength is a *symmetric* cycle, because its fatigue limit is of the minimal value (Fig. 2.31). *The maximum and minimum stresses are equal to the absolute value and opposite by sign:*

$$\sigma_{max} = -\sigma_{min}, \quad R = -1.$$

Asymmetric cycle (Fig. 2.32): *the maximum and minimum stresses are not equal by absolute value ($\sigma_{max} \neq -\sigma_{min}$).*

Asymmetric cycles can be:
- *sign-changing ($\sigma_{max} \neq -\sigma_{min}$, $R < 0$, $R \neq -1$)*
- *constant-sign ($\sigma_{max} \neq -\sigma_{min}$, $R > 0$, $R \neq +1$).*

116

Pulsating (zero-to-tension) cycle (Fig. 2.33): the maximum or minimum stresses are equal to zero:

$$\sigma_{min} = 0 \text{ or } \sigma_{max} = 0; \; R = 0 \text{ or } R = \infty$$
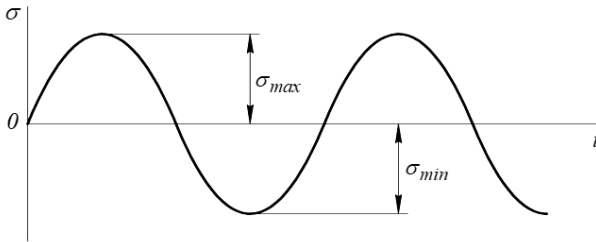
Fig. 2.31. Symmetric cycle of stress
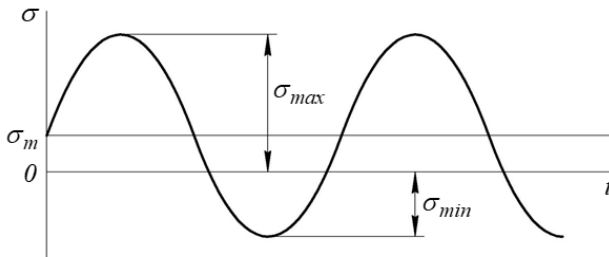
Fig. 2.32. Asymmetric cycle of stress
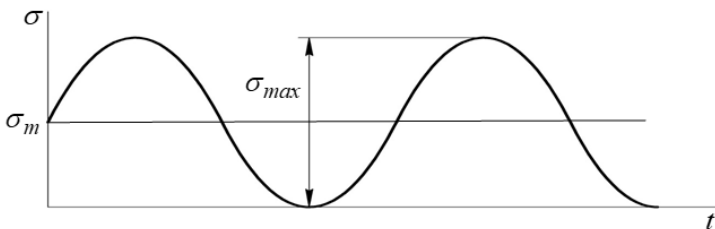
Fig. 2.33. Pulsating cycle of stress

At a constant stress (Fig. 2.34), when $\sigma_{max} = \sigma_{min} > 0$, $R = +1$.

Such a cycle is called *the cycle of constant static loading*.

Cycles of equal asymmetry coefficients R are called *similar*.
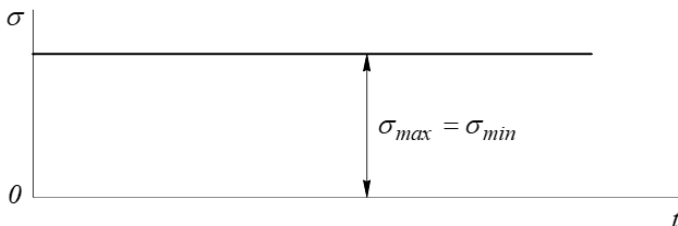
Fig. 2.34. The cycle of constant static loading

Fatigue limit. Fatigue curve

Endurance limit (fatigue) is the largest (limiting) stress of a cycle, at which a test-piece does not suffer from the fatigue failure after a random number of cycles.

Generally, in endurance calculations *the limit of endurance* is indicated σ_R (τ_R). And for a *symmetry* cycle it is σ_{-1} (τ_{-1}), for *pulsing* it is σ_0 (τ_0), for *a constant static loading cycle* it is σ_{+1} (τ_{+1}).

In order to determine the limit of endurance, test-pieces are tested for endurance, and the most popular of which is the test for pure flexure at a symmetric cycle.

By the results of the tests *the stress-number of cycle diagram (S-N diagram)* is built (*the endurance curve, August Wöhler's curve*) which is the dependency of maximum stress σ_{max} on the number of cycles N (Fig. 2.35)
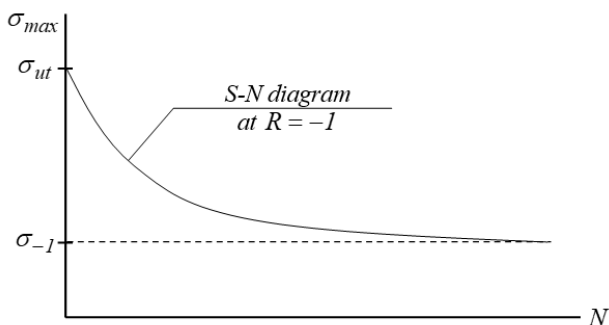
Fig. 2.35. Stress-number of cycle diagram

The maximum number of cycles at which a test is made, is called *the base cycle number* (for steel and iron cast the base number is taken equal to 10^7). If a test-piece bears the base cycle number, it is considered that the stress in it does not exceed the limit endurance and it can bear any more number of cycles without failure.

For non-ferrous metals and their alloys the base of tests increases to $N = 10^8$.

A diagram of limiting stresses

The endurance limit, at any cycle ratio, can be determined with *the diagram of limiting stresses* built in the coordinate system $\sigma_a = f(\sigma_m)$ for which a fatigue test is made at different values of R (Fig. 2.36)

Fig. 2.36. The diagram of limiting stresses

Point A corresponds to the endurance limit at an *asymmetry cycle*: $\sigma_a = \sigma_{-1}, \sigma_m = 0$.

Point B corresponds to the endurance limit of *a constant static loading cycle*: $\sigma_a = 0, \sigma_m = \sigma_{ut}$.

Point C corresponds to the endurance limit at *a pulsing cycle*: $\sigma_a = \sigma_m = \dfrac{\sigma_0}{2}$.

The area of a diagram limited by curve ACB and coordinate axes determines the zone of safe stress cycles (in terms of fatigue failures).

Ray OC characterizes a pulsing cycle and is the border of the zones of sign-changing and sign-constant cycles:

- for sign-changing cycles $\sigma_a > \sigma_m$ (*the zone of these cycles is located higher than ray OC*);
- for constant-sign cycles $\sigma_a < \sigma_m$ (*the zone of these cycles is located lower than ray OC*).

Random ray OD is a geometric place of points characterizing similar cycles for which

$$tg\alpha = \frac{\sigma_a}{\sigma_m} = \frac{1-R}{1+R} = const$$

.

If point K, characterizing a specified cycle, is located inside area $OACB$, the cycling strength of the material is guaranteed.

Influence of structural and technological factors on the endurance limit

Influence of stress concentration. The stress concentration is the phenomenon of a rapid increase in stresses in the zone of a rapid change of shape and cross section of some area of a detail (*holes, groove, key grooves, dents, carvings, etc.*):

The stress concentration *is evaluated*: by the theoretic concentration coefficient, and also by the efficient concentration coefficient.

Theoretical coefficient of stress concentration:

$$\alpha_{k\sigma} = \frac{\sigma_{max}}{\sigma_n}, \quad \left(\alpha_{k\tau} = \frac{\tau_{max}}{\tau_n}\right),$$

where σ_{max}, τ_{max} are the maximum local stresses near a concentrator;

σ_n, τ_n are the nominal stresses.

Efficient coefficient of stress concentrations:

$$K_\sigma = \frac{\sigma_{-1}}{\sigma_{-1k}}, \quad \left(K_\tau = \frac{\tau_{-1}}{\tau_{-1k}}\right),$$

where σ_{-1}, τ_{-1} are the endurance limits for a symmetric cycle of the test-piece without a stress concentrator;

σ_{-1k}, τ_{-1k} are the endurance limits for a symmetric cycle of the test-piece with a stress concentrator;

Stress concentrations considerably decrease
the endurance limit of a detail.

Influence of the sizes of a detail on the value of the endurance limit is considered by *the scale parameter* (*coefficient of influence of the absolute sizes of a cross section*):

$$\varepsilon_{M\sigma} = \frac{\sigma_{-1d}}{\sigma_{-1d_0}}, \quad \left(\varepsilon_{M\tau} = \frac{\tau_{-1d}}{\tau_{-1d_0}} \right),$$

where σ_{-1d}, τ_{-1d} are the endurance limits of specified diameter d;

σ_{-1d_0}, τ_{-1d_0} are the endurance limits of a laboratory test-piece of the similar configuration ($d_0 = 7.....10 \ \text{мм}$).

When the sizes of a test-piece increase the endurance limit decreases. Influence of the surface state is evaluated by *the coefficient of surface quality:*

$$\beta_{n\sigma} = \frac{\sigma'_{-1}}{\sigma_{-1}}, \quad \left(\beta_{n\tau} = \frac{\tau'_{-1}}{\tau_{-1}} \right),$$

where σ'_{-1}, τ'_{-1} are the endurance limits for a set of test-pieces with a
specified surface treatment;
σ_{-1}, τ_{-1} are the endurance limits of a polished test-piece.

The endurance limit can be increased by several times through
a decrease in the roughness of the surface of a detail.

Influence of the temperature. Generally, when the temperature increases the endurance limit decreases, and when the temperature decreases, the endurance limit increases.

Strength calculation at variable stresses

Safety factor at a symmetrical cycle:

$$n_\sigma = \frac{(\sigma_{-1k})_d}{\sigma_a},$$

121

where $(\sigma_{-1k})_d$ is the actual endurance limit of a detail,

$$(\sigma_{-1k})_d = \frac{\sigma_{-1}}{K_{-1}},$$

where K_{-1} is the overall coefficient of change in the endurance limit at a symmetric cycle,

$$K_{-1} = \frac{K_\sigma}{\varepsilon_{M\sigma} \cdot \beta_{n\sigma}},$$

where K_σ is the effective coefficient of stress concentrations,

$\varepsilon_{M\sigma}$ is the scale parameter,

$\beta_{n\sigma}$ is the coefficient of surface quality,

σ_{-1} is the endurance limit for a symmetric cycle.

σ_a is the amplitude of a symmetric cycle.

Safety coefficient under torsion is determined similarly:

$$n_\tau = \frac{(\tau_{-1k})_d}{\tau_a}.$$

Under the commutative action of normal and tangential stresses the safety factor is determined with the empirical dependency:

$$\frac{1}{n^2} = \frac{1}{n_\sigma^2} + \frac{1}{n_\tau^2} \qquad \text{whence} \qquad n = \frac{n_\sigma \cdot n_\tau}{\sqrt{n_\sigma^2 + n_\tau^2}}.$$

In order to determine the safety factor for non-symmetrical cycles for any type of loading (*flexure, torsion, compression, bending*) the following dependencies can be used:

$$n_\sigma = \frac{\sigma_{-1}}{\sigma_a \dfrac{K_\sigma}{\beta_{n\sigma} \cdot \varepsilon_{M\sigma}} + \psi_\sigma \sigma_m} \qquad \left(n_\tau = \frac{\tau_{-1}}{\tau_a \dfrac{K_\tau}{\beta_{n\tau} \cdot \varepsilon_{M\tau}} + \psi_\tau \tau_m} \right),$$

where ψ_σ and ψ_τ are the coefficients which characterize the material sensitivity to asymmetry of a cycle under tension, compression, flexure and torsion, respectively.

122

On determining the safety factor by fatigue resistance, it should be compared with the safety factor by resistance to plastic deformations [58]. The latter ones are determined by the formulae below:

$$n_\sigma = \frac{\sigma_y}{\sigma_{max}} = \frac{\sigma_y}{\sigma_a + \sigma_m}; \quad \left(n_\tau = \frac{\tau_y}{\tau_{max}} = \frac{\tau_y}{\tau_a + \tau_m} \right).$$

where σ_y, τ_y are the limits of yield.

The stability of a detail in calculations is evaluated by the least safety factor, obtained by corresponding formulae in both cases.

Ways to increase the endurance limit:
- grinding or polishing the surface;
- surface treatment with high-frequency currents;
- thermo-chemical treatment of the surface with azotizing or cement stabilization; and
- rolling the surface or blowing with steel or iron shot.

2.11. Conceptual basis of thermocontrollability in railway braking tribopairs

Analysis of the results of recent research and the allocation of an outstanding problem.

An analysis of the results of an expert survey within the framework of the study of the International Union of Railways has led to the processing of about 100 questionnaires of industry researchers from participating countries, representing individual research experience, along with experience in addressing specific tasks of the railway industry in their countries, showed that the most sought after directions were development rail transport:

1. Robust construction of rolling stock (cluster "Rolling stock").

2. Traffic safety and personal safety of passengers (cluster "System as a whole").

3. Technologies for monitoring the rolling stock and compatibility (cluster "Infrastructure").

4. Development of new materials and technologies for infrastructure (cluster "Infrastructure").

5. New materials and production processes for rolling stock (cluster "Rolling stock") [14]

6. Interaction in the wheel-rail system (cluster "Infrastructure").

Analyzing the 6 most priority areas of research, one can distinguish the pattern with the highest concentration and demand directions within the framework of scientific clusters Infrastructure and Rolling Stock. Experts-specialists determine the reliable and safe operation of infrastructure and rolling stock as the basis for efficient operation of the railway transport complex.

The effectiveness of brake facilities is one of the most important conditions that determine the possibility of increasing the weight and speed of trains, the throughput and freight capacity of railways. From the properties and condition of the brake equipment of the rolling stock to a large extent the safety of the movement depends.

Due to the constant increase in the speed of trains, high requirements for braking devices are imposed. The application of the well-known design of the brake shoe, which involves the interaction of the brake pad with the wheel's surface, is limited by the limits of their permissible heating. The use of disc brakes is becoming more widespread, because the required braking power is not achieved with the help of shoe brakes. The use of shoe brakes at high speeds is also undesirable due to the fact that the wear of the wheels increases significantly.

In the course of operation, the surface of the riding and the rudder of the running wheels interact with the rails, and in the case of clutch braking - and with the blocks on the brake axles. As a result, both friction pairs mutually influence the process of wearing the wheels and rails, forming a contact zone between them and the level of contact stresses that arise, and, consequently, on the coupling forces that determine the size of the traction and braking forces of the rolling stock.

Modern world studies to improve the effectiveness of friction interaction consist of work on the following main areas:

- mathematical modeling of thermo physical and mechanical processes in the zone of friction contact in the wheel-brake system, necessary for the analysis of existing and advanced brake equipment;

- assessment of reliability and technical risks of operation of brake equipment;

- computer simulation of thermo physical and mechanical processes in the zone of frictional contact of brake elements using finite element models and analysis of its results;

- research on computational hydro-gas dynamics;

- experimental studies of friction processes with cyclic temperature stabilization at high speed;

- development of tools aimed at controlling friction processes, including for the improvement of brake devices;

Significant influence on the process of braking the rolling stock is dynamic. In this case, special attention is paid to improving the methodology to determine the appropriate effort. Also, promising directions for improvement of the respective qualities of freight wagons are currently proposed, and some separate positive results are presented [3].

Among the modern studies, a significant place is occupied by the research of thermal stresses of disc brakes, in particular the study of dynamic loads, research of the ventilation apparatus of brake discs, analysis of the mechanisms of heat transfer of brake friction elements.

The need to supplement existing research does not call into question the characteristics of the friction processes presented in the studies. The authors of the works point to the need to ensure a stable coefficient of friction of the friction surfaces, reduce the temperature and reduce the probability of occurrence. Consequently, based on the world's leading research, the task is to develop a scientific basis for thermo coupling in the rail brake tribo parts and effective methods for improving the brake friction system in order to increase the braking performance by controlling the temperature in the friction pair.

Purpose. Definition and substantiation of the most effective methods of perfection of the brake friction system in order to increase the braking efficiency by controlling the temperature in the friction pair, increasing the thermoregulation and energy dissipation capacity in the braking systems. Creation of a method for increasing the efficiency of the braking system by controlling the cooling of the friction surfaces by adaptive air supply; the creation of a mathematical model of the dependence of the optimal diameter of the friction lining holes on the air pressure supplied in them, the air flow from the pressure and the method of assessing the influence of factors on the operation of the braking equipment during the supply of compressed air to the frictional contact.

Research methodology. Presentation of the main research material. To study the question put in the article used the method of expert evaluations.

The method of expert evaluations allows to work with insufficiently formalized and structured tasks, which are not clearly defined algorithms, properties and relations [71]. The ease of use of the expert estimation method, its flexibility and the ability to obtain the necessary information led to its use to assess the options for improving the braking system elements to stabilize the temperature in tribo-contacts. The group of experts included scientists and engineers from universities, depot and manufacturers of rolling stock components. Factors for evaluating innovative methods for increasing the efficiency of the braking system of the modern rolling stock are as follows:
  • increased security;

• stable friction characteristics (coefficient of friction, temperature);
• wear resistance;
• Noise level during braking;
• cost of construction and operation;
• ecological factor.

Setting up the task of expert evaluation:

1. Object of research - braking systems.

2. Number of options proposed by experts n.

3. The evaluation of options involves m experts.

4. Each expert has his rank, which is determined by the level of his competence and sources of assessment arguments.

5. Each expert conducts a qualitative assessment of the proposed options.

6. All variants of improvement of brake elements should be distributed on their significance.

Innovative methods of increasing the efficiency of the braking system of the modern rolling stock are as follows:

IM1 - forced air supply to the contact of tribo elements;

IM2 - forced air supply, the temperature of which is regulated depending on conditions and modes of operation;

IM3 - application of pads with powdered inserts;

IM4 - application of pads with cooling ribs;

IM5 - application of brake linings whose outer surface is made of heat-dispersing material;

IM6 - supply to the contact area of tribo elements of friction activators;

IM7 - the application of brake elements in the construction of which provides for phase transitions.

The processing of the results of the expert evaluation was carried out with the help of the program developed by the authors (Table 2.1).

As a result of the conducted expert research the estimation of innovative methods of increasing the efficiency of the braking system of the modern rolling stock has been evaluated. It has been established that the most promising method of increasing the braking efficiency is the supply of air with adjustable temperature, depending on braking and operating conditions. This method received the highest rank of 0.237. However, other methods can also be considered promising, since the difference in estimates is negligible. According to experts' opinion, the slightest effect on temperature stabilization has the edges of cooling pads (the sum of ranges is 0.114).

Table 2.1

Results of the expert evaluation

Factor	Expected value	Weight factor	Variation in swing	Standard deviation	The coefficient of variation
Factor1	4,909	0,175	2	0,905	18,4
Factor2	6,636	0,237	1	0,651	9,8
Factor3	4,273	0,153	1	0,603	14,1
Factor4	3,182	0,114	2	0,778	24,5
Factor5	4,273	0,153	3	1,168	27,3
Factor6	3,273	0,117	2	1,015	31
Factor7	5,455	0,195	1	0,674	12,4
Coordination factor = 0,4					

On the basis of the analysis of leading modern researches and patents of technical solutions aimed at improving the frictional properties of brake tools, the following classification of methods for the implementation of thermoregulatory and energy dissipation functions in braking systems has been developed.

1. Thermal regulation is based on the absorption or allocation of heat by metallic or non-metallic friction elements of brake devices. In this case, you can use [19]:

1.1. Chemical reactions to materials of friction overlays with release or absorption of heat.

1.2. Effects of allocation and absorption of energy when the aggregate state of friction elements changes (melting, evaporation, sublimation, crystallization, etc.).

1.3. Physical properties of materials of friction elements, which provide high heat output.

2. The thermoregulation is based on the removal of heat outside of the friction pair of friction elements.

2.1. Ventilation and self-ventilation.

2.2. Extraction of heat with special cooling elements.

The analysis of the results of the processing of expert data indicates that, according to experts, the most effective methods are cooling of frictional contact, improvement of the ventilation device of disc brakes.

This task can only be performed on the basis of new scientific and technical solutions in the field of brake equipment, which will allow the creation of a system of forced cooling of the disc brakes, which will provide

effective characteristics of the cooling process, will have acceptable mass-dimensional and fire performance and significantly reduce the dependence of the coefficient of friction on temperature, which is generated in the contact zone of the working elements during braking.

Method of cooling the brake frictional contact by supplying compressed air. The mechanical part of the disc brakes of the freight car consists of brake discs, which are pressed on two on each wheel set, brake linings and brake blocks (fig. 2.37).
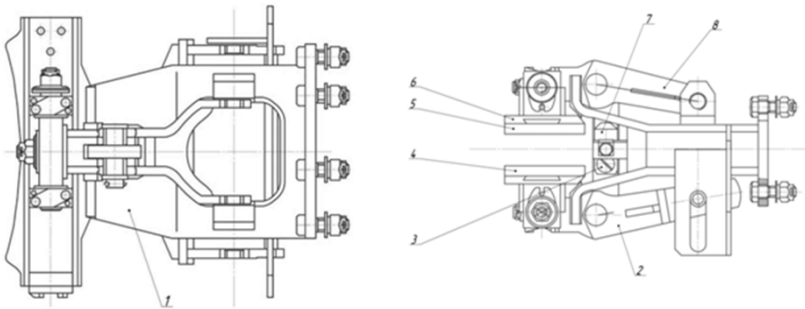

Fig. 2.37. Brake block

Braking made disc brake , which consists of brake blocks (Fig. 2) fixed by means of bolted connections to the transverse beams frame brackets cart. Brake blocks consist of case 1 (Fig. 2.32) respectively, and tick-borne mechanisms. Internal mite lever mechanism pivotally connected according to the rod and casing brake cylinder longitudinal rods. Tick-borne mechanism consists of two levers and 8-tightening divider 7, 6 shoe, brake linings 5 and 4, nuts, washers and pins. With pincers shaped bilateral arrangements made to effect brake linings, brake discs, mounted on axes wheel sets. The pulling divider that works as hard rod and gear lever effort from one to another, moving them toward the brake disk, while providing uniform gaps between the pads and the disc brakes with vacation. Fixing levers pincers shaped skid mechanism configured to move them in two mutually perpendicular directions, providing uniform pressing the brake pads to the brake disc surface. Cover installed in the guide holders and closed blocking bolt that kept locking spring. Both wheel pairs cars found two brake disk (Fig. 2.38).

The proposed method of braking a railway vehicle and equipment for its implementation is as follows [15].

1 Compressor pumps in the main tank 2 compressed air, which in the feed line 3 goes to the crane driver 4. The crane driver connects the main tanks 2 and feed line 3 from brake manifold 5.
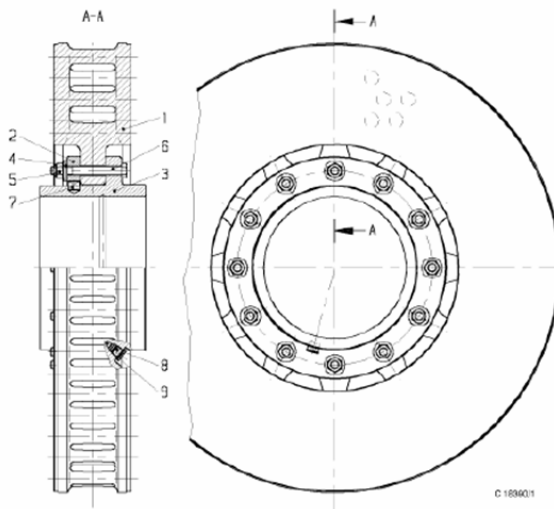
Fig. 2.38. Vented brake disc:
1 – Friction ring, 2 – Clamping ring, 3 – Hub, 4 - Washer or clamping sleeve,
5 – Lock Nuts, 6 – Hex bolt, 7 – Screw for locking rotation, 8 – Threaded plug,
9 – A sealing ring

Before sending the train brake charge, which handle the crane driver 4 put in the selling position (Fig. 3.34), in which air from the main reservoir 2 through the feed line 3 via crane driver 4 enters the brake lines 5 and then through distributor air 6 - in reserve tank 8. this brake cylinder 7 through the air distributor 6 and a check valve 10 communicates with the bellows 9, which accumulates compressed air. The check valve 10 provides compressed air moving in one direction with a brake cylinder bellows and prevents air movement in the opposite direction.

For the train braking the crane handle for a driver 4 is transferred to the braking position, feed line 3 is disconnected and the brake lines 5 through valve 4 communicates with the atmosphere *Am*. When lowering the pressure in the air distributor line 5 6 comes into effect, divides brake cylinder 7 with bellows 9 and combines it with a spare tank 8 filled with compressed air. When applying compressed air in the brake cylinder piston rod 7 moves and transfers braking force through longitudinal rod 13 to chuck mechanisms 14 press brake shoes with brake plate 15 and brake disc 19. Further work control valve bellows 9 and 11 compressed accumulated air through a rubber pipe 12 under pressure is fed into the hole 16 (Fig. 2.40) brake pads 15. This contact helps to cool "brake pad - brake disc" [9, 20]
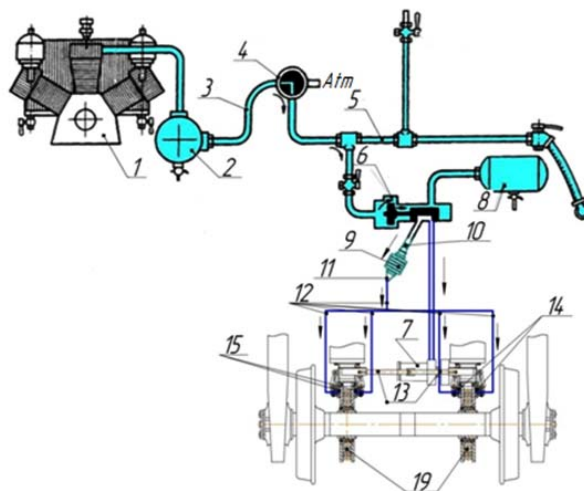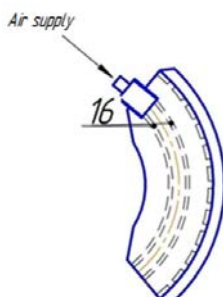
Fig. 2.39. Method of braking a railway vehicle

Fig. 2.40. Composite brake lining with holes

Also developed a disc brake of a railway vehicle, comprising brake discs, brake cylinders, brake pads, shoes, according to a prototype and the forced cooling system frictional contact disc and cover with compressed air from the brake line. The technical result of the use of project equipment includes braking efficiency and reduce the intensity of wear of brake linings through the timely removal of products frictional wear of the friction zone, cooling zone frictional contact "brake pad - brake disc" improving traffic safety by increasing braking reliability.

When supplying compressed air between the brake linings and the brake disk during braking, one can identify the factors that will affect this process:

• The air pressure supplied between the brake disc and the brake linings;

• the diameter of the inlet openings of the fittings in the brake linings;

• Optimal clearance between the brake disc and brake pads (before the braking process so that the air has time to blow off the pads).

The parameters governing the operation of the braking mechanism, when the compressed air is supplied between the brake pads and the brake disk, are as follows:

• air flow from the receiver;

• coefficient of friction, coefficient of efficiency and coefficient of stability of the brake mechanism;

• the uniform distribution of air over the surface of the friction pad during braking;

• Specific braking force.

In view of this, it is necessary to define and recommend the value of pressure of compressed air and the diameters of the inlet holes so that the force of counteraction from the compressed air does not lead to deterioration of the above parameters.

That is, it is necessary to numerically determine the factors that affect the process of supplying compressed air between the brake disc and brake linings during the braking process and the dynamics of their action.

In the case of forced cooling by compressed air, the surface of the brake lining should be considered as an aerostatic slip resistance. Its basis will be a friction pad with symmetrically located holes for the supply of compressed air, relative to the longitudinal axis (Fig. 2.41).

The calculation of the aerostatic support is based on the approximation of the pressure field in the gap by difference algebraic equations. The method takes into account the two-dimensional distribution of the gas flow in the supports of different configurations and gives results close to the real ones. In each of the points it is necessary to consider the integrated equations, using known formulas for the approximate calculation of derivatives.

There are several methods of supplying and distributing gas in the gap. Very effective is the sectional system of gas supply with its distribution in the working gap on the micro cavities. The calculation scheme of a single-channel straight-line aerostatic support, applied with a guide width of less than 40 mm.

The gas is fed to the pressure bearing ρ_0. Passing through the hole of the submersible diameters d, the gas with pressure p_d enters the micro curve length l; moving along the last, through the gap goes to the environment. The

micro cavity, in combination with the stationary part of the support, forms a capillary feeding channel having a split in the form of an equilateral triangle of height t (depth of the groove). Due to the small amount of air flow that flows through the lubrication gap, the flow along the capillary can be considered laminar.
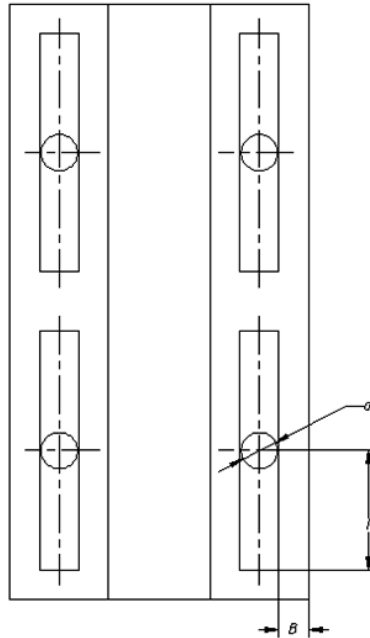

Fig. 2.41. Settlement scheme

A more precise solution of the problem of laminar lubrication of the support is associated with great difficulty, since the flow of lubrication through the hole-spatial: the flow velocity, in addition to the constituent $\frac{\partial y}{\partial t}$,, also has the component $\frac{\partial x}{\partial t}$. These components are proportional to the corresponding pressure gradients. The pressure gradient $\frac{\partial p}{\partial x}$ along the capillary is small in comparison with the pressure gradient $\frac{\partial p}{\partial y}$. from which it can be assumed that the flow along the y axis is flat and directed perpendicular to the

capillary axis. The current line received confirms the admissibility of such a simplification of the task.

Consider an element of the lubricating layer of width dx and height h, located at a distance x from the inlet. The gas flow through the separation of the capillary decreases with increasing x due to leakage through the gap, at $x=l$. Reducing the mass flow dm_x on the segment of the capillary dx should be equal to the mass flow through the gap (on both sides of the capillary) on the same segment in the direction y. This condition of continuity of the flow is used to construct a differential equation of support.

In the laminar flow, the volume flow of gas through a capillary with a transverse intersection of an equilateral triangle is associated with a pressure gradient formula:

$$q_x = -\frac{\partial p}{\partial x} \cdot \frac{\sqrt{3}t^4}{180\mu},$$

Where t is the depth of the microcavity;
p is changeable pressure in the channel;
μ is the dynamic viscosity of the gas.

Fluctuations in temperature of gas during its slow flow along the capillary are insignificant; so there is a correlation

$$\rho = Ap,$$

where p is the density of the gas;
A -Some permanent.

Taking into account (1) and (2) the increase in the mass flow of gas along the capillary on the element dx will be

$$dm_x = \frac{\partial}{\partial x}q_x Apdx = -A\frac{\sqrt{3}t^4}{360\mu}\frac{d^2p^2}{dx^2}dx,$$

Because $\frac{\partial p}{\partial x}p = \frac{1}{2}\frac{\partial p^2}{\partial x}$.

The mass flow in the direction of the y axis on the same segment dx equals the gain $\frac{1}{2}dm_y$, the capillary in the direction of the y axis:

$$\frac{1}{2}dm_y = q_y Ap_3 dx = -A\frac{h^3}{24\mu}\frac{\partial p_3^2}{dy}dx;$$

Here p_3- alternating along the axis y pressure in the gap; ρ - pressure in the capillary.

Expression (4) is a linear differential equation of the first order

$$\frac{\partial p_3^2}{\partial y} = const,$$

because dm_y is a constant value for the intersection x. Its integration with allowance for the boundary conditions $p_3 = p$ for $= 0$; $p_3 = p_a$ for $y = B$ leads to the equation of distribution of pressure along the y axis:

$$p_3^2 = -\frac{p^2 - p_a^2}{B} y + p^2.$$

Where

$$\frac{\partial p_3^2}{\partial y} = -\frac{p^2 - p_a^2}{B}$$

Substituting (6) in expression (4) we give the latter to the form

$$dm_y = A \frac{h^3}{12\mu} \cdot \frac{p^2 - p_a^2}{B} dx.$$

The sum of elementary increases in costs in the direction of x and y hould be zero. This condition leads to a differential equation

$$\frac{h^3}{B}(p^2 - p_a^2) = \frac{\sqrt{3}t^4}{30} \cdot \frac{d^2 p^2}{dx^2}$$

Substituting the function $p(x)$ obtained in the equation (5) as a result of the solution of the last equation, we find $p_3 = p_3(y)$.

Indicate the characteristic of a flat support with a microcavity

$$K = 17{,}3 \frac{l^2 h_0^3}{B t^4}$$

and dimensionless parameters:

$P = \frac{p}{p_a}$ – relative pressure in the capillary;

$X = \frac{x}{l}$ – relative coordinate;

$H = \frac{h}{h_0}$ – relative clearance (h_0 – estimated clearance).

In addition, we will denote the reduction of the record

$$m^2 = KH^3 = 17{,}3 \frac{l^2 h_0^3}{B t^4}.$$

The differential equation of pressure distribution along the capillary will have the form

$$\frac{\partial^2 p^2}{\partial X} - m^2 P^2 + m^2 = 0$$

The general solution of this equation will be

$$P^2 = C_1 e^{mX} + C_2 e^{-mX} + 1$$

Taking into account the boundary conditions, $P = P_d$ at $X = 0$ (at the exit of the throttle with a diameter d) and $\frac{\partial P}{\partial X} = 0$ at $X = 1$ (since the gas flow at the end of the capillary can be taken to be zero), we determine constant integration and find the law of pressure distribution along the length of the capillary:

$$P^2 = \frac{(p_d^2 - 1)e^{mX}}{1 + e^{2m}} + \frac{(p_d^2 - 1)e^{-mX}}{1 + e^{-2m}}$$

The results of calculations by the equation (11), as well as the dependence of the specific rigidity of the resistance to pressure P_d, are calculated and presented in the form of tables and nomograms.

For further calculations, a number of known parameters are given and the required ones are calculated. For the design brake pad we find an expression that determines the optimal hole diameter, depending on the pressure p_0.

$$d = \sqrt{\sqrt{\frac{K_1 \gamma_0}{g} \frac{t^4}{102 \alpha l \mu}}},$$

where K_1 – specific stiffness of the support,

γ_0 - specific gravity of air at pressure p_0,

t – groove depth

α – coefficient of production,

μ – is the dynamic air viscosity.

Figure 2.42 shows the results of calculating the optimal hole diameter, depending on the pressure at different values of the length of the groove l

According to the data obtained, under the pressure of air, which is fed into the openings of the brake lining up to 0.4 MPa (pressure in the brake cylinder during braking of the car), the estimated diameter of the holes does not exceed 8 mm.

It is also necessary to analyze the force of counter pressure, which is formed when compressed air is used to cool the frictional contact and to classify the products of wear. It is calculated by the formula

$$Q = p_a p_0 B l n K_{\text{н}},$$

where $K_{\text{н}}$ is the specific strength of the counterweight. By varying the number of holes n, the geometric parameters of the element of the aerostatic support (overlays) and the pressure, different values of the force of the counterweight Q can be obtained.
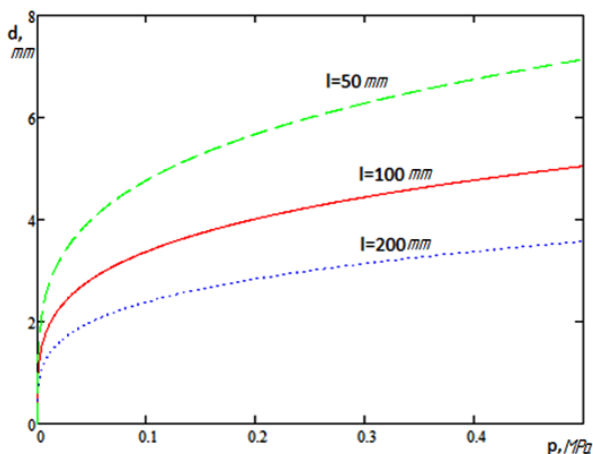

Fig. 2.42. Calculating the optimal hole diameter

Here is a plot of the dependence of the force of the counterweight Q on the number of holes n in one overlay. According to the formula, it is linear (Fig. 2.43

Figure 3.43 shows the dependence of air flow rate on pressure during braking.

Thus, for $p_0 = 0{,}4$ МПа, $l = 10$ см, В $= 2$ см, $p_a = 0{,}1$ MPa of the pressure compensation is 1.44 kN for two apertures in the overlay and 14.4 kN for twenty holes in the overlay. Depending on the force of pressing the brake linings on the axle and other parameters of the braking system, the parameters of the design brake lining are determined.

Conclusions and prospects for the development of the direction. According to the results of the planned strategic principles of the

development of the world rail system, analysis of the expert survey of specialists of research organizations in the field of rail transport, increasing the efficiency of the operation of brake equipment is one of the most important factors for increasing the speed of traffic, safety and energy efficiency of rail transport [36].
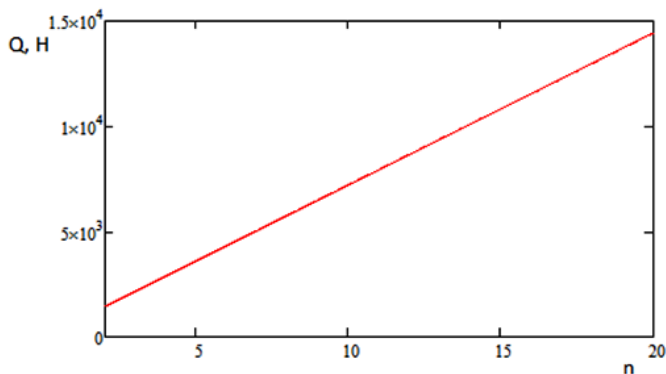

Fig. 2.43. The graph of the strength of the counterweight Q from the number of holes n in one overlay
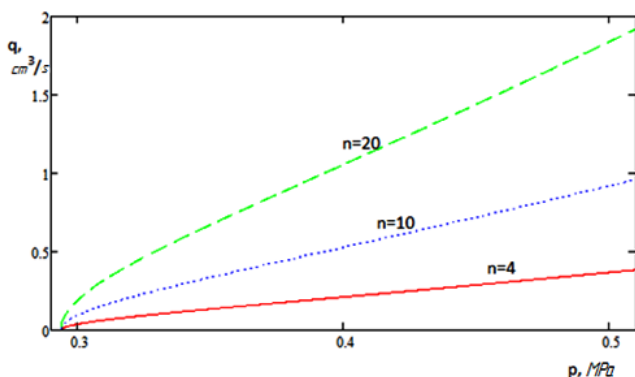

Fig. 2.44. Dependence of air flow rate on pressure

An innovative method for controlling the temperature of brake friction surfaces is suggested, which will promote further development of high-speed locomotive movement. The method differs from the novelty of the developed

solutions, represents the theoretical and practical value in the direction of improving the performance characteristics of brakes [34]. For the proposed method, an assessment of the influence of factors on the operation of the braking equipment during the supply of compressed air to the frictional contact is made. The scientific novelty of the research consists in the creation of a mathematical model of the dependence of the optimal diameter of the friction lining holes on the air pressure supplied to them, the air flow from the pressure.

3. FUNDAMENTALS OF MACHINE DESIGN

3.1. Classification of machine building products

All products of machine building plants, *various engineering means, separate aggregates, mechanisms, devices or other structures,* consist of details.

Detail is the element of a structure made of some grade material without assembly operations.

Details are divided into:
- *simple* – bolt, screw, clout, bung, etc.
- *compound* – crankshaft, reducer shell, etc.

Assembly unit is the set of details joined by a manufacturer by special assembly operations (*welding, screwing, riveting, soldering, etc.*) which fulfils some joint action (e.g. connecting rod of a diesel locomotive engine, rolling and sliding bearings, pumps, compressors, reducers, etc.).

"Complexes" and *"complete sets"* are a totality of assembly units made by a manufacturer which provide certain functions within a corresponding structure after its assembly at a destination place (e.g. pump stations, diesel generator stations, automated machine lines, sets of spare parts, etc.).

Basic criteria requirements for machine details
- operational integrity,
- reliability,
- manufacturability,
- efficiency,
- aesthetics, and
- ecological compatibility.

OPERATIONAL INTEGRITY is the state of a facility, at which it can perform its functions (*can function*), maintaining the basic parameters established by the normative documents.

OPERABILITY CRITERIA

- strength (*main criterion*),
- rigidity,
- stability,

- vibration resistance,
- wear resistance, and
- heat resistance.

Strength is the capacity of details bear integrity under the loads applied.

Rigidity is the capacity of details to resist deformations (*change in shape and size*) under the loads applied.

Stability is the capacity of details to maintain the initial (*rectilinear*) equilibrium form even under small lateral loads.

Vibration resistance is the capacity of a facility to function in operational modes without inadmissible levels of vibrations.

The mathematic modelling of vibration characteristics in order to provide the required level of vibration resistance through construction of appropriate systems of vibration protection is of special attention of design engineers dealing with modern transport engineering facilities [48-49, 95-96].

Vibration is the process of mechanical oscillations in movable engineering systems. A level of vibration activity is the vibroactivity.

Vibration negatively affects operation of a facility (*change of needed operational characteristics*), and the maintenance personnel (*visual and hearing impairment, disorders in biochemical composition of blood, etc.*).

Vibroprotection *is a set of operations aimed at decreasing vibration of a facility to a needed level in terms of their normal operation, and also with consideration of the influence of vibration on people and environment.*

Regarding vibroprotection in mechanical systems two subsystems are distinguished: SV and *OB,* which are connected with links *L:*

$$SV \xrightarrow{\ L\ } OV$$
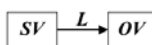
SV (source of vibration). It is a subsystem in which physical processes directly run and cause vibration.

OV (object of vibroprotection). This subsystem is part of a mechanical system, vibrations in which should be decreased.

Forces emerging in link *L* which connects the object and source of vibrations and causes vibrations of the object are called *the force* (*dynamic*) *action*.

The design of transport facilities requires evaluation of their vibroprotection by the value of *the coefficient of vibroprotection*.

$$\gamma = \frac{\left| Z_{max}^{OB} \right|}{\left| Z_{max}^{HB} \right|},$$

where $\left|Z_{max}^{OB}\right|$ and $\left|Z_{max}^{UB}\right|$ are the maximum amplitudes of vibrations of an object of vibroprotection and a source of vibrations, respectively.

The vibroprotection task is fulfilled if the coefficient of vibroprotection $\gamma < 1$ (*the vibroprotection condition for a facility*).

The designing techniques in terms of vibroprotection use the systems which provide *vibration insulation* of vibroactive objects or *vibration damping* of corresponding vibrations.

The vibration insulation systems provide for insulation of vibro-active structural modules or a whole facility from adjacent modules (use of rubber-to-metal silent-blocks, rubber pods, designing vibration insulation armchairs, etc.).

Vibration damping systems are divided into static and dynamic.

Static vibration damping systems provide for:

❖ introduction of elements increasing viscous resistance of vibration processes in the structure of a facility (*use of hydraulic and pneumatic dampers [shock absorbers], dry friction dampers [springs], etc.*).

❖ design and use of special multilayer details, which increase viscous resistance to vibration processes due to friction between adjacent layers, in vibroactive mechanisms.

❖ design of a facility by the condition of a low initial level of vibroactivity (the use of self-balancing or structural balancing with counterweights, balance-beams, rotors, etc.).

Dynamic (active) vibration damping systems provide for the use of special devices, vibration dampers, which create dynamic counterinfluences to acting vibrations and decrease their effect. The simplest example of such systems is a mechanical gear linkage system of Lanchester used for balancing the inertia forces of the reciprocating masses in an internal combustion engine.

In order to protect facilities and biological objects (humans, first of all) from vibrations of the low-frequency range, where static systems are of low-inefficiency (especially from time-variant vibration spectra), automated dynamic vibro-protection systems are used.

Structural diagram of a vibro-protection dynamic system
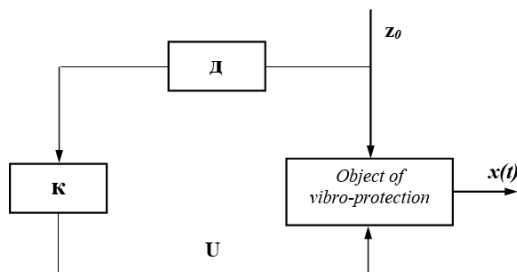*controlled by the excitation compensation method*

Fig. 3.1. Vibro-protection dynamic system

Such systems are controlled on the basis of excitation compensation methods, compensation of the deviations of a regulated variable, or their combination.

Control of such a system requires a possibility to register (*modeled in design*) vibration excitations and have appropriate execution modules of the structure for their compensation.

The diagram (Fig. 3.1) demonstrates that exaltation z_0 (e.g. vertical vibration displacements of an internal combustion engine) is perceived by sensitive element Д (*sensor*), the signal from which is transmitted to bucking-out system К which fulfils regulated counteraction U, which compensates excitation z_0 and supports the specified law of motion of object *x(t)*, while satisfying the requirements for the vibration level (*degrees of compensations* z_0).

Wear resistance is the capacity of material to resist wear.

The wear resistance of details considerably decreases under corrosion. Corrosion is the process of constant damage of surface layers of metal due to oxidation.

Heat resistance is the capacity of details of a facility to maintain operating capacity within the prescribed limits of a temperature change conditioned by the working process and friction in its mechanisms and units.

Excessive heating of details can cause:
- lower material strength,
- additional deformations and stresses,
- breakage of normal lubrication conditions (*increased wear*), and
- change in gaps of mating parts.

Calculations aimed at support and control of operation capacity
are divided into two groups: design and test.

The objective of design (*preliminary*) calculations is determination of the basic sizes of details which satisfy most important criteria for the operation capacity.

Complete mechanical stress:

$$\overline{p_n} = \overline{\sigma} + \overline{\tau},$$

where $\overline{\sigma}$ is the normal stresses;

$\overline{\tau}$ are the tangential stresses.

For example: the strength condition for a detail which bears tensile deformation:

$$\sigma_{max} \le [\sigma], \quad [\sigma] = \sigma_{on} / n,$$

where σ_{on} is the unsafe stresses;

n is the safety factor.

Under complex deformation (e.g., calculation of shafts):

$$\sigma_{экв} \le [\sigma], \quad \text{where } \sigma_{экв} \text{ is the equivalent stresses.}$$

Revised calculations

The objective of revised calculations is determination of the safety factors in unsafe sections of details of facilities.

Condition of a safety factor:

$$S \ge [S],$$

Where *S* is the safety factor in an unsafe section of a detail,

[S] is the permissible values of a safety factor.

RELIABILITY is the capacity of a facility to fulfill the prescribed functions (*to maintain the operation capacity*) during a needed time or running hours.

CRITERIA OF RELIABILITY

- refusal,
- durability,
- maintainability, and
- safety.

Refusal is a loss of operational capacity of a facility.

Durability is maintenance of operational capacity of a facility to the boundary state at which its further operation is impossible or inefficient.

Maintainability is the capacity of a facility regarding regeneration of operational capacity to prevent failures, reveal and remedy faults in maintenance and repair.

Safety is assurance of operation capacity during and after the prescribed terms of storage and transportation [40].

The probability of no-failure operation is widely used as a factor to assess operational reliability of a device in solving technical and engineering tasks; it demonstrates that within a given interval (running hours) no failures of the facility are registered [16].

Probability of no-failure operation: $\quad P(t) = 1 - \dfrac{N(t)}{N},$

where $N(t)$ is the number of test facilities in which failures are registered,

N is the general number of test facilities.

Probability of no-failure operation of an engineering system:

If structural modules are connected in series:

$$P_{\Sigma nocn} = P_1(t) \cdot P_2(t) \cdot ... \cdot P_n(t) = \prod_{i=1}^{n} P_i(t).$$

If structural modules are connected in parallel:

$$P_{\Sigma nap} = 1 - \prod_{i=1}^{n} \left[1 - P_i(t) \right].$$

MANUFACTURABILITY of details and assembly units is characterized by the minimal expenditures of materials, time and labor in production, operation and maintenance.

Major ways to provide manufacturability of details:

▪ simple outline surfaces of details (*cylindrical, conical, etc.*) which are easy in the mechanical and physical treatment;

▪ use of building materials which require low-waste and resource-saving treatment technologies for manufacture of details (*pressing, precision casting, laser, explosive, welding etc.*); and

▪ effective use of a single system of tolerances and fits (*grounded technical specification for manufacturing*).

EFFICIENCY is characterized by achieving a high cost-effectiveness of a facility in design, production and maintenance.

The basic quantitative factor of economic efficiency is the annual saving rate

$$E_{\varepsilon} = (E_n + E_{\vartheta}) \cdot A_n,$$

where E_n, E_{ϑ} are the savings at production and maintenance of a new facility, in comparison with the values of the facility replaced, respectively;

A_n is the annual output of a new facility.

AESTHETY is the level of perfection and attractiveness of forms, exterior view of details, assembly units and the whole facility.

ECOLOGICAL COMPATIBILITY is the no adverse effect level for humans and environment.

3.2. Basic types and characteristics of modern materials

A choice of materials for details and units of mechanisms is a very significant stage for a designer engineer. Therefore, some *special requirements* should be satisfied so that to provide operational capacity and reliability. *For example,* for mechanisms of aviation and space engineering the basic requirements are provision of the minimal mass and overall dimensions; for details working at sliding friction – wear resistance, at high temperatures – heat resistance etc [26]. The technological characteristics of materials should conform to production methods (*casting, press forming, cutting*) and production types (*series or mass*). Besides, cost of the material chosen is of considerable importance.

Machine engineering uses the following materials for machine elements:
- ferrous metals:
  - ⇨ *steels,* and
  - ⇨ *iron casts.*
- non-ferrous metals:
  - ⇨ *copper-based alloys (brass, bronze),*
  - ⇨ *tin-based alloys (babbits),*
  - ⇨ *aluminum alloys,* and
  - ⇨ *titanium alloys.*
- combined materials:
  - ⇨ *composite,*
  - ⇨ *reinforced,* and
  - ⇨ *metal-ceramic.*

- non-metal materials:
  - ⇨ *plastics,* and
  - ⇨ *rubber.*

The choice of a material is determined by:
- functionality of a detail,
- conditions of its operation,
- structural requirements,
- technological requirements, and
- efficiency requirements.

<center>*STEELS*</center>

Steels are iron-carbon alloys in which the carbon content does not exceed 2%.

Steels are divided into carbon and alloy.
Carbon steels are divided into:
- low-carbon ($C < 0,25\%$),
- medium-carbon ($C = 0,25......0,6\%$), and
- high-carbon ($C > 0,6\%$).

Carbon steels are divided into:
- steels of regular quality (Steel 0, Steel 1, … , Steel 6)

They are used for production of basic and fastening details, and also additional, non-responsible details, which operate at low stresses.
- quality structural steels
  - ➤ grades $7......10$: used for details operating at constant stresses;
  - ➤ grades $15......20$: used for details bearing insufficient dynamic loads;
  - ➤ grades $30......55$: used for loaded details.

Marking of carbon steels uses figures indicating the carbon content in hundredth of percent (e.g. steel grade *40* means the carbon content is *0.40%*).

The steel with low amount of carbon is characterized by *high plasticity and weldability*. When the carbon content increases the strength increases, the plasticity decreases and weldability worsens.

Alloy steels are produced from carbon steels by adding *alloying elements* (*Cr* – chromium, *Ni* – nickel, *W* – wolfram, *Al* – aluminum, *Mn* – manganese, *Mo* – molybdenum, *Ti* – titanium, etc.) in order to increase the indices of strength, yield, impact elasticity etc. The element factor in percent is indicated with figure after letter. If the figure is not included in the marking, the content of alloyed element is less than *1 %*.

<center>146</center>

According to the amount of alloying elements (*AE*) the steels are divided:

➢ low-alloy ($AE < 3\%$),
➢ medium-alloy ($AE = 3.0......5.5\%$),
➢ high-alloy ($AE > 5.5\%$).

For example, steel 38Cr2Al
0.38% - carbon, 2% - chromium, 1% - aluminum.

Alloy steels are divided into:

➢ quality, and
➢ high-quality (letter *A* is added in marking):
  (e.g., steel 12Cr2N4A – 0.12% carbon, 2% chromium, 4% nickel, A – high-quality steel).

Carbon and alloy steels are tempered, the process includes three stages: heating to a required temperature, soaking at this temperature and cooling with a prescribed speed. The basic types of the steel thermal treatment are:

- *anneal:* mainly used to decrease the hardiness in order to facilitate mechanical treatment and relieve the internal stresses in steel. The annealing temperature depends on the carbon content in steel.

- *normalization:* used to improve the steel structure, relieve the internal stresses and provide better conditions for cutting. It differs from anneal by cooling in open air and not in a furnace.

- *hardening:* heating steel to a certain temperature, annealing at this temperature with a further rapid cooling in water, oil, melted salts or in air. Annealing is used together with tempering to increase hardness, strength and wear resistance of steel.

At rapid cooling during anneal there appear internal stresses in metal, which can cause cracks, distortion and brittleness. These defects are eliminated with further tempering.

- *tempering:* heating steel to the temperature much lower than that during annealing, soaking at this temperature and cooling in air.

Details bearing the maximum stresses on the surface (flexure, torsion, contact stresses), are exposed to the surface hardening to increase the fatigue resistance. There exist the following methods of surface hardening: mechanical, thermal, surface, laser hardening, ion implantation.

Mechanical method. Better resistance of a detail to damages can be achieved by generating tension stresses on the surface. It is obtained with cold hardening by bead blasting with rolls or bullets. Bead blasting is the plastic deformation of the surface layer of a detail at a depth of *0.15 ... 0.30 mm* with steel or iron shot which forcefully beats the surface. Cold hardening increases the surface hardness and the fatigue strength. With the same purpose

cylinder-surface details are exposed to pressure rolling (axles of transport facilities, crankshafts).

Thermal method. Hardening is the basic method, at which a thin surface layer is heated and hardened with high-frequency currents, and the detail core remains viscous. The depth of a hardened layer is *0.5-1.0 mm*, surface hardening is *HRC 50-55*, and the fatigue resistance increases *1.5* times on average.

Surface methods.

Cementation is saturation of the surface layer with carbon at heating to a temperature of *880-950°C* with further hardening. Its objective is to gain a better hardiness and wear resistance of the surface layer of a detail. Cementation is used for carbon and alloy steels with the carbon content to *0.25 %*. Carbonization of steel gives the cemented layer of a depth of *0.8-2.5 mm* and surface hardness *HRC 56-62*.

Nitriding (surface saturation of steel nitrogen at heating to a temperature of 500-700°C in ammonia) increases the corrosion resistance in the atmospheric conditions, and the surface hardness. The depth of the nitriding layer is *0.3-0.5 mm*. Nitriding is used for a better hardiness, wear resistance of a surface layer and the corrosion stability mainly for a detail made of steels containing aluminum, chromium and molybdenum [64].

Cyanidation is surface saturation of steel with carbon and nitrogen simultaneously at a temperature of *530-550°C*. It can be conducted in liquid, solid and gas media. Cyanidation is used to increase strength of twist drills and other high-speed steel tools and details of irregular shapes.

Laser hardening. It is used for hardening surface layers. The process implies melting a very thin layer under emission with rapid hardening and, thus, obtaining new properties. Advantages of laser hardening in comparison with traditional methods are a possibility to treat limited areas of a detail at a specified depth, including nooks of irregularly-configured details.

Ion implantation. It implies bombardment of the surface of a detail with ions of various chemical elements (*carbon, nitrogen, boron, titanium*), causing changes in the structure and chemical composition of the surface layer, and also increasing micro hardness and durability by several times. It is used to increase the strength of cutting tools.

IRON CASTS

Iron casts are ferricarbonic alloys, with the carbon content $C > 2\%$.

According to the structure, iron casts are divided into:
- white (characterized by a high hardness and brittleness),
- annealed (characterized by a high strength and low plasticity), and

- grey (characterized by a relatively high strength, wear resistance and damping capacity – vibration damping).

COPPER-BASED ALLOYS (BRASS AND BRONZE)

They are characterized by high antifriction, casting and anticorrosion capacities, besides, they have sufficient strength.

Brasses (basic alloying element is zinc) are divided into:
- double (copper and zinc alloys). For example, grades Л59, Л62, Л90 with the content of copper – *59, 62, 90 %*, respectively,
- multicomponent (alloys with such elements as lead, silicon, manganese, aluminum, iron, nickel, brass, apart from copper and zinc). For example: grades CuSiPb 80-3-3 – *80%* - copper, *3%* - silicon, *3%* - lead; CuMnPb 58-2-2 – *58%* - copper, *2%* - manganese, *2%* - lead).

Brasses have good corrosion resistance, antifriction properties, electric conductivity, and good technological properties. And their cost is higher, than that, for example, of steels 45 by five times on average.

Bronzes (all copper alloys with the exception of brass) are divided by content of the basic alloying element into:
- tin, and
- tinless.

For example, bronze grades: tin-phosphorous БрОНФ 10-1-1 (basic – copper, *10%* - tin, *1%* - nickel, *1%* - phosphorus); aluminum-iron БрАЖ 9-4 (*9%* - aluminum, *4%* - iron).

Bronzes have high antifriction and anticorrosion properties. And the cost of bronze is higher than that of steel 45 by ten times on average.

TIN-BASED ALLOYS (BABBITS)

Babbits are fusible alloys based on tin, lead, zinc and aluminum with high antifriction properties; they are used as an antifriction material of liners for friction bearings.

The babbits are divided into:
- high-tin (alloy of tin with stibium and copper) the tin content is *>70%*,
- tin-lead – the content of tin is *5.....20%*, of stibium is *15%*, of lead is *65......75%*, and
- lead – the lead content is *>80%*.

For example, babbit grade Б83 has *83%* of tin. The cost of babbits is several times higher than that of bronze.

ALUMINUM ALLOYS

Among aluminum-based alloys are:
- silumins (alloys of aluminum with silicon),
- duraluminium (alloys of aluminum, copper and magnesium).

Aluminum alloys are used as a casting material for making details of irregular shape, and also various bodies, shells, containers, pipes etc., of sufficient strength, and the specific weight of more than three times less in comparison with that of steel.

TITANIUM ALLOYS

They are mostly used in aviation, rocket engineering and chemical machine building for manufacture of critical parts of high strength, heat resistance, corrosion resistance, but with low antifriction properties and low heat conductivity.

By specific weight they are 1.7 *times lighter in comparison with steel, and by stability they are of the highest strength level among alloy steels.*

NON-METAL MATERIALS

Plastics by their strength characteristics are similar to some metals, and by corrosion resistance can be even better.

Among medium-strength materials are laminated plastics, such as getinax (paper-based laminate), textolite (cloth-based laminate), lignofol (lignin-based laminate).

Among high-strength materials are glass-fiber plastics.

Rubber is characterized by high elasticity, weather resistance, and shock absorbing properties.

3.3. Production specifications for machine tools

At present the machines and equipment production as well as their operation and maintenance is based on the principle of interchangeability of parts, assembly units and aggregates.

Interchangeability is the principle to design and manufacture details, which provides a possibility to assemble or change units, manufactured separately and with prescribed quality, without additional treatment and adjustment by maintaining the corresponding quality during repairs.

Interchangeability can be:
- complete (implies connection of all adjacent details in the process of assembly operations without additional treatment); and
- incomplete (implies connection of part of details produced with lower precision without additional treatment).

Size (quantitative value of parameters of a detail) is a numerical value (diameter, length, height, etc.) in chosen measuring units.

Sizes are divided into:
- actual is the dimension set by measuring with a permissible error;
- limiting is two permissible dimension (largest and smallest) between which an actual dimension should be; and
- nominal is the dimension relative to which the boundary dimensions are determined and which is used to read errors (set in designs).

There are upper and lower limiting deviations (Fig. 3.2).
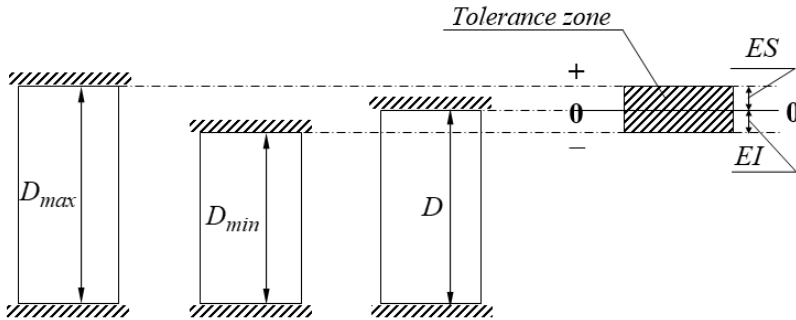
Fig. 3.2. Types of limiting deviations
Positive deviations are above a zero line while negative deviations are under a zero line

In standards:
- upper deviation in size is indicates as *ES*-holes, *es*-shaft,
- lower deviation – as *EI*-holes, *ei*-shaft.

Limiting deviations:

$$ES = D_{max} - D, \qquad EI = D_{min} - D,$$
$$es = d_{max} - d, \qquad ei = d_{min} - d,$$

where D, d are the nominal size of a hole and a shaft,

D_{max}, d_{max} are the largest limiting size of a hole and a shaft,

D_{min}, d_{min} are the smallest limiting size of a hole and a shaft.

Limit sizes and tolerance zone for holes

Tolerance zone is the area limited with upper and lower deviations.

Tolerance (*always positive*) is the difference between the largest and smallest limit sizes or the absolute value of an algebraic difference between upper and lower deviations:

$$T_D = D_{max} - D_{min} = ES - EI,$$
$$T_d = d_{max} - d_{min} = es - ei.$$

> *Tolerancing for detail sizes is regulated*
> *by "The Unified System of Tolerances and Fits"*

Increased sizes of a detail complicate accuracy of its production, therefore for determination of appropriate tolerances, the following dependency is used

$$T_D = i \cdot a,$$

where i is the tolerance unit (*scale factor, mkm*),

a is the number of tolerance units (*precision factor*).

> *Subject to a in tolerance T_D the standards for sizes to 500 mm*
> *establish 19 quality classes (degrees of accuracy).*
> *01, 0, 1, 2, 3, 4, 5,......., 17.*

- quality classes $01.........4$ are used for production of finite measures of length, calibers, and measuring instruments;
- quality classes $5.........11$ are used for tolerances for sizes of mating elements of a detail;
- quality classes $12.........17$ are used for free (mismatched) sizes.

The location of a tolerance zone relative to a zero line (*nominal size*) is marked with one or two Latin letters, capital letters for holes and small letters for shafts.

For example, for a hole: $\varnothing$ 20H7 is the hole of the diameter 20 mm, the tolerance zone corresponds to location of letter H, and by value of quality class 7.

Fit is the character of connection of mating coaxial surfaces of details (*hole and shaft*) (Fig. 3.3).

The nature of a fit depends on the ratio of tolerance zones of the shaft and the hole; it is determined by values of:

- clearances (the size of the hole is larger than the size of the shaft), and
- tightness (the size of the shaft is larger than the size of the hole).

Clearance fit is the fit which always accompanies formation of a clearance.

Interference fit is the fit which always accompanies tightness.

Transition fit is the fit with a possibility to obtain both gap and interference.
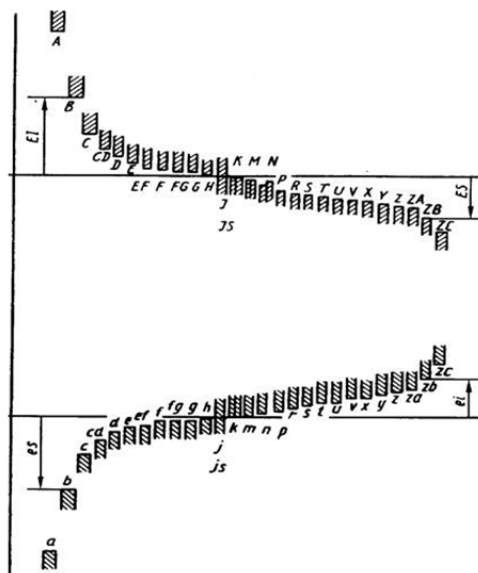
Fig. 3.3. Regarding positions of tolerances zones for sizes of holes and shafts
The Unified System of Tolerances and Fits stipulates formation of fits
in the hole system and fits in the shaft system

153

Fits in the hole system are the fits in which different clearances and interferences are produced by connecting different shafts with *the basic hole*. *The basic hole*, marked with letter H, has lower deviation $EI = 0$.

For example, fit $\varnothing 20H7/g6$ has the nominal diameter 20 mm, the tolerance zone of the hole corresponds to letter H, by value – to quality class 7, the shaft – to letter g by quality class 6.

Fits in the shaft system are the fits in which different clearances and interferences are produced by connecting different holes with *the basic shaft*. *The basic shaft*, marked with letter h, has upper deviation $es = 0$.

For example, fit $\varnothing$ 20K7/h6 has the nominal diameter 20 mm, the tolerance zone of the hole corresponds to letter h by quality class 6, the shaft corresponds to letter K by quality class 7.
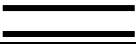
One of the basic components of the production specification for machine parts is standardization *of deviations in forms and surface position*.

Deviation of form is the deviation of the form of an actual surface limiting the body and separating it from the environment, from the form of the nominal surface (ideal surface, the form of which is prescribed by the diagram or the specifications).

The largest deviation of the form is called the *tolerance on form* (Table 3.1)

Table 3.1

Types of deviation

Tolerances on form		Tolerances on position	
Linearity		Parallelism	
Planeness		Perpendicularity	
Cylindrical shape		Inclination	
Roundness		Coaxiality	
Longitudinal section		Symmetry	
		Positional	
		Intersection of axes	

Deviation of surface position is the deviation of an actual position of an element of the surface, axis or symmetry area from the nominal position (Table 3.2).

The limit of the permissible deviation value for position is called *the tolerance on position* (Table 3.1).

<div align="right">Table 3.2</div>

Cumulative tolerances on form and position

Radial motion	
Face motion	
Prescribed motion	
Total radial motion	
Total axial motion	
Forms of prescribed profile	
Forms of prescribed surface	

In order to evaluate the accuracy of surface position the bases are set. The base can be a surface (e.g. plane), *its generatrix or point (e.g. the vertex of cone)* (Fig. 3.4).

If the base is the surface of revolution (cylindrical, conic) or thread, their axis *is considered as the base.*

Fig. 3.4. to evaluate the accuracy of surface position

The basic axes and surfaces in diagrams are marked with a shaded triangle linked with the frame with a capital letter for the base.

In working diagrams of details the notation conventions for tolerances on form and position, as well as marking of bases are located in a frame divided into 2 or 3 parts: in the first – the tolerance sign, in the second – its numerical value in millimeters, in the third (if needed) – symbol of the base (Fig. 3.5).

In design actual detail surfaces differ from the nominal surfaces by periodic irregularities produced in treatment:

• if the irregularity width to high ratio does not exceed *50*, such irregularities are called *roughness*;

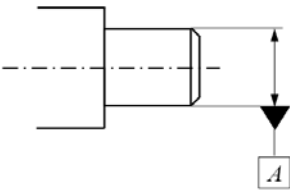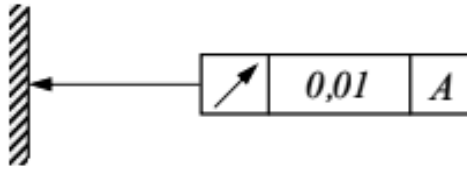• if the irregularity width to high ration exceeds *50,* such irregularities are called *waviness*.

Fig. 3.5. Working diagrams of details

The roughness values are determined (*controlled*) by profilograms produced from detail surfaces with profilographs within the prescribed basic length *l*.

Pure surfaces of small roughness: increase strength and corrosion resistance of details, decrease running-in friction in mating movable details (*kinematic pairs*), *however the cost of their mechanical treatment considerably increases.* (Fig. 3.6, 3.7) [64]
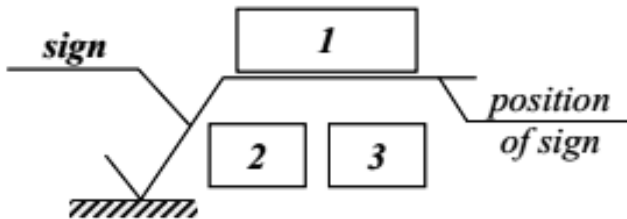

Fig. 3.6. Types of surfaces treatment:
1 – type of surfaces treatment (if needed). For example*,* polishing, grinding;
2 – roughness value (*for example* R_a or R_z),
where Ra (preferred) is the average arithmetic deviation in profile;
R_Z is the height of profile irregularities in ten points (*five highest and five deepest*);
3 – roughness value (in *mkm*)

Details which compose the structure of a facility are joined with links. They can be divided into *movable* (*various joints, bearings, clutches, etc.*) and *immovable* (*threaded, welded, key etc.*). In engineering immovable links are called joints (Table 3.3).
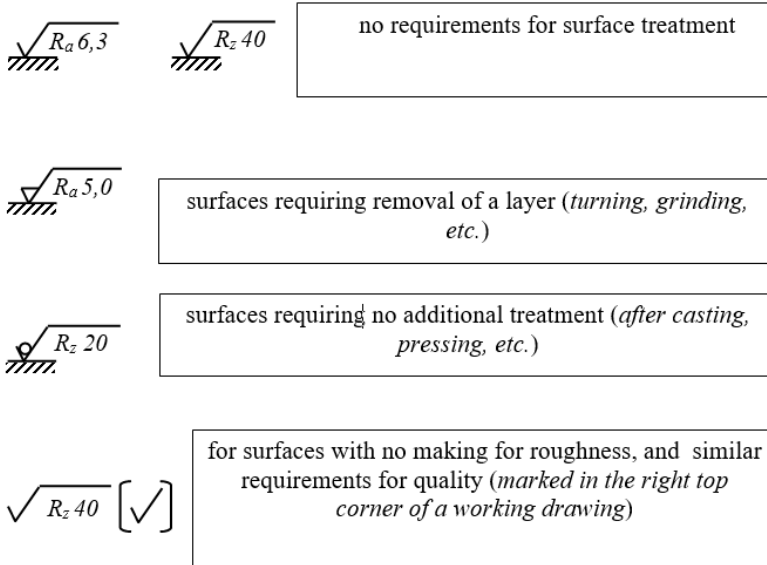
$\sqrt{R_a\,6,3}$ $\sqrt{R_z\,40}$ | no requirements for surface treatment

$\sqrt{R_a\,5,0}$ | surfaces requiring removal of a layer (*turning, grinding, etc.*)

$\sqrt{R_z\,20}$ | surfaces requiring no additional treatment (*after casting, pressing, etc.*)

$\sqrt{R_z\,40}\ [\checkmark]$ | for surfaces with no making for roughness, and similar requirements for quality (*marked in the right top corner of a working drawing*)

Fig 3.7. Joints of machines parts

Table 3.3

Disassembly joints types

detachable – the joints can be dismantled without breaking the details:	*permanent* the joints cannot be dismantled without breaking the details:
- thread; - key; - spline; - profile; - pin.	- weld; - rivet; - interference; - solder; - adhesive.

DETACHABLE JOINTS
Thread joints

Thread joints are the joints made of details with external (*bolts, screws, pins, etc.*) and internal (*nuts, threaded openings in basic parts*) threads.

Thread is projections on the base surface
of screws or nuts and located along the spiral line.

     Thread is manually made with taps or dies, and also on special machines with cutting tools, cutting heads or milling tools. In mass production thread is done with *rolling* (*under pressure*) on thread-rolling automatic machines by plastic deformation of a rough part; rolled threads have a higher durability thanks to cold hardening of the external thread [11].

     Threads are classified by:
- form of the base surface:
  - cylindrical,
  - conic.
- profile shape:

⇨   triangular,

⇨   rectangular,

⇨   trapezoidal,

⇨   round,

⇨   buttress.

- spiral line direction:
  - right-hand,
  - left-hand.
- number of starts:
  - single-start,
  - multiple start (two- and three-start).
- position on a detail:
  - external,
  - internal.

   By functions threads are divided into:

     ❖ fastener (characterized by: comparatively high friction forces preventing self-unfastening; high reliability; manufacturability):

     - metric is the basic fastener thread,

   Its profile is an equilateral triangle, therefore, the thread angle is $\alpha = 60°$. All its sizes are measured in millimeters. Crests and roots become blunt by straight line or arc, which decreases the stress concentration and prevent the thread from breakage. A radial clearance in the thread makes it untight.

     - inch,

The profile is an isosceles triangle with the angle $\alpha = 55°$ in vertex. All its sizes are in inches. It is used in repair of details for import machines.

- pipe,

A small inch thread with rounded crests and roots (the thread angle $\alpha = 55°$). Absence of radial clearances makes it tight. It is used for joining pipes.

- round,

The thread profile consists of arcs, mated by short straight lines (the thread angle $\alpha = 30°$). The thread is characterized by high dynamic strength. It is used only in the harsh operational conditions for polluted environment.

❖ of screw mechanisms (characterized by: small friction forces, which allows decreasing efficiency and wear resistance):

- rectangular,

The thread profile is a square. It has lower strength. The wear generates axial clearances which are difficult to eliminate. (substituted with trapezoidal threads). It is used only in low-load screw-nut transmissions.

- trapezoidal symmetrical,

The thread profile is an isosceles trapezium with the thread angle $\alpha = 30°$. It is characterized by low friction losses. The efficiency is higher than that for threads of triangle profile. It is used for on-load reverse motion (lead-screws of machines).

- thrust (trapezoidal non-symmetrical).

It has the unequal-sided trapezium profile of the angle $\alpha = 27°$. The efficiency is higher than that of a trapezoidal thread. The root rounding increases the fatigue resistance of a screw. It is used in screw-nut gears at high one-sided axial loads (screw-jacks, presses).

Advantages:
o high reliability,
o easy assembly and disassembly,
o high loading capacity, and
o relatively low cost.

Disadvantages:
o stress concentrators in roots which decrease the fatigue stability of a thread joint,
o necessity to actively use locking devices (*to prevent self-unscrewing*).
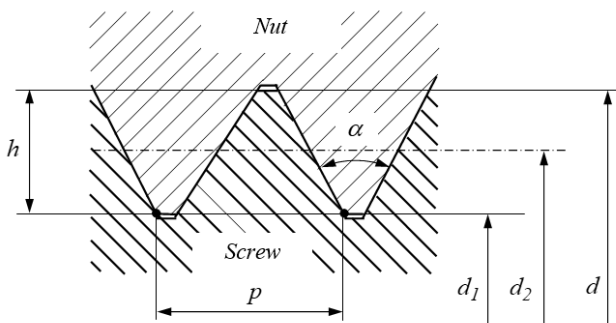
Basic geometrical parameters of a thread (Fig. 3.7):

Fig. 3.7. Basic geometrical parameters

d is the external diameter;
d_1 is the internal diameter;
d_2 is the average diameter;
h is the working profile height;
p is the thread pitch;
p_1 is the thread pitch, $p_1 = p \cdot n$, where n is the number of starts;

α is the angle of thread;
ψ is the angle of helix by average diameter,

$$tg\,\psi = \frac{n \cdot p}{\pi \cdot d_2}.$$

The static loading is characterized by two types of breakage in thread joints – break of the screw body and cut of thread turn.

The minor diameter (*an internal diameter of the thread*):

$$d_1 = \sqrt{\frac{4 \cdot Q_з}{\pi \cdot [\sigma]}},$$

where $Q_з$ is the pre-tightening force,

$[\sigma]$ is the permissible normal stress.

A strength test of the thread at cut

$$\tau = \frac{Q_з}{\pi \cdot d_1 \cdot H \cdot k \cdot m} \leq [\tau_{cp}],$$

where H is the nut height;

k is the total factor depending on the thread type;

m is the factor of irregular load distribution;

$[\tau_{cp}]$ is the permissible stress of cutting.

KEY JOINTS

Key joints are used to transfer the torque moment from shaft to hub of the detail on it (*tooth gear, gin, clutch*), or, vise versa, from hub to shaft. Key joints use additional parts, keys, which are mounted in slots between shaft and hub (Fig. 3.8) [42, 47, 56, 59-60].
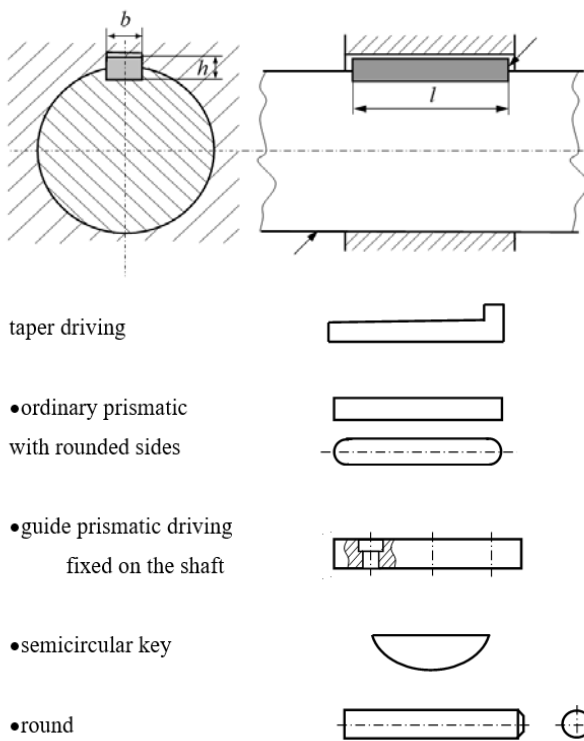

taper driving

•ordinary prismatic
with rounded sides

•guide prismatic driving
    fixed on the shaft

•semicircular key

•round

Fig. 3.8. Key joints

Advantages:
o   simple and reliable structure,

- o easy assembly and disassembly, and
- o low price.

Disadvantages:
- o weakened solid sections of mating details,
- o stress concentrators.

Ordinary prismatic keys work for crumpling edge faces and cutting.

The sizes of the key cross section ($b \times h$) are chosen from tables of standards according to the diameter of shaft d.

Required key length

$$l = \frac{4T}{h \cdot d \cdot [\sigma_{cм}]}$$ - *from the condition of crumbling prevention,*

$$l = \frac{2T}{b \cdot d \cdot [\tau_{cp}]}$$ - *from the condition of cutting prevention,*

where T is the torque moment transmitted by the joint,

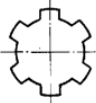$[\sigma_{cм}]$, $[\tau_{cp}]$ are the permissible stresses of crumbling and cutting.

Out of two calculated length values
of keys the larger one should be chosen.

Spline joints

The spline joints can be conditionally described as the multi-key joint in which keys are directly produced on the shaft.

Table 3.4

Types of spline joints

straight-spline (Fig. 3.9)	*involute*	*with triangular* *splines*

Spline joint is calculated for crumbling side faces of splines.

It is used for transmission of considerable torsion moments.

Advantages:
o higher strength of key shafts in comparison with that of spline shafts, and
o better detail centering.

Disadvantages:
o complex manufacture of spline shafts
o increase of stress concentrators.

Irregularity in load distribution between splines is considered by the coefficient $\psi = 1,2......1,3$.
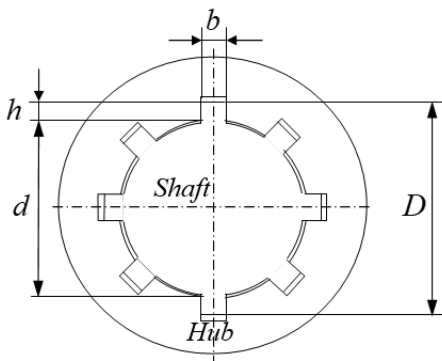

Fig. 3.9. Straight-spline joint

The maximum torque moment

$$T_{max} = z \cdot h \cdot l \cdot \frac{D+d}{\psi} [\sigma_{CM}],$$

where z is the number of splines;

h is the height of the contact surface;

l is the working spline length equal to the hub length of the detail connected to the shaft;

$[\sigma_{CM}]$ is the permissible stress of crumbling.

Profile joints

In the profile joint enveloping and enveloped surfaces of a detail have the non-round shape of a section, therefore it provides transmission of large torque moments.

Advantages:

o lower stress concentration (*in comparison with that of key and spline joints*), and

o better centering.

Disadvantages:

o complex manufacture of mating details.

Profile joint with contoured profile is calculated by crumbling stresses on working surfaces.

It is recommended to take $b = 0,75 \cdot d$ for square joints.

Maximum torque moment (Fig. 3.10)

$$T_{max} = \frac{b^2 \cdot l}{3} [\sigma_{cм}].$$

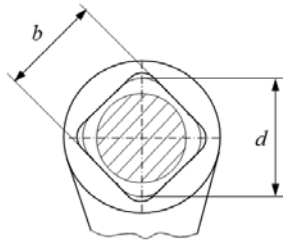The recommended joint length: $l = d .....2d$.

Fig. 3.10. Torque moment

Pin joints

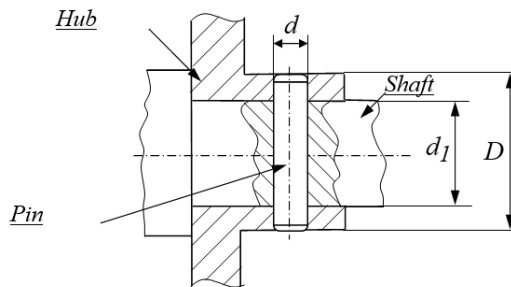Pin joint includes an additional detail – the pin (Fig. 3.11).

Fig. 3.11. Pin joint

164

It is used for transfer of the axial load or torque moment, and also for providing exact position of connection details.

Advantages:
- o simple structure, and
- o easy assembly.

Disadvantages:
- o weakened basic details with pin holes,
- o low structural manufacturability, and
- o limitation of the loads transmitted.

Pins are calculated for cutting and crumbling.

When transmitting torque moment T

$$\tau = \frac{4T}{\pi \cdot d_1 \cdot d^2} \leq [\tau_{cp}],$$

$$\sigma = \frac{2T}{d_1 \cdot d \cdot (D - d_1)} \leq [\sigma_{cm}].$$

PERMANENT JOINTS

WELD JOINTS are non-detachable connections formed by atomic bonds between details through fusion of connection edges, their plastic deformation or the combination of both. The weld joints are widely used in industry and, in particular, in transport and military engineering.

Advantages:
- • high manufacturability and low cost of welding;
- • material saving and low mass of welded details in comparison with that of moulded and riveted details by *25...30%*;
- • welded seams can be similarly strong as the base metal (under appropriate design and production);
- • possibility to obtain details of irregular shape from simple rough parts;
- • possibility to obtain tight joints;
- • high efficiency and manufacturability of the welding process; and
- • high maintainability of welded products.

Disadvantages:
- • shape distortion (self-deformation) of products in welding and wear;
- • possibility to create forceful stress concentrators at welding;
- • complex quality control of welded seams without their damage; and

• complication in providing high reliability under impact and cycle loads (including vibration).

By seam formation the weld joints are divided into: seams formed with edge fusion (fusion welding) and seams formed without edge fusion of connection details.

Among the most commonly used ways of fusion welding are joints made with:

- *electric arc* welding and its modifications (manual arc welding with melting and non-melting electrodes, hidden arc welding, gas-shielded welding, etc.),
- *gas* welding (with heating melted edges with a gas flame),
- *electroslag* welding,
- *laser* welding,
- *electron beam* welding.

The joints *without edge melting* include ones made with:

- *forge* welding,
- all types of *contact* welding (*butt-seam, spot, seam*),
- welding with *plastic cold deformation*,
- *explosion* welding,
- *diffusion* welding in vacuum,
- *friction* welding.

At present most welded seams made by electric arc welding are standardized. By mutual position of welded parts they can be divided into five basic types (Fig. 3.12) [43]: butt – flat butt seams, corner – fillet seams, T-joint – flat butt or fillet seams, lap – fillet seams and edge – fillet seams.
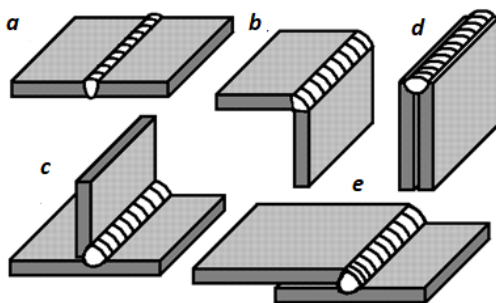

Fig. 3.12. Types of welded seams:
a – butt, b – corner, c – T-joint, d – lap, e – edge

The metal hardened after melting and joining of welded connection details are called the welded seam.

The tensile stresses in *a flat butt seam* are calculated as if for the base metal

$$\sigma = \frac{F}{\delta \cdot l} \leq [\sigma]'_p,$$

where F is the force bearing by a welded seam;

δ is the thickness of a smaller welded sheet;

l is the seam length;

$[\sigma]'_p = (0{,}85 \dots 1{,}0) \cdot [\sigma]_p$ is the permissible normal tensile stress for the metal of a seam ($[\sigma]_p$, the permissible normal stresses for the weld metal).

Fillet seams are usually calculated by cutting along an unsafe (least) section. Here, the tangential stresses

$$\tau = \frac{\sqrt{2} \cdot F}{l \cdot k} \leq [\tau]'$$

where k is the leg of a fillet seam,

$[\tau]' = (0{,}5 \dots 0{,}65) \cdot [\sigma]'_p$ are the permissible tangential stresses for the seam metal.

While determining the permissible stresses for the seam metal (*added metal*), the values of coefficients in brackets are taken in dependency on the welding type and quality of added metal.

RIVET JOINT is the permanent joint formed with use of special inserts, rivets of high-plastic material.

The rivets connecting the edges of several details are called the rivet seam. Rivets are made of low-carbon and alloy steels, copper and copper alloys (mostly, brass), aluminum and aluminum alloys.

Advantages:
- possibility to connect unweldable details,
- simple structure and easy technology process,
- less detail damages at dismantling, and
- lower stress concentration.

Disadvantages:
- lower strength of connection details due to rivet holes,
- high metal consumption for joints,
- high labor intensity and cost, and

• density failure of seams in operation.

Variety of applications for rivet joints results in a great number of their variants (Fig. 3.13).
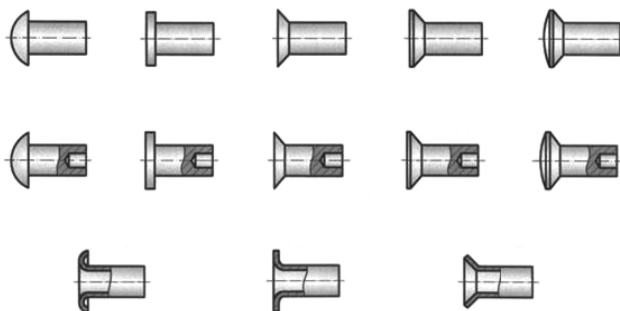
Fig. 3.13. Variety of rivet joints

Solid round-head rivets are used for power and impervious seams, solid *flat-head* rivets – for corrosive environments, *hidden-head* solid rivets – for a decrease in aero- and hydro-resistance (*aircraft, boats*).

Semi-tubular and *tubular* rivets are used for connecting thin sheets and non-metal details (*at low loads*).

Among the basic types of rivet joints are lap joint *with one liner* and *two liners*. (Fig. 3.14)
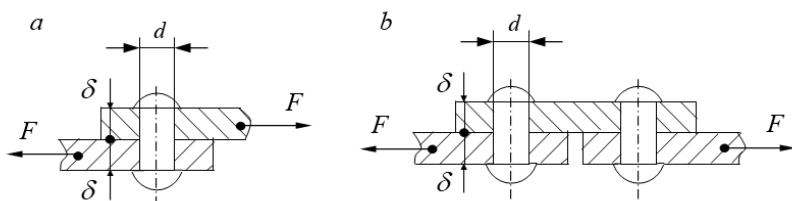
Fig. 3.14. Basic types of rivet joints:
a – with one liner, b – two liners

Rivets in joints under axial loads are calculated for cutting and tested for crumbling.

Strength condition in calculation for cutting

$$\tau = \frac{4F_1}{i \cdot \pi \cdot d^2} \leq [\tau_{3p}],$$

168

where F_1 is the load on one rivet;

i is the number of shear sections.

Strength condition in calculation for crumbling: $\sigma = \dfrac{F_1}{\delta \cdot d} \le [\sigma_{\text{ЗМ}}],$

where δ is the thickness of connection details.

INTERFERENCE JOINT (pre-stressed joint). The interference joints provide an immovable connection of details due to friction forces emerging between external and internal surfaces in assembly of details.

The basic advantage of interference joint is its simplicity and manufacturability. It provides a comparatively low cost of joint and a possibility to be used in mass production.

A significant disadvantage of interference joint is dependency of the loading capacity on a number of factors which are difficult to consider: a wide dissipation of values of coefficients of friction and interference, and influence of working temperatures on joint strength. Among disadvantages of the joint are high assembly stresses in details and a decrease of their fatigue resistance due to pressure concentration at hole edges.

Interference joints are used to connect gears, flywheels, rolling bearings, motor spindles, turbine disks and others with the shaft. Besides, interference fits are used for manufacture of stackable crankshafts, screw wheels, etc.

SOLDER JOINTS are the joints formed by chemical and physical (adhesion, solution, formation of eutectics) interaction of fusion material, solder, with connection edges of details. The use of a fusion solder implies heating connection details. However, a solder is characterized by absence of fused connection surfaces.

Solder joints are widely used in transport engineering (soldered radiators of cooling systems), in instrument engineering and electronic engineering (assembly of printed-circuit boards and hook-up elements).

Advantages:
❖ possibility to join heterogeneous materials;
❖ possibility to joint thin-walled details;
❖ possibility to obtain joints in nooks;
❖ corrosion resistance;
❖ low stress concentration due to solder plasticity; and
❖ tightness of solder joint.

Disadvantages:
❖ low seam strength in comparison with the base metal;
❖ requirements for high accuracy in surface treatment, assembly and fixation of details for soldering;

❖ low mechanical and thermal strength; and

❖ high cost of solders and fluxes.

Different metals and some alloys, the melting temperature of which is considerably lower than the melting temperature of the material of connection details, are used for solders. ᵣ

All solders, by the melting temperature, can conditionally be divided into three groups: low-temperature (*melting temperature is* $T_{пл} < 150...200°C$) tin, lead, bismuth, cadmium, indium alloys; *middle-temperature* or soft ($150...200°C < T_{пл} < 350...400°C$) tin, lead, stibium, zinc alloys; *high-temperature* or *hard* ($350...400°C < T_{пл} < 850...1000°C$) copper, zinc, silver and their alloys, most famous and cheap of them are brass.

The marking and functions of some solders are: *ПОС-90* (*tin 90%, the rest is lead, $T_{пл}$ = 222 ℃*) – for dishware; *ПОС-30* ($T_{пл}$ =256 ℃) – for radio equipment; *ПМЦ-48* (*copper 48%, the rest is zinc, $T_{пл}$ = 865 ℃*) – for copper alloys with the melting temperature no less than *920℃*; *ПСр-72* (*silver 72%, the rest is copper, $T_{пл}$ = 779 ℃*) – for ferrous and non-ferrous metals with the melting temperature no less than *800℃*; *ПСр-40* (*silver 40%, copper $\sim$ 16,7%, zinc $\sim$ 17,0%, cadmium$\sim$ 26,0%, nickel $\sim$ 0,3% $T_{пл}$ = 605 ℃*) - for ferrous and non-ferrous metals with the melting temperature no less than *650℃*.

In order to protest metal and remove the oxide coating, fluxes are used in soldering; they can be hard, liquid or gaseous. The most widely used of them are: for soft solders – colophony, ammonium (*sal ammonia*), soldering acid; for hard solders – borax (*sodium borate*), boric acid, chlorous and fluoride metal salts.

So that to fill a clearance in a solder joint, the clearance should not be very large: for low-melt solders the clearance is usually taken to *0.2...0.3 mm* per side, and for hard solders it is a little smaller – to *0.15 mm*. The value of a clearance depends on both the structure of a solder joint and the soldering technique: furnace soldering requires one size of clearances, but salt soldering – another.

ADHESIVE JOINTS are formed directly by adhesive forces emerging in the hardened and polymerized glue coat spreading on connection surfaces. The difference between an adhesive joint and solder joint is that adhesives are not metals, while solders are either metals or their alloys. In accordance with composition and properties of adhesives their polymerization can run both at room temperature and at heating [99-101].

The basic advantage of this joint is its density, and also a possibility to glue heterogeneous metal and non-metal materials in various combinations.

A disadvantage is low heat resistance (60^0C for most adhesives and 250^0C for heat-resistant adhesives), and low strength.

All adhesives can be divided into structural (which can bear loading for tear and shear after hardening) and non-structural (compounds which cannot bear loads for a long time).

Among structural adhesives are butvar-phenolic, epoxy, cyanoacrylyte adhesives, etc. Among non-constructive adhesives are 88H, some rubber adhesives, etc.

Most adhesive joints require an ageing under pressure for gripping and subsequent after-baking in free condition. Some adhesives require heating for evaporation of solvent with subsequent polymerization. Adhesive joints are frequently used as retaining for thread joints. Generally, adhesive joints better work for shear than for tear.

3.5. Shafts and axles. Bearings. Clutches

SHAFT is the part of a machine or mechanism used for transmission of the twisting or torque moment along the axial line. Most shafts are rotation (movable) details of mechanisms on which the details, directly transmitting the torque moment (gear wheels, pulley wheels, chain wheels, etc.), are fixed.

Axis is the detail of a machine or mechanism used to support rotating parts and not to transmit the torque or twisting moment. Axis can be movable (rotating) or immovable (Fig. 3.15).

The axle operates only for flexure, and the shaft operates for flexure and torsion.

Axles are straight bars.
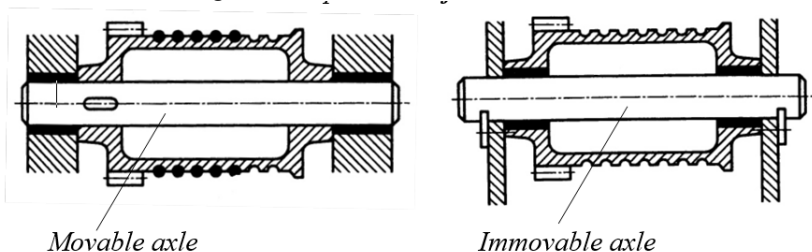

Movable axle   Immovable axle

Fig. 3.15. Axel of winch barell

Shafts and axles are made of carbon steels (chiefly, grades of 30 40, 45 and 50) and alloys (40X, 40XH, 40XHMA, 18XHBA, 18XΓT, etc.). in the form of sheet and forged pieces, typical, mostly, for shafts of reducers (Fig. 3.16).
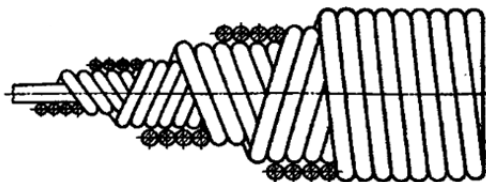
Fig. 3.16. Shaft

According to the longitudinal geometric axle shape shafts are divided into:

❖ straight: longitudinal geometric axle is a straight line. For example: reducer shafts, transmissions of track-type and wheel machines;

❖ crankshaft: longitudinal geometric axle is divided into several parts, parallel and radially-displaced relative to each other. For example: crankshaft of an internal combustion engine;

❖ flexible: longitudinal geometric axle is a variable-curvature line which can vary in operation of the mechanism or at assemble-dissemble processes. It is mostly used in the speedometer drive of a car.

By functions they are divided into:

❖ *transmission shafts:* bear elements transmitting the turning moment (*gear or worm wheels, pulley, sprockets, clutches, etc.*) and chiefly equipped with end parts exceeding the dimensions of the mechanism case;

❖ *transmission shafts:* intended for power distribution from one source to several consumers;

❖ *mainshafts:* bear all movable operating elements of the actuating units (*mainshafts of machines with work pieces or instruments, called the spindle*)

By production form of the external surface, straight shafts are divided into:

❖ *smooth:* shafts with equal diameter along the whole length;

❖ *stepped:* shafts with sections of different diameters;

❖ *hollow:* shafts with through or blind holes which are co-axial to the external surface of the shaft and expend deep along the shaft;

❖ *spline:* shafts with ruffs, splines, on the external cylinder surface, equispaced along the circle, and intended to transmit the momentary load from or to the details which directly transmit the turning moment;

❖ *key:* shafts with the key-slot profile along a certain length; and

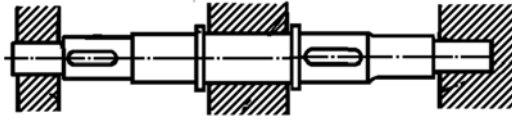❖ *shafts* matched with elements which directly transmit the rotational moment (shaft-bearing, shaft-worm).

Fig. 3.17. Structural elements of shafts and axles

Journals are support sections of the shaft and the axle. They are divided into *end*, *neck* and *thrust journals*.

End journal is the journal located at the end of the shaft and transmitting chiefly the radial force.

Neck journal is a journal in the middle part of the shaft or axle. *Bearings support end and neck journals.* End and neck journals can be cylindrical (*a, b*), conic (*c*) or spherical (*d*) by form. *Cylindrical journals* are the
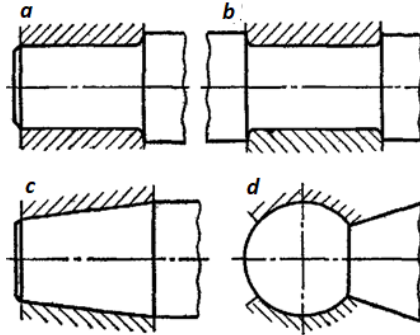

Fig.3.18. Bearings support end and neck journals

most popular. Journals of this shape are rather technological in manufacture and repair, and widely used both with sliding and rolling bearings. The conic journals are, mostly, end journals, generally acting with sliding bearings, thus, giving a possibility to regulate a clearing and fix the axial shaft position. *Spherical journals* well compensate alignment errors in bearings, and also decrease the effect from shaft torsion under working loads to the work of the bearings.

Thrust journal is the journal transmitting the axial force. *Thrust bearings* are supports for thrust journals.

Thrust journals, by form and number of friction surfaces, are divided into *solid (a), ring (b) and collar (c)*. (Fig.3.19)
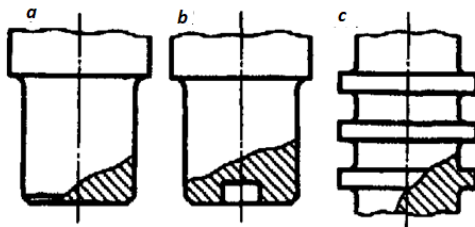

Fig.3.19. Thrust journal

The bearing backs of shafts and axles for hubs of set details are of cylindrical or conic shape.

Transient sections of shafts and axles between two levels of different diameters are made: with a rounded groove for a grinding disk; with a hollow chamfer of a constant radius (hollow chamfer is the surface of gradient transition from a smaller section to a larger section); and with a hollow chamfer of a variable radius. Transition sections are stress concentrators.

BEARINGS are supports for shafts and axles. They bear the radial and axial loads applied to the shaft or axle, and, besides, maintain the rotation axis of a shaft or axle in position [18].

By direction of force loads, bearing are divided into:

❖ *radial:* bear the load perpendicular (by radius) to the rotation axle;

❖ *thrust:* bear the load directed along the rotation axle (thrust bearings are sometimes called *footstep bearings*);

❖ *radial-thrust:* bear radial and axial loads simultaneously, and the radial load value is usually much higher than axial;

❖ *thrust-radial:* bear the radial and axial loads, but the value of radial load is much lower than axial.

According to the friction type, bearings are divided into:

❖ rolling bearings;

❖ sliding bearings.

ROLLING BEARINGS (Fig.3.20) are an assembled group, the basic elements of which are rolling bodies – balls 3 and rolls mounted between rings 1 and 2 which are hold at a certain distance from each other with separator 4. When the bearing acts, the rolling bodies roll along the ring slots – rolling tracks.

Separators are mostly pressed of soft carbon steel. Separators for high-speed bearings are massive and made of textolite, teflon, brass and bronze [33]. There are many types of of separators (Fig. 3.21, 3.22)
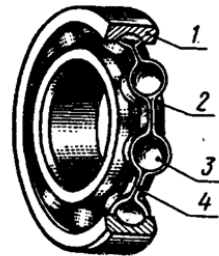

Fig. 3.20. Rolling bearings

Advantages of rolling bearings are:

- considerably low cost due to its mass production;

- low friction losses and insignificant heating in operation (*friction losses at run-ups and steady-state mode are virtually similar*);

- high interchangeability which facilitates the machine assembly and repair;

- low consumption of scarce non-ferrous metals in production and lubricants in operation; and

- low axial dimensions, simple assembly and operation.

Disadvantages of rolling bearings:

- large radial dimensions;
- high sensitivity to impact and vibration loads; and
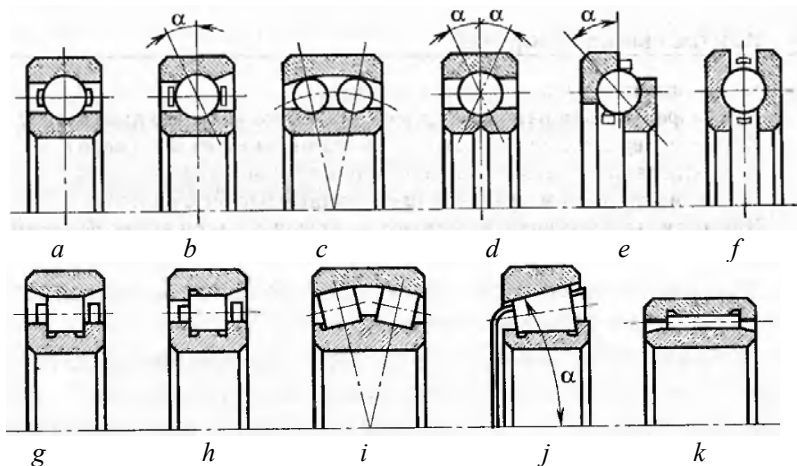- high resistance to rotation and noise, and low durability at high rotation

Fig. 3.21. Classification of rolling bearings:
a – radial; b – thrust-radial;
c – radial double-row spherical; d – radial-thrust one-row four-point;
e – thrust-radial; f – thrust, g-h – radial with short cylindrical rollers;
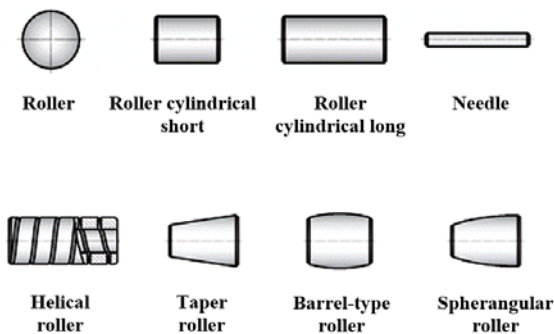i – radial spherical double-raw; j – conic; k - needle-shaped

Fig. 3.22. Rolling elements of bearings

- Ball bearings are used at high speeds and high loads (Fig. 3.23).
- Roller bearings are used at mean and low speeds and high loads (Fig. 3.24).
- Helical roller bearings are used at dynamic loads.
- Barrel-type and spherangular roller bearings are used at the axis misalignment of internal and external rings.
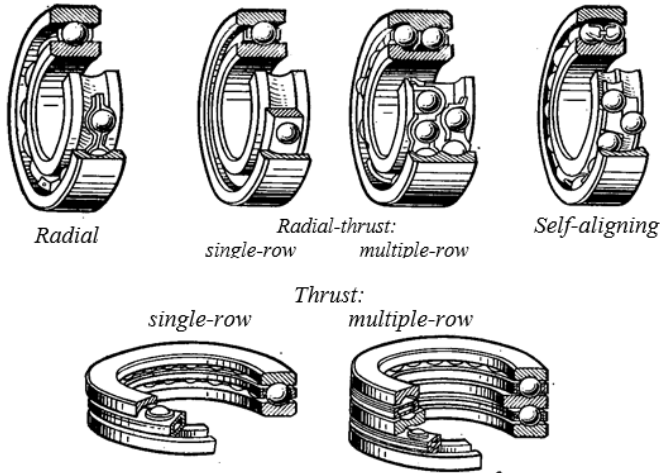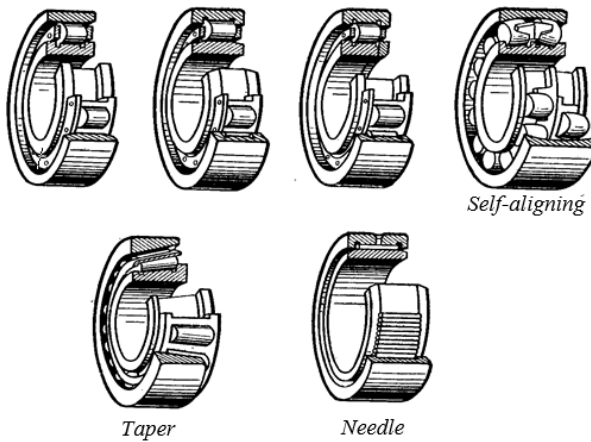

Fig. 3.23. Ball bearings

Fig. 3.24. Roller bearings

SLIDING BEARINGS consist of body 1, insert 2, lubricating tools and strips (Fig. 3.25).

The bearing body is usually a separate detail at which shaft journal 4 rests. The inserts are made of antifriction materials (babbits, bronze, brass, zinc alloys). Bimetal inserts are frequently used; here, a thin layer of antifriction material spreads on a less costly metal base. The lubricant goes to the working surface from canal 3 through lubricant tracks 5.
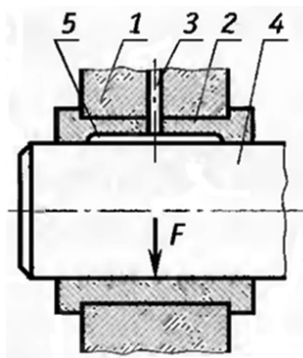
Fig. 3.25. Sliding bearings

Advantages of sliding bearings:
   - low dimensions in the radial direction;
   - good sensitivity to dynamic (impact and vibration) loads;
   - high mating accuracy;
   - well conformability;
   - high service life in flood lubricant conditions;
   - possibility to work in water, abrasive and corrosive environment (*under an appropriate choice of materials and manufacture methods*);
   - possibility to be assembled (*subject to the structure*) in both axial and radial directions;
- simple structure and low cost.
   Disadvantages of sliding bearings:
   - large dimensions in the axial direction;
   - considerable lubricant consumption;
   - needed control over a constant supply of lubricants to working surfaces;
   - high starting moment and high wear at the start-up stage; and
   - necessity to use expensive antifriction materials in bearings.
   By load direction sliding bearings are divided into radial and thrust.

By structural features sliding bearings are divided into: one-piece (solid) and two-piece (separable).

One-piece sliding bearings find wide application when loads and sliding speeds are low ($v_{sl} \leq 3$ m/sec) in devices and control mechanisms.

Two-piece bearings are mostly applied in cases where axial assembly (crankpins of crankshafts for internal combustion engines) is impossible of undesirable, and also in heavy engineering for fastening heavy loaded shafts.

Sliding bearings are used when it is impossible or inefficient to use rolling bearings: for separable supports; at impact and vibration loads; at high

177

rotation frequencies. They are used in internal combustion engines, compressors, turbines, pumps, rolling mills, heavy reducers and other machines.

CLUTCHES. Most machines are equipped with mechanisms in the form of an aggregate each, thus, they are completely interchangeable. Besides, when motion transmits from the engine to the actuating mechanism, the latter should periodically be actuated without stoppage of the engine. These tasks and some others are solved with application of clutches.

Clutch is the device for connecting shafts, drives, pipes, cables and ropes. Clutches are divided into: coupling and machine drives. And the latter are considered in the course of machine parts. Machine drive clutches are the devices intended for connection of shafts, and torque moment is transmited without changes in value and direction [76-77, 98, 102-103].

Functions of clutches:
- *compensation* of mismatches of connection shaft ends;
- *torque shock softening and vibration damping;*
- *prevention of mechanisms from damages* at abnormal loads*;*
- *periodic coupling and uncoupling* of shafts in motion or during stops;
- *transmission of unit-directed motion* or prevention of counter motion from the driver to the driving shaft;
- *limitation of parameters of transmitting motion* – speed (*rotation frequency of the driving shaft*) or torque moment.

Classification of clutches:
- by type of energy for motion transmission – *mechanic, hydraulic, electromagnetic;*
- by coupling of connection shafts – *clutches of permanent coupling (uncontrolled), claw clutches, controlled clutches* (shafts are connected and disconnected by an operator), *and automatic clutches* (automatic connection or disconnection when a controlled parameter is reached);
- by capacity to damp dynamic loads – *rigid,* which cannot decrease dynamic loads and damp torsional vibrations, and *elastic*, which damp vibrations and impacts due to elastic elements and elements absorbing vibrations of energy;
- by degree of shaft connection – immovable (dead), movable (compensating), coupling, free travel, preventive;
- by principle of action – sleeve-type, linear-separable, transverse-separable, compensating, rolling, elastic, friction, cum, gear*, with crushable elements (cutting), with coupling (cam and roll);*
- by structural features – lengthwise compensating, lateral compensating, universally-compensating, hinge, elastic (constant and variable rigidity), conic, cylindrical, friction free-travel, and ratchet free-travel.

3.6. Creation of the Image of the New Generation Freight Car Bogie

Improvement of dynamics and strength of freight car bogie is an actual task for industrial and scientific organizations [3, 25]. Studies are carried in the mainstream of the EU Road Map, according to which, in order to reduce the energy dependence of the transport sector and to reduce emissions of harmful substances into the atmosphere, it is planned that by 2030 30% of goods transported by road will be redirected to river and railway transport, and by 2050 50% of freight will be transported by river and railway transport. This background requires the introduction of significant innovations and modernization of the fleet of cars, for example, the working program Shift2Rail aims to achieve [6]:

- reducing the weight of the body up to 30% and the weight of the bogie (reducing unspring weight, which allows to reduce wear, noise and vibration and will reduce by 20% the life cycle cost of the bogie) [62];

- reducing the dynamic impact on the track through the use of active suspension;

- reducing maintenance costs by 20% through the introduction of monitoring systems, mechatronic systems, etc.;

- reducing wheel and rails wear by 25%, including when passing the curved track sections;

- increasing the speed of movement, especially for freight rail transport demonstrates the dynamic development of passenger rail transport and the "stagnation" of freight rail transport in terms of speed on the example of Sweden.

Constantly used in the European Union and Commonwealth of Independent States countries bogie designs, such as Y25, G-type, UIC Link suspension, Barber (type 18-100), have a long history and have undergone only minor transformations during their existence, their schematic development history is shown in Fig. 3.26 and was created by article authors [5, 7-8, 50]. The innovation matrix created as a part of SUSTRAIL project has shown that the leading research centers in Europe consider Y25 bogie as the basis of the freight bogie of the future. Within the framework of the conventional approach, it should be modified in the primary spring suspension, use two Lenoir dampers, material with good damping properties, new wheel contour and new wheel steel type. Within the futuristic concept, in addition to the outlined, the use of wedges, hydraulic dampers, and changes in the stiffness of the supports are supposed. Yet it should be noted that the Y25 bogie is very sensitive to the track irregularities, and also requires the improvement of the dynamic qualities for the passage of curved track sections [25].

179

Unlike the authors, S. Stichel and P. A. Jonsson consider it promising to use Link suspension bogie with hydraulic dampers [8], which allows to achieve speeds of up to 160 km/h. Authors in their previous works suggest the development of the Barser cart (18-100), as well as the use of elastic-dissipative bearing elements (Fig. 3.26).
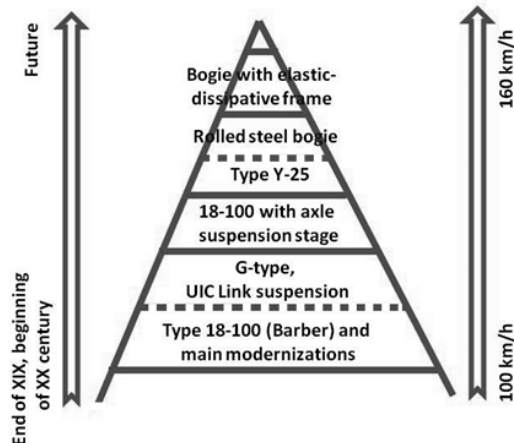

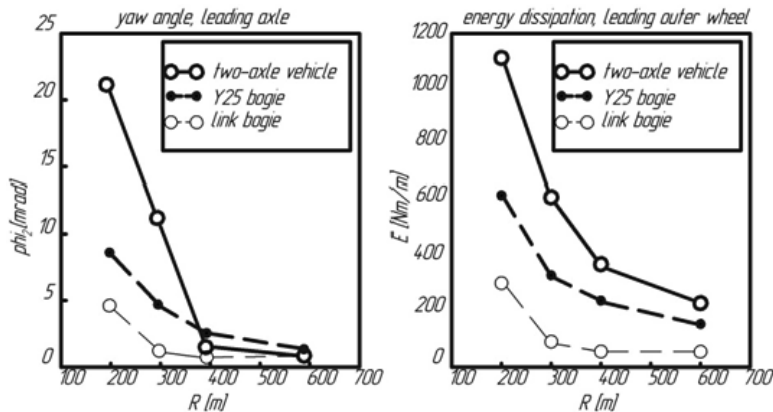Fig. 3.26. Development of bogie constructions

Fig. 3.27. The angle of attack and the dissipation energy of the first wheel pair of different types of bogies when passing curves of different radii

In the countries of Central and Eastern Europe, a three-piece bogie is widely used (18-100 type or Barber) which is no better: maximum operating speed does not exceed 90-100 km/h, the high dynamic impact on the railway track is one of the main causes of its wear and damage, high dynamic loading of the supporting members, absence of the pedestal bogie primary suspension, cast bogie frame. In different years, attempts have been made to optimize the characteristics of bogie suspension, the use of elastic elements in the pedestal, transition from cast to welded elements, but no significant breakthrough and tangible results have been achieved (Fig. 3.27) [51, 52]

Methods for Creating a New Design for a Freight Car Bogie

In this way and relying on, actual task is to introduce new concepts and technologies, to create a new bogie design, with the implementation of advanced construction techniques, such as multi-functional components, design modularity, the use of innovative materials, the use of pre-stressed elements. In the near future, it is almost impossible to introduce significant changes in the design of widely used bogies due to the repair base, therefore there is a need for creating a new design for a freight car bogie and upgrading a freight car bogie [3, 63].

The authors suggest a number of ways to improve freight car bogies of different types on the basis of the approach outlined above:

- using of pre-stressed structures;
- using of rolling materials, the creation of a specialized profile;
- using of elastic-damping multifunctional elements with modularity units.

Methods for upgrading a Freight Car Bogie

The causes of lateral frame fractures are found out. Following reasons are known from the literature:

1. Excess value of load (impact loads) for jaws on the sorting roller coaster (up to 100 kN on the jaw).

2. Fatigue failures due to the running of the side frames (if technically faulty bogie) [16].

3. The presence of internal defects in side frames.

4. Operation of bogies after stairs from rails

5. Combination of longitudinal jaw loading and bends of the side frames.

Skewed wheel pair during impact are accompanied longitudinal force on the jaw up to 100 kN and force moment 4.5 kNm. This reason is established experimentally during impact tests. Scheme of strain gages and the general view of the car (Fig. 3.28).

Fig. 3.28. Scheme of strain gages and the general view of the car

The authors developed and patented constructions of pre-stressed elements of the bogie design: truck bolster, side frame (for upper and lower belts); side frame pedestal jaw opening (Fig. 3.29-3.30) [29].
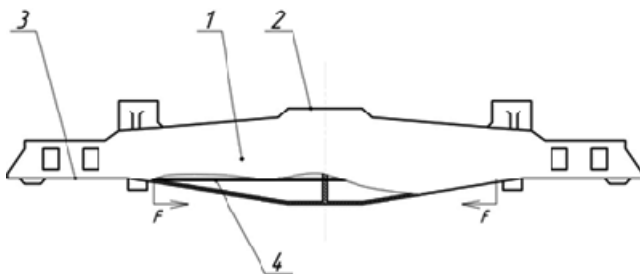

Fig. 3.29. Pre-stressed bolster of a three-piece bogie:
1 – truck bolster; 2 – bolster bowl; 3 – support bearing; 4 – rod

As a result of strength calculations, by the finite element method (general view (a) and side frame (b) of calculation model, it was found out that by changing the force creating a preliminary stress in the pedestal jaw opening, it is possible to reduce the level of maximum stresses in the most stressed zone by 1.5 to 2 times (Fig. 3.31-3.32) [83, 94].

As the development of the idea of using a load-bearing element that closes the pedestal jaw opening, the authors developed technical solutions for the creation of primary bogie suspension in a three-piece bogie (Fig. 3.33). An examples of a design with coil springs. A preliminary calculation of the distribution of equivalent stresses in the side frame of the created structure the change in the scheme of application of forces did not lead to an increase in the level of stresses (Fig. 3.34) [13, 22, 35, 73-74, 93].
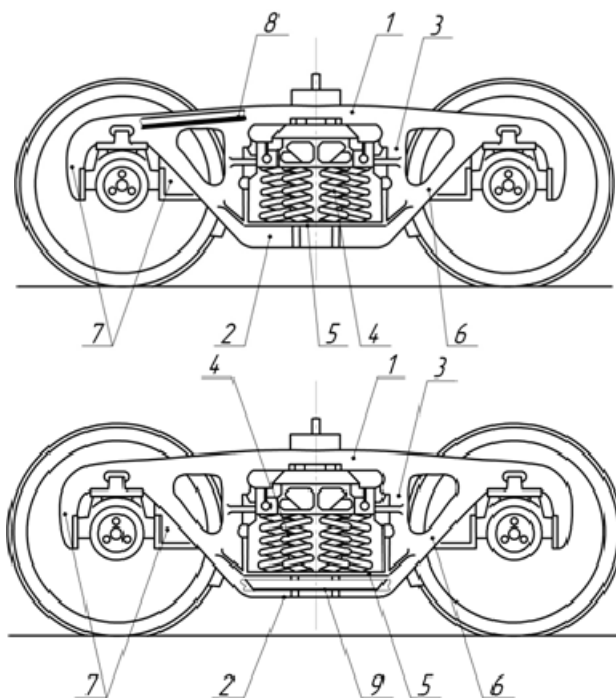
Fig. 3.30. Pre-stressed side frame of three-piece bogie concept:
1 – top sole bar member; 2 – lower sole bar member; 3 – vertical columns;
4 – spring opening; 5 – bearing surface; 6 – diagonal sole bar member;
7 – jaw pedestal; 8, 9 – rod

According to the previous calculation and other studies, applying in the primary bogie suspension allows to reduce resistance to movement (increase of energy efficiency) of the freight car by 11%, and also to increase the speed of movement by 30% with an equivalent level of impact on the track (Fig. 3.35). Visualization of the dynamic model, structural scheme (Fig. 3.36).

The first stage of verification is using simple model:

$$m \cdot \ddot{z} + \beta \cdot \dot{z} + Ж \cdot z = 0$$

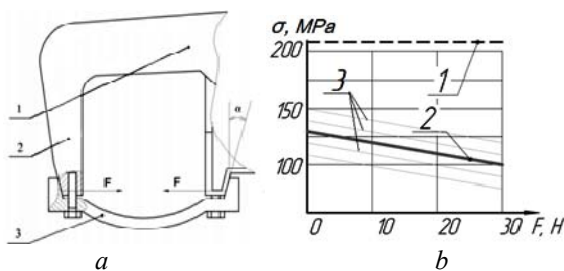where m – mass, β – attenuation coefficient of vibration, Ж – elasticity.

Fig. 3.31. Pre-stressed pedestal jaw opening of a three-piece bogie concept
a – pre-stressing circuit in pedestal jaw opening, 1 – top sole bar member,
2 – pedestal jaw, 3 – pedestal brace, α – angle of inclination, providing the preliminary
tension of the structure, F – force providing pre-stressed state of a structure;
b – dependence of the level of maximum stresses in the zone R55 (at maximum
vertical and axial loads) on the force of preliminary tightening of the jaws with
pedestal brace (metal string), 1 – stress level in the existing side frame,
2 – stress level when using a pedestal jaw, cross-section 20 sm2,
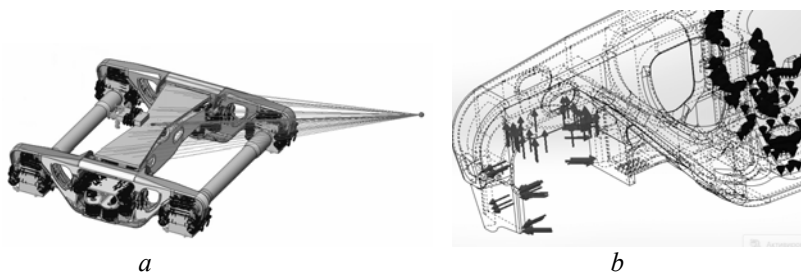3 – dependence of stress level when changing the cross-section of the pedestal jaw

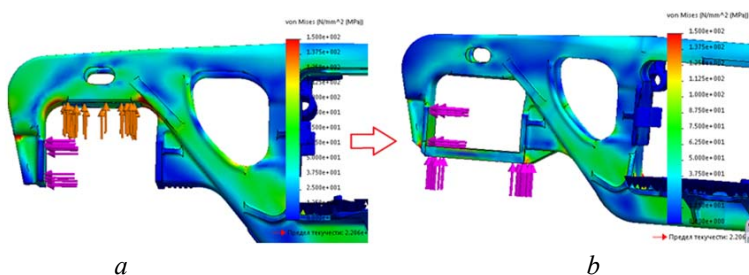Fig. 3.32. General view (a) and side frame (b) of calculation model

Fig. 3.33. Distribution of equivalent stresses in the side frame:
a – in existing bogie, b – in a bogie with a pre-stressed pedestal jaw opening

184
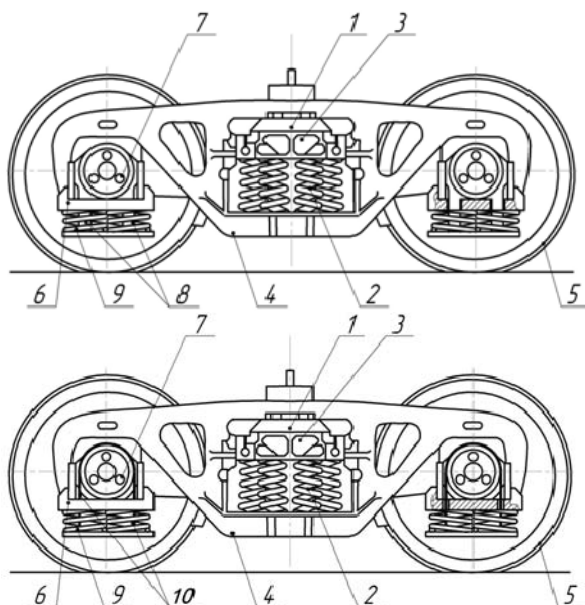
Fig. 3.34. Three-piece bogie with the pedestal brace and primary bogie suspension
a – with rigid connection, b – with flexible connection:
1 – bolster, 2 – bolster suspension, 3 – friction shock absorbers, 4 – side frame,
5 – wheelsets, 6 – pedestal brace, 7 – axle-box, 8 – rods connecting the bearing
with a stiffener, 9 – primary spring suspension, 10 – cable
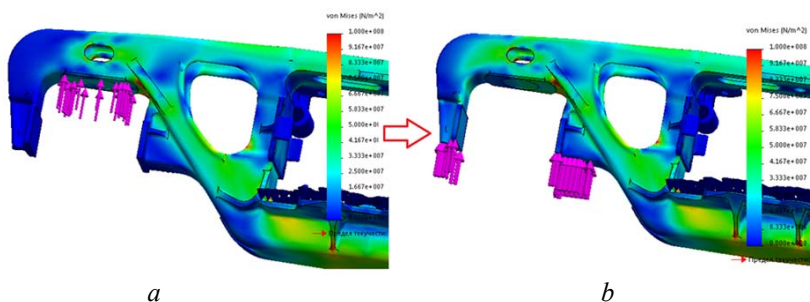
Fig. 3.35. Diagrams of equivalent stresses for the existing (a) and prospective (b)
schemes of vertical forces application
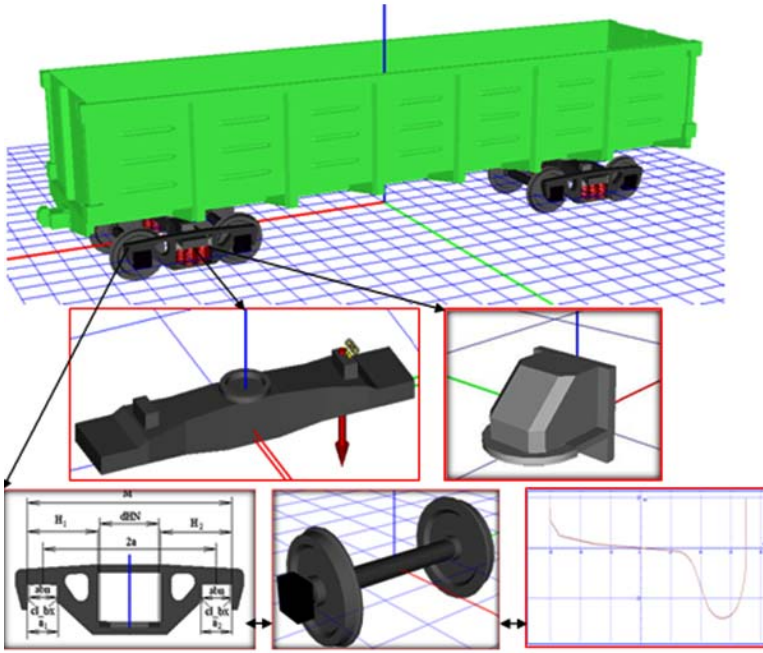
Fig. 3.36. Visualization of the dynamic model

The second stage of checking the computer model of the car's dynamics is comparison with testing results in an empty and loaded state. Places of installation of accelerometers in tests is shown on fig. 13. As the estimates of the adequacy of the mathematical model, the difference coefficient is used:

$$\varepsilon = \frac{\sqrt{\sum_{i=1}^{n}\left(x_i^e - x_i^м\right)^2}}{\sqrt{\sum_{i=1}^{n}\left(x_i^e\right)^2} + \sqrt{\sum_{i=1}^{n}\left(x_i^м\right)^2}},$$

where $x_i^м$ and x_i^e – predicted and experimental values; n – the number of verifiable values.

Obtained values below 0.11, this indicates a slight difference in calculation and experimental data. The total relative average deviation of calculated and received by results of measurements of frequencies is 7.47%.
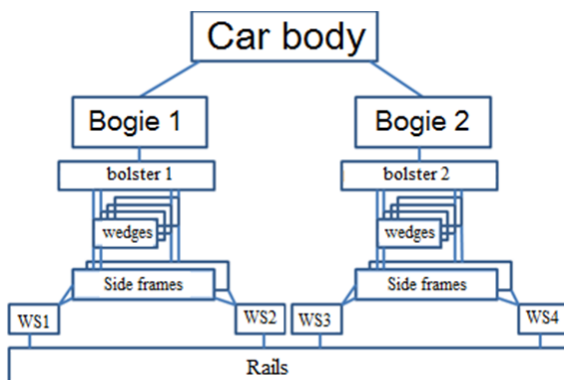
Fig. 3.37. Structural scheme of the model

Fig. 3.38. Places of installation of accelerometers in tests

The average value of reducing the resistance of the car is 11% [67]. Reduction of the coefficient of side frame dynamics is 21%. Iincrease in the coefficient of stability of the wheel from rolling on the head of the rail for 3%.

Using of Elastic-Damping Multifunctional Elements with Modularity Units

The most promising approach to the creation of a freight car bogie from a number of technical solutions developed by the authors is the use of modular multifunctional load-bearing structural elements [27].

The authors developed new technical solutions and concepts:
- concept of bogie with an elastic-dissipative frame with cradle suspension;
- concept of bogies like type Barber/18-100 and type Y-25 with an elasto-dissipative frames (Fig. 3.39-3.40).
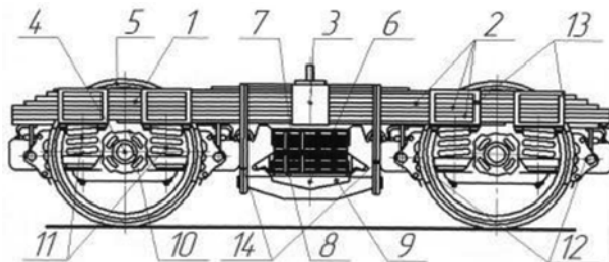
Fig. 3.39. Concept of bogie with an elastic-dissipative frame with cradle suspension:
1 – frame with 2 – leaf springs, 3 – clamp, 4 – axle-boxes, 5 – wheels,
6 – central suspension (7 – springs), 8, 9 – tie and balk, 10 – primary spring
suspension (11 – springs), 12 – braking equipment, 13, 14 – support nodes
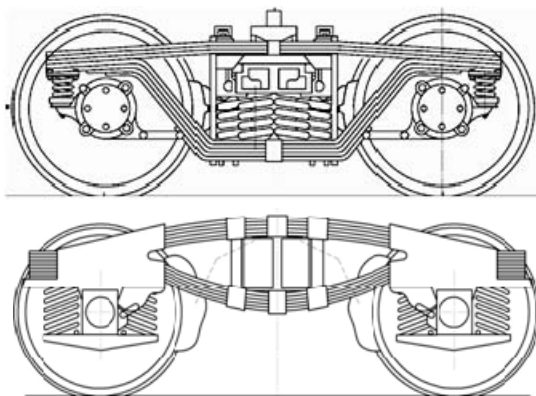
Fig. 3.40. Concepts of bogies with an elastic-dissipative frame

Considering the international experience in the field of contact evaluation of wheel and rail stresses, bench and road tests of wheel-rail contac, dynamics modeling of a bogie etc., the object of further research is the simulation of the dynamics of cars with new types of bogies and their testing [68].

REFERENCES

1. Alyamovskiy, A. A. (2007). SolidWorks/COSMOSWorks 2006–2007. Inzhenerniy analiz metodom konechnyh elementov. Moscow: DMK, 784.

2. Antipin, D. Y., Racin, D. Y., Shorokhov, S. G. (2016). Justification of a Rational Design of the Pivot Center of the Open-top Wagon Frame by means of Computer Simulation. Procedia Engineering, 150, 150–154. doi: https://doi.org/10.1016/j.proeng.2016.06.738

3. Chandra Prakash Shukla, Bharti, P. K. (2015). Study and Analysis of Doors of BCNHL Wagons. International Journal of Engineering Research & Technology (IJERT), 4 (04), 1195–1200. doi: https://doi.org/10.17577/ijertv4is041031

4. Chernova, N. I. (2007). Matematicheskaya statistika. Novosibirsk: Novosib. gos. un-t. Novosibirsk, 148.

5. Code UIC 430-4 OR. Wagons. Circulation entre des réseaux à écartement de 1435 mmet des réseaux à écartement de 1520 mm. Prescriptions techniques et conditions d'homologation. 1re édition, Mai 2004.

6. Code UIC 430-5 O – Regulations for the exchange and use of new generation freight wagons between railways with gauges of 1435 mm and 1520 mm; 1st edition, November 2003.

7. Code UIC 505 - 1 OR. Railway transport stock - Rolling stock construction gauge.

8. Code UIC 510-3 O. Wagons - Essais de résistance au banc des bogies à 2 essieuxet 3 essieux. 1re éditiondu 01.01.89 - Nouveautiragedu 01.07.94.

9. Code UIC 535-2 O - Standardisation and positioning of steps, end platforms, gangways, handrails, tow hooks, automatic coupler and brake valve controls on wagons in connection with the fitting of the automatic coupler of the UIC Member Railways and OSJD Member Railways 3rd edition of 1.1.78 and 7 Amendments.

10. Code UIC 577 OR Wagon stresses* 105 3rd edition, May 2004.

11. CodeUIC581 OR. Wagons – Lifting – Rerailing.1st edition of 1.1.83 and 1 Amendment.

12. Domin, Yu. V., Cherniak, H. Yu. (2003). Osnovy dynamiky vahoniv. Kyiv: KUETT, 269.

13. D'yakonov, V. (2000). MATHCAD 8/2000: special'niy spravochnik. Sankt-Peterburg: Piter, 592.

14. Eaton J., Kortum S.,1996: Trade in ideas: Patten, you and productivity in OECD. / Journal of the global economy. Number 40. p. 251-278.

15. EN 12663–2. Railway applications - structural requirements of railway vehicle bodies – Part 2: Freight wagons. [Valid from 30.04.2010]. B.: BSI, 2010. 54 c.

16. European Standard 14363. Railway applications – Testing for the acceptance of running characteristics of railway vehicles – Testing of running behaviour and stationary tests. – June 2005. – 113 p.

17. Eurostat. Yourkeyto Europeanstatistics [Електронний ресурс] :[Веб-сайт]. – Електронні дані. – Режим доступу: https://ec.europa.eu/eurostat/tgm/refreshMapView.do?tab=map&plugin=1&init=1 &toolbox=types&pcode=t2020_rk320&language=en(дата звернення 03.12.2018). – Назва з екрана.

18. Fomin O., Gerlici J., Lovskaya A., Kravchenko K., Prokopenko P., Fomina A., Lack T. Determination of the durability of the bearing structure of the body of an open goods wagon from round pipes during transportation on the railway ferry. International Scientific Conference on Aeronautics, Automotive and Railway Engineering and Technologies BulTrans-2018; Sozopol; Bulgaria; 15-17 September 2018 through 8 September 2018; Code 135294. MATEC Web of Conferences. Volume 157, 14 March 2018, Article number 02010.

19. Fomin, O. Scientific Substantiation of Thermal Leveling for Deformations in the Car Structure / Oleksiy Fomin, Oleksandr Logvinenko, Oleksiy Burlutsky, Andriy Rybin // International Journal of Engineering & Technology. – Vol. 7, No 4.3 (2018) – P. 125-129. (DOI: 10.14419/ijet.v7i4.3.19721)

20. Fomin, O. Determining strength indicators for the bearing structure of a covered wagon's body made from round pipes when transported by a railroad ferry [Text] / O. Fomin, A. Lovska, V. Masliyev, A. Tsymbaliuk, O. Burlutski // Eastern-European Journal of Enterprise Technologies. – 2019. – Vol. 7, Issue 1 (97). – P. 33–40. doi: 10.15587/1729-4061.2019.154282

21. Fomin, O. Experimental confirmation of the theory of implementation of the coupled design of center girder of the hopper wagons for iron ore pellets [Text] / O. Fomin, I. Kulbovskiy, E. Sorochinska, S. Sapronova, O. Bambura // Eastern-European Journal of Enterprise Technologies. – 2017. – Vol. 5, Issue 1 (89). – P. 11–19. doi: 10.15587/1729-4061.2017.109588

22. Fomin, O. The influence of implementation of circular pipes in load-bearing structures of bodies of freight cars on their physico-mechanical properties / O. Fomin, A. Lovskaya, A. Plakhtiy, V. Nerubatsky // // Scientific Bulletin of National Mining University . 2017, Issue 6 (162), p.89-96

23. Fomin, O. V. Synopsis of development of wagon materials fatigue failure / O. V. Fomin, A. V. Tsymbaliuk/ Scientific and technical journal «Metallurgical and Mining Industry». 2017, No. 8 – P.24-29.

24. Gallager, R.; Banichuk, N. V. (Ed.) (1984). Metod konechnih elementov. Osnovy. Perevod s angliyskogo. Moscow: Mir, 428.

25. Gerlici J. Gorbunov M. , Nozhenko O., Pistek V., Kara S., Lack T., Kravchenko K. 2017 About creatiion of bogiie of the freiight car // VOLUME 19 COMMUNICATIONS 2A/2017. P. 29-35.

26. Gibel' "Merkuriya – 2". Kak eto bylo… Available at: https://www.pravda.ru/accidents/9720-parom/

27. Gorbonov, Mykola Creation of the Image of the New Generation Freight Car Bogie / Mykola Gorbonov, Sergii Kara, Olena Nozhenko, Oleksii Fomin, Gediminas Vaičiūnas, Viačeslav Petrenko // Transport Means - Proceedings of the International Conference 2018. – P. 1277-1283

28. Gorbunov M., Gerlici J., Kara S. et al. 2018 New principle schemes of freight cars bogies // Manufacturing Technology, Apr. 2018, Vol.18, No. 2, P. 233-238.

29. Gorbunov, N. I.; Mokrousov, S. D.; Nozhenko, E. S.; Kravchenko, E. A.; Kara, S. V. 2013. The Question of the Truck Freight Cars (in Russian). Vestnik V. Dahl East: Ukrainian National University, No. 18 (207), P. 87-93.

30. Harak, S. S., Sharma, S. C., Harsha, S. P. (2014). Structural Dynamic Analysis of Freight Railway Wagon Using Finite Element Method. Procedia Materials Science, 6, 1891–1898. doi: https://doi.org/10.1016/j.mspro.2014.07.221

31. Heebyung K.,2006: A functional approach for studying technological progress: Application to information technology / K Heebyung, L Christopher A Magee// Technological Forecasting & Social Change –p.1061–1083.

32. Heebyung K.,2008: Functional approach for studying technological progress: Extension to energy technology / K Heebyung, L Christopher A Magee /Technological Forecasting & Social Change –, V.75, Issue 6, Pages 735-758.

33. Iwnicki, S. D. et al. 2013. The 'SUSTRAIL' High Speed Freight Vehicle: Simulation of Novel Running Gear Design, in 23rd Symposium on Dynamics of Vehicles on Roads and Tracks (IAVSD 2013), Qingdao.

34. Jonsson, P-A.: Dynamic Performance of Freight Wagons and their Influence on Cost for Track Deterioration. KTH Rail Vehicles, Teknikringen Royal Institute of Technology SE-100 44, Stockholm Sweden.

35. Kir'yanov, D. V. (2006). Mathcad 13. Sankt-Peterburg: BHV. Peterburg, 608.

36. Komarova, A. N. 2015. The Impact on the Energy Efficiency Characteristics of Carts of Freight Cars (in Russian), PhD Thesis, Sankt-Petersburg, 88 p.

37. Kosmin, V. V. (2007). Osnovy nauchnyh issledovaniy. Moscow: GOU «Uchebno-metodicheskiy centr po obrazovaniyu na zheleznodorozhnom transporte», 271.

38. Lack, T.; Gerlici, J. 2013. Wheel/rail Contact Stress Evaluation by Means of the Modified Strip Method. Communications - Scientific Letters of the University of Zilina, University of Zilina, vol. 15, No. 3, P. 126-132.

39. Lack, T.; Gerlici, J. 2014. Wheel/rail Tangential Contact Stress Evaluation by Means of the Modified Strip Method. Communications - Scientific Letters of the University of Zilina, vol. 16, No. 3A, P. 33-39.

40. Lisowski E., Czyzycki W. Transport and storage of LNG in container. Journal of KONES Powertrain and Transport, 2011, 18, 3, P. 193–201. Trejo-Escandón J. O., Leyva-Díaz A., Tamayo-Meza P. A., Flores-Herrera L. A., Sandoval-Pineda J. M. Study of the effect of liquid level on the static behavior of a tank wagon. International Journal of Engineering Research and Science and Technology. 2015. Vol. 4, No. 1. P. 18 – 25.

41. Logvinenko A. A. Peculiarities of stress calculation of basic parts of valve timing gear of modern locomotive electric power installations // Metallurgical and mining industry (Machine building). – Dnipropetrovsk, 2014. – No.6. – P. 59-63.

42. Lovska, A. O., Vizniak, R. I. (2012). Pat. No. 108214 UA. Vuzol nesuchoi konstruktsiyi kuzova vahona dlia yoho zakriplennia vidnosno paluby zaliznychno-poromnoho sudna. MPK: B60P 3/06, B60P 7/135, B60P 7/08, B61F 1/12, B63B 25/00. No. a201206115; declareted: 21.05.2012; published: 10.04.2015, Bul. No. 7.

43. Makhnenko, O.V.; Saprykina, G. Y.; Mirzov, I. V.; Empty, A.D. 2014. Prospects for the Creation of Welded Structures of Load-Bearing Elements of a Freight Wagon Bogie. Automatic welding, No. 3 (730), P. 36-42 (in Russian).

44. Malkov V., Vlasova A., Nosko **P**., Stavitsky V.2011: Method of the dynamic analysis the mechanism.TEKA Kom. Mot. i En erg. Roln. –OL PAN,11A. – Lublin, p. 145-150.

45. Mario H.,2005: Technometrics: Origins, historical evolution and new directions / Technological Forecasting & Social Change –p.944-979.

46. Myamlyn S.V.,2009:Prohnozuvannya design of biaxial trolley car / SV Myamlyn AS Matsyuk Bulletin of DIIT-p.24-29.

47. Nastavlenie po krepleniyu general'nyh gruzov pri morskoy perevozke dlya t/h "Geroi Shipki". Cargo securing manual for m/v "Geroi Shipky" No. 2512.02 (1997). Odessa, 51.

48. Oleksij Fomin, Juraj Gerlici, Alyona Lovskaya, Kateryna Kravchenko, Oleksii Burlutski and Vladimír Hauser Peculiarities of the mathematical modelling of dynamic loading on containers in flat wagons transportation // MATEC Web of Conferences 254, 02039 (2019)

49. Oleksij Fomin, Juraj Gerlici, Alyona Lovskaya, Mykola Gorbunov, Kateryna Kravchenko, Pavlo Prokopenko and Tomas Lack Dynamic loading of the tank container on a flat wagon considering fittings displacement relating to the stops // MATEC Web of Conferences. 2018. Vol. 234. 05002 (DOI: https://doi.org/10.1051/matecconf/201823405002)

50. Onsson, P-A, 2007. Dynamic Vehicle-Track Interaction of European Standard Freight Wagons with Link Suspension. Doctoral Thesis, Report TRITA AVE 2007:36, KTH Rail Vehicles.

51. Orlova A. M.; Rudakova E. A.; Turutin I. V.; Saidova. A. 2011. The Choice of the Design of the First Stage of Suspension of Three-Element Bogie of Innovative Freight Cars (in Russian), Izvestiya: Petersburg University of Communications, No 3, P. 88-99.

52. Orlova N., 1988: Guidelines for the study of the level and trend of technological development based on patent information. - M.: Fire Prevention –p.42.

53. Orlova, A. M. 2008. Hierarchical-iterative Method of Choosing Parameters of Power Characteristics and Constructive Solutions for Hanging Freight Wagon Carriages. Transport of Ural (in Russian), No. 2(17), P. 35-42.

54. Park **V**., 2006: International patents, patent rights and technology gaps / / Working Paper. American University, Department of Economics, 2001.

55. RailwayMarketAnalysis2016. December2016. - Bundesnetzagentur für Elektrizität, Gas, Telekommunikation, Post und Eisenbahnen. [Електронний ресурс] : [Веб-сайт]. – Електронні дані. – Режим доступу: https://www.bundesnetzagentur.de/SharedDocs/Downloads/EN/Areas/Rail/Downl oads/MarketAnalysisRailway2016.pdf?__blob=publicationFile&v=3(дата звернення 03.12.2018). – Назва з екрана.

56. Rakshit, U., Malakar, B., Roy, B. K. (2018). Study on Longitudinal Forces of a Freight Train for Different Types of Wagon Connectors. IFAC-PapersOnLine, 51 (1), 283–288. doi: https://doi.org/10.1016/j.ifacol.2018.05.074

57. Rudraprasad Bhattacharyya, Abhishek Hazra. A study on stress analysis of ISO tank container. 58th Congress of The Indian Society of Theoretical and Applied Mechanics, 2013. P. 1–5.

58. Sapronova, S. Research on the safety factor against derailment of railway vehicles [Text] / S. Sapronova, V. Tkachenko, O. Fomin, V. Gatchenko, S. Maliuk // Eastern-European journal of enterprise technologies. 2017. – Vol. 6, Issue 7 (90). – P. 19-25 (DOI: 10.15587/1729-4061.2017.116194)

59. SHIFT2RAIL. Joint Undertaking. Multi-Annual. Action Plan. Brussels, November 2015, 818 p.

60. Shmakov, M. G. (1975). Special'nye sudovye ustroystva. Leningrad: Sudostroenie, 344.

61. Skornyakov E.,2000: Guidelines for conducting patent research / Skornyakov E., Omarov T., Chelisheva O., M.: INIT Rospatent-p.245.

62. Spiryagin M., Spiryagin V., Kostenko I.,2011: Modelling of a controlled tractive wheelset for a bogie of a rail way vehicle based on noise spectrum analysis TEKA Kom. Mot. i En erg. Roln. –OL PAN,11A. –Lublin, p. 232-244.

63. Sukolenov, A. E., Zahariev, E., Gutin, I. G. et. al. (1989). Mezhdunarodnaya paromnaya pereprava Illichevsk – Varna. Moscow: Transport, 103.

64. Talu M. The Influence of the Corrosion and Temperature on the Von Mises Stress in the Lateral Cover of a Pressurized Fuel Tank. Hidraulica. 2017. Iss. 4. P. 89–97. Д. В. Mathcad 15 / Mathcad Prime 1.0. СПБ: БХВ-Петербург, 2012. 432 с.

65. Tichel, S, Jonsson, P-A. 2009. Is there a Future for Freight Wagon with Link Suspension? Proc. of the 9th Intern. Heavy Haul Conference, IHHA'09, Shanghai, June.

66. Timofeev N.,M.,1970:Opyt forecasting the development of machinery industry on the basis of statistical analysis of patents. / N.,M., Timofeev, N.,M., Madatov /-M.: Clarendon Press Atomizdat p.58.

67. Tkachenko, V. Research of resistance to the motion of vehicles related to the direction by railway [Text] / V. Tkachenko, S. Sapronova, I. Kulbovskiy, O. Fomin // Eastern-European Journal of Enterprise Technologies. – 2017. – Vol. 5, Issue 7 (89). – P. 65–72. doi: 10.15587/1729-4061.2017.109791

68. UIC Code 518.Testing and approval of railway vehicles from the point of view of their dynamic behaviour.Safety – Track fatigue – Ride quality.– International Union of Railways. – September 2009. – 119 p.

69. UIC Code 519.Method for determining the equivalent conicity. – 1st edition, 2004.

70. White paper: Roadmap to a Single European Transport Area - Towards a competitive and resource efficient transport system /* COM/2011/0144 final.

71. Yoon, S. C., Kim, J. G., Jeon, C. S Choe, K. Y. (2009). Evaluation of Structural Strength in Body Structure of Freight Car. Key Engineering Materials, 417-418, 181–184. doi: https://doi.org/10.4028/www.scientific.net/kem.417-418.181

72. Yuan, Y. Q., Li, Q., Ran, K. (2011). Analysis of C80B Wagon's Load-Stress Transfer Relation. Applied Mechanics and Materials, 148-149, 331–335. doi: https://doi.org/10.4028/www.scientific.net/amm.148-149.331

73. Алямовский А. А. COSMOSWorks. Основы расчета конструкций на прочность в среде SolidWorks. М.: ДМК Пресс, 2010. 784 с.

74. Алямовский А. А. SolidWorks Simulation. Инженерный анализ для профессионалов: задачи, методы, рекомендации. М.: ДМК Пресс, 2015. 562 с.

75. Белорусская железная дорога. Стратегия инновационного развития транспортного комплекса Республики Беларусь до 2030 года [Електронний ресурс]:[Веб-сайт]. – Електронні дані. – Режим доступу:http://www.rw.by/corporate/press_center/reportings_interview_article/2015/03/strategija_innovacionnogo_razv/(датазвернення 27.11.2018). – Назвазекрана.

76. Горбунов, М.I. Комплексний розрахунок виконання кришки люка напіввагона з різнотипних матеріалів із проміжним ш-подібним обв'язуванням / М.I. Горбунов, О.В. Фомін, А.О. Ловська, В.В. Коваленко// Наука та прогрес транспорту. Вісник Дніпропетровського національного університету залізничного транспорту імені академіка В. Лазаряна: науковий журнал. – м. Дніпро: ДНУЗТ ім. В. Лазаряна, 2018. – Вип. 3(75) – С. 138-148. doi 0.15802/stp2018/132863

77. Горбунов, М.I. Уточнення показників міцності кришки люка напіввагона, моделюванням додаткових розрахункових режимів / Горбунов М. I., О.В. Фомін, А.О. Ловська, В.В. Коваленко // Вісник Національного технічного університету «ХПІ». Серія: Транспортне машинобудування, № 29 (1305) 2018. - С. 38-45.

78. ГОСТ 33211–2014. Вагоны грузовые. Требования к прочности и динамическим качествам. [Действителен от 22.12.2014]. М.: Стандартинформ, 2016. 54 с.

79. Державна служба статистики України [Електронний ресурс] : [Веб-сайт]. – Електронні дані. – Режим доступу: http://www.ukrstat.gov.ua/(дата звернення 03.12.2018). – Назва з екрана.

80. ДСТУ 7598:2014 Вагони вантажні. Загальні вимоги до розрахунків та проектування нових і модернізованих вагонів колії 1520 мм (несамохідних). [Дійсний 01.07.2015]. 2015. 162 с.

81. Законодавство України. Національна транспортна стратегія України на період до 2030 року[Електронний ресурс] : [Веб-сайт]. – Електронні дані. – Режим доступу: http://zakon.rada.gov.ua/laws/show/430-2018-%D1%80(дата звернення 20.11.2018). – Назва з екрана/

82. Ивченко Г. И., Медведев Ю. И. Математическая статистика: учебник. М.: Книжный дом "ЛИБРОКОМ", 2014. 352 с.

83. Макеев С. В., Буйленков П. М. Особенности расчета напряженно-деформированного состояния танка-контейнера с учетом реального нагружения в эксплуатации. НАУКА–ОБРАЗОВАНИЕ–ПРОИЗВОДСТВО: Опыт и перспективы развития: сборник материалов XIV Международной научно-технической конференции, посвященной памяти доктора технических наук, профессора Е. Г. Зудова (8-9 февраля 2018 г.): в 2-х т. – Т. 1: Горно-металлургическое производство. Машиностроение и металлообработка. – Нижний Тагил: НТИ (филиал) УрФУ. 2018. С. 174–184.

84. Маковкин Г.А., Лихачева С.Ю. Применение МКЭ к решению задач механики деформируемого твердого тела: учебное пособие. Часть 1. Н.Новгород: Изд-во ННГАСУ, 2012. 71 с.

85. Маталыцкий М. А., Хацкевич Г. А. Теория вероятностей и математическая статистика: учебник. Минск: Вышэйшая школа, 2017. 591 с.

86. Памятка UIC/ОСЖД 430-4 ОР. Вагоны грузовые. Движение по сетям железных дорог с шириной колеи 1435 мм и 1520 мм. Технические условия и испытания на соответствие техническим условиям.

87. Памятка ОСЖД О+Р 516. Грузовые вагоны сообщения между железными дорогами колеи 1435 мм и железными дорогами колеи 1520мм. Технические предписания и технические условия для допуска вагонов.

88. Памятка ОСЖД О+Р-500. Габариты подвижного состава и приближения строений. Варшава, 30 сентября - 4 октября 1996.

89. Памятка ОСЖД О+Р-535. Унификация и размещение ступенек, концевых площадок, переходных мостиков, поручней, канатных крюков и воздухозапорных кранов грузовых вагонов 20.11.1998.

90. Правила пользования вагонами в международном сообщении (ППВ). Приложение №1 к Договору о ППВ. Действует с 1 января 1956 года (переиздано с изменениями и дополнениями на 1 июня 2004 года).

91. Руденко В. М. Математична статистика: навч. посіб. К.: Центр учбової літератури, 2012. 304 с. Zhong, Y.-G., Zhan, Y., Zhao, G. (2014). Fatigue Analysis of Structure of Gondola Car Body Based on Rigid-flexible Coupling Multi-body Systems. 11th World Congress on Computational Mechanics (WCCM XI). Barcelona.

92. Соколов С. А. Строительная механика и металлические конструкции машин: учебник. СПб.: Политехника, 2011. 422 с.

93. Третьяков А. В., Третьяков О. А., Зимакова М. В., Петров А. А. Экспериментальная оценка спектров ударного отклика подвижного состава. Наука та прогрес транспорту. Вісник Дніпропетровського національного університету залізничного транспорту, 2017, № 3 (69). С. 147–159.

94. Фомін, О.В. Зміцнення несучих вагонних систем методом навивання/ О.В. Фомін, А.А. Стецько, В.Е. Осьмак // Международный информационный научно-технический журнал «Вагонный парк». – Харків. – № 11-12(128-129), 2017. – С. 38-41.

95. Фомін, О.В. Математичне моделювання варіаційних характеристик плям нагріву при термічній правці каркасних елементів піввагонів / О.В. Фомін, О.В. Бурлуцький, М.І. Горбунов, О.А. Логвіненко, А.М. Фоміна // Збірник наукових праць Державного університету інфраструктури та технологій: Серія «Транспортні системи і технології». – Київ: ДУІТ, 2018. – Вип. 31. – С. 186-195

96. Фомін, О.В. Математичне описання термічної правки вагонних металоконструкцій / О.В. Фомін, М.І. Горбунов, О.В. Бурлуцький, О.А. Логвіненко, А.М. Фоміна // Вчені записки Таврійського національного університету імені В.І. Вернадського:Серія: Технічні науки. – Київ: ТНУ імені В.І. Вернадського, 2018 – Том 29 (68) № 1 2018, Частина 3 – С. 151-155

97. Фомін, О.В. Поліпшення несучої здатності вагона-хопера для перевезення зерна з метою підвищення опору динамічним зусиллям / Фомін О.В., Прокопенко П.М., Горбунов М.І. Сапронова С.Ю.// Науковий журнал – Вісник Східноукраїнського національного університету імені Володимира Даля. – Сєверодонецьк: СНУ ім. В.Даля, 2017. – № 5(235) – С. 88-99.

98. Фомін, О.В. Структурно-функціональне описання конструкції кришки люка/ О.В. Фомін, М.І. Горбунов, Н.С. Кочешкова, В.В. Коваленко// Наука та прогрес транспорту. Вісник Дніпропетровського національного університету залізничного транспорту імені академіка В. Лазаряна: науковий журнал. – м. Дніпро: ДНУЗТ ім. В. Лазаряна, 2018. – Вип. 2(74) – С. 133-146. doi: 10.15802/stp2018/130014

99. Фомін, О.В. Теоретично-практичний базис правки деформованих вагоноконструкцій термічним впливом / О. В. Фомін, О. А. Логвіненко, О. В. Бурлуцький, А. М. Фоміна // Наука та прогрес транспорту. Вісник Дніпропетровського національного університету залізничного транспорту імені академіка В. Лазаряна: науковий журнал. – м. Дніпро: ДНУЗТ ім. В. Лазаряна, 2018. – Вип. 6(78) – С. 155-164.

100. Фомін, О.В. Термічна правка технологічно-деформованих верхніх обв'язувань піввагонів / О.В. Фомін, О.В. Бурлуцький, М.І. Горбунов, О.А. Логвіненко, А.М. Фоміна // Вісник Національного технічного університету «ХПІ». Серія: Динаміка та міцність машин. – 2017. – N 39. - С. 76-80. – Режим доступу : DOI : 10.20998/2078-9130.2017.39.115771

101. Фомін, О.В. Концептуальні основи термічної правки / Фомін О.В.,Бурлуцький О.В, Горбунов М.І., Логвіненко О.А.// Науковий журнал –

Вісник Східноукраїнського національного університету імені Володимира Даля. – Сєвєродонецьк: СНУ ім. В.Даля, 2018. – № 2(243) – С. 233-236.

102. Фомін, О.В. Формалізовані описання конструкцій кришок люків напіввагонів (частина 2) / Фомін О. В., Горбунов М. І., Коваленко В. В., Флярковська В.О. // Науковий журнал – Вісник Східноукраїнського національного університету імені Володимира Даля. – Сєвєродонецьк: СНУ ім. В.Даля, 2018. – № 1(242) – С. 145-152.

103. Фомін, О.В. Формалізовані описання конструкцій кришок люків напіввагонів (частина 1) / Фомін О.В., Горбунов М.І, Коваленко В.В, Міщук І.Р.// Науковий журнал – Вісник Східноукраїнського національного університету імені Володимира Даля. – Сєвєродонецьк: СНУ ім. В.Даля, 2018. – № 2(243) – С. 216-224.

104. Центр транспортных стратегий. – Российский транзит: страны Прибалтики остаются на голодном пайке [Електронний ресурс]:[Веб-сайт]. – Електронні дані. – Режим доступу:http://cfts.org.ua/articles/rossiyskiy_tranzit_strany_pribaltiki_ostayutsya_na_golodnom_payke_749(дата звернення 03.12.2018). – Назва з екрана.

Scientific Publication

Oleksii V. FOMIN
Mykola I. GORBUNOV
Oleksii V. BURLUTSKI
Olexandr A. LOGVINENKO
Olexandr V. KAZANKO
Olena V.EL KASSEM

THEORETICAL ASPECTS
OF APPLIED TRANSPORT MECHANICS

(Part 1)

Monograph

English version